

The influence of TGF- β signaling on precursor cells in the mouse retina



Dissertation zur Erlangung des Doktorgrades der
Naturwissenschaften (Dr. rer. nat.) der Fakultät für Biologie
und vorklinische Medizin der Universität Regensburg

vorgelegt von

Martina Klupp
aus
Landau a.d. Isar

im Februar
2013

Das Promotionsgesuch wurde eingereicht am: 24.09.2012

Die Arbeit wurde angeleitet von:

Prof. Dr. Ernst Tamm
Prof. Dr. Ludwig Aigner

Prüfungsausschuss:

- Vorsitzender: Prof. Dr. Kurtz
- Erstgutachter: Prof. Dr. Tamm
- Zweitgutachter: Prof. Dr. Schneuwly
- Drittprüferin: Prof. Dr. Wagner
- Ersatzprüfer: PD. Dr. Fuchshofer

Unterschrift:

Contents

Contents	i
1 Introduction	1
1.1 Abstract	1
1.2 Introduction	2
1.3 Stem cells	2
1.3.1 Definition of stem cells	2
1.3.2 Embryonic versus adult stem cells	3
1.3.3 Asymmetric cell division	3
1.4 Possible stem/progenitor populations in the eye	3
1.4.1 The architecture of the neural retina and its surroundings	3
1.4.2 The ciliary marginal zone as a source of progenitor cells . .	4
1.4.3 The retinal pigment epithelium as a source of progenitor cells	6
1.4.4 Müller glia cells as progenitor cells	6
1.5 A closer look at Müller glia cells	7
1.5.1 Architecture of Müller glia	7
1.5.2 Müller glia in development	7
1.5.3 Functions of Müller glia	9
1.5.4 Gliosis	9
1.6 The TGF- β pathway	10
1.6.1 Functions of the TGF- β pathway	10
1.6.2 TGF- β : a transforming growth factor	11
1.6.3 The TGF- β /ALK receptors	11
1.6.4 The TGF- β signaling	11
1.6.5 Structure and regulation of the Smads	12
1.6.6 TGF- β in embryonic and neural stem cells	12
1.6.7 TGF- β in the retina and in Müller glia	13
1.7 Nestin	14
1.7.1 Nestin as a cytoskeletal protein	14
1.7.2 Nestin: a marker for neural stem cells	15
1.7.3 Nestin and its role in proliferation and differentiation . . .	15
1.8 Aims of my work	16
2 Materials and Methods	17
2.1 Materials	17
2.1.1 Chemicals and reagents	17

2.1.2	Laboratory Consumables	19
2.1.3	Laboratory Instruments	20
2.1.4	DNA and protein ladders	21
2.1.5	Reaction kits	21
2.2	Animal models	22
2.2.1	Animal housing and maintenance	22
2.2.2	Wistar rats	22
2.2.3	The Cre/loxP recombination system	22
2.2.4	EIIa Cre mice	23
2.2.5	Rosa26 LacZ Reporter mice	23
2.2.6	CAG Cre ERT - Tamoxifen inducible mice for the breeding of a TGF- β full knockout	23
2.2.7	Smad7 ^{fl/fl} mice	24
2.2.8	TGF- β RII ^{fl/fl} mice	24
2.2.9	β -B1 CTGF overexpressing mouse strains	25
2.2.10	Breeding of Smad7 ^{fl/-} and TGF- β RII ^{fl/-} mice	25
2.3	Genotyping	26
2.3.1	Extraction of genomic DNA from mouse tails	26
2.3.2	DNA precipitation	26
2.3.3	PCR - polymerase chain reaction	27
2.3.4	Genotyping EIIa Cre mice	27
2.3.5	Genotyping the Smad7 ^{fl/fl} and TGF- β RII ^{fl/fl} mice	27
2.3.6	Genotyping the Smad7 ^{fl/-} and TGF- β RII ^{fl/-} mice by dele- tion PCR	29
2.3.7	Genotyping Rosa LacZ mice	29
2.3.8	Genotyping β -B1 CTGF mice	30
2.3.9	Agarose gel electrophoresis	30
2.4	Histology and Immunohistochemistry	32
2.4.1	Buffers and equipment for histology	32
2.4.2	Tissue preparation	32
2.4.3	Histological stainings	34
2.4.4	Measurement of retinal thickness	35
2.4.5	Determination of axon number in optic nerves	36
2.4.6	Intravitreal injection - the NMDA lesion model	36
2.4.7	TUNEL staining	36
2.4.8	BRDU assays and stainings - methods to quantify cell pro- liferation	38
2.4.9	Apoptosis assays (TUNEL) and proliferation assays (BRDU) in newborn mice	39
2.4.10	LacZ staining of EIIa Cre x Rosa LacZ	39
2.4.11	Immunostaining of tissue	40
2.4.12	Nestin and GFAP stainings	42
2.4.13	Glutamine synthetase staining (GS) - Evaluation of the number of Müller glia cells in different mouse lines	43
2.4.14	Light- and fluorescence microscopy	43
2.5	Quantification of mRNA expression	45
2.5.1	Retina preparation for mRNA isolation	45
2.5.2	RNA isolation with TriFast TM	45
2.5.3	RNA-quantification	45

2.5.4	cDNA synthesis	46
2.5.5	Quantitative real-time (RT)-PCR	46
2.6	Protein biochemical techniques	48
2.6.1	Protein isolation with the trizol method	48
2.6.2	Sodium-dodecyl-sulfate polyacryl-amid gel electrophoresis: SDS PAGE	49
2.6.3	Western blot protein transfer	50
2.6.4	Western blot immunostaining	51
2.6.5	Coomassie staining for loading control	52
2.7	Cell culture	53
2.7.1	Cell culturing techniques	53
2.7.2	Cell counting with the CASY Cell Counter	53
2.7.3	Enrichment of rat Müller glia cells for cell culture	54
2.7.4	Colorimetric cell proliferation ELISA	54
2.7.5	TGF- β 1 treatment and RNA isolation from Müller glia cells	55
2.8	Diagrams and Statistics	55
3	Results	57
3.1	Aims and ideas	57
3.2	Expression of EIIa Cre recombinase - EIIa mice x Rosa LacZ	57
3.3	Effects of an altered TGF- β pathway	58
3.3.1	Breeding of Smad7 ^{fl/-} and TGF- β RII ^{fl/-} mice	58
3.3.2	Confirmation of gene deletion and gene product deficiency	59
3.3.3	Phenotype analysis	61
3.3.4	Measurements of retina thickness	63
3.3.5	Evaluation of the number of Müller glia	65
3.3.6	Proliferation and Apoptosis in newborn Smad7 mice	67
3.3.7	Nestin and GFAP expression	71
3.3.8	Activated pathways in Smad7 ^{fl/-} mice	75
3.4	NMDA lesions in Smad7 and TGF- β RII deficient mice	76
3.4.1	Axon number after an NMDA lesion	76
3.4.2	Retinal apoptosis after an NMDA lesion	79
3.4.3	Proliferation after NMDA treatment	81
3.4.4	Nestin and GFAP expression after NMDA treatment	83
3.5	β -B1-CTGF overexpressing mice	86
3.5.1	Increased retinal thickness	86
3.5.2	Number of Müller glia cells	86
4	Discussion	91
4.1	Generation of mouse models with diminished or enhanced TGF- β signaling	91
4.2	Influence of an altered TGF- β signaling on retinal thickness and cell number	92
4.2.1	Smad7 deficiency causes a thickened retina around the optic nerve head	92
4.2.2	Induceable TGF- β RII homozygous deletion causes a thinned retina	92
4.3	Influence of the TGF- β pathway on proliferation	92
4.3.1	Increased proliferation in Smad7 deficient mice	92

4.3.2	Direct effects of TGF- β on adult neural cells and embryonic stem cells	93
4.3.3	CTGF as a potential mediator	94
4.3.4	Possible influence of an crosstalk between TGF- β and EGF-pathway on proliferation	94
4.3.5	Possible influence of an crosstalk between TGF- β and Wnt-pathway on proliferation	95
4.4	The possible role of Nestin in the progenitor cell population . . .	96
4.4.1	Increased Nestin expression in Smad7 deficient mice	96
4.4.2	Nestin expression as a sign of activation, gliosis and structure stabilization	96
4.4.3	Polarized distribution of cell components	96
4.4.4	The possible role of Nestin in cell cycle control	96
4.4.5	Nestin expression after NMDA lesion	97
4.5	Proliferation in the lesioned adult retina	97
4.6	Constriction of the effects to the central retina	98
4.7	Outlook	99
5	Summary	101
	Abbreviations	103
	List of Figures	105
	List of Tables	107
	List of publications	109
	Bibliography	111
	Danksagung	125

Chapter 1

Introduction

1.1 Abstract

Age-related macular degeneration and glaucoma are among the most frequent causes of vision loss in the USA [1]. Like retinitis pigmentosa or diabetic retinopathy, they cause a loss of retinal neurons, that can not be compensated by the human or mammalian retina. Fish or urodeles (salamander), in contrast, are able to not only regenerate single cells, but also complete and functioning retinæ from their somatic stem cells. Based on this, many studies aim to clarify the signaling pathways that lead to regeneration in the retina or that keep the human and mammalian stem/progenitor cell populations from forming a regenerative reaction.

One pathway that is part of the control mechanism of neural stem cells is the transforming growth factor (TGF)- β signaling pathway. As TGF- β is known to reduce neurogenesis in the brain and in neural stem and progenitor cell cultures, we formed the hypothesis that it also has an influence on the stem/progenitor cells in the eye.

Focusing on the precursor cells of the retina we were especially interested in Müller glia cells, as they present an important stem cell population in fish and birds.

To demonstrate the influence of the TGF- β pathway on Müller glia in developing and lesioned adult mouse eyes, we used mice with a heterozygous deletion of the promoter region and exon I of Smad7 (mothers against decapentaplegic homolog 7) and of exon II of TGF- β Receptor II. With histological and biochemical methods we could show that a deficiency of Smad7, an inhibitor of the TGF- β pathway, lead to a thickened inner and outer retina and an elevated number of Müller glia in the adult animal, caused by enhanced proliferation in newborn mice. Interestingly the stem cell marker Nestin could be shown to be elevated in Müller glia cells in adult animals as well.

Additionally, we conducted N-methyl-D-aspartate (NMDA) lesions to provoke a proliferative reaction in the progenitor cell populations of the retina, but no effect could be shown. Experiments were also done with TGF- β receptor II deficient - and partly with TGF- β receptor II knockout mice, where a thinned retina in the adult animals could be found.

We conclude that TGF- β influences proliferation during the development of the central retina, but not in the normal or injured adult retina.

1.2 Introduction

Regeneration is a fascinating phenomenon that mankind has been interested in for centuries. As early as 1768 Lazzaro Spallanzani reported that snails could regenerate their heads, when decapitated, unfortunately without the brain. This led the public to search their gardens for snails, to replicate this experiment [2]. Many animals in nearly all phyla show these vast regenerative capacities. Salamanders for example regrow limbs and tails even including the spinal chord, and planarians are even able to regenerate whole animals from single body parts [3]. In mammals the regenerative capacities are much more limited, the loss of cells is often irreparable. This applies in particular to the central nervous system, about which the neuroanatomist Cajal stated in 1928 [4]: 'Once development was ended, the founts of growth and regeneration of the axons and dendrites dried up irrevocably. In adult centers, the nerve paths are something fixed and immutable: everything may die, nothing may be regenerated.' In 1962 however the limited occurrence of new neurons forming in injured adult rat brains was discovered [5]. This sparked new interest in research in the field of regeneration in neural tissues including the neural retina as part of the brain. The retina is subject to many degenerative diseases like age related macula degeneration (AMD) or glaucoma, causing cell loss and leading to considerable visual impairment. Cells that are lost in these processes in the human retina can not be replaced. Therefore the study of regenerative processes holds big hopes for the future medical care of these diseases, most of all, hopes that the process of regeneration can be stimulated in a clinical setting.

1.3 Stem cells

In order to regenerate, a tissue has several options: the proliferation of differentiated cells, the activation of reserve stem cells, the formation of new stem cells with a limited capacity for self renewal (progenitor cells) or a combination of these strategies [3]. For our attempts to manipulate regenerative processes, the knowledge of stem cells and the mechanisms that control their behavior is the key.

1.3.1 Definition of stem cells

Stem cells have the remarkable potential to develop into many different cell types in the body, during early life and growth [6].

The following features define a stem cell:

1. Multipotency: The cell is not terminally differentiated and can differentiate into a variety of cells [7].
2. Self renewal: The cell can proliferate infinitely [7].
3. Each daughter cell can decide if it becomes a stem cell or a differentiated cell [7], see Fig. 1.1.

4. Even if stem cells can proliferate infinitely, in unlesioned tissue mammalian stem cells are predominantly in a quiescent non dividing G0-state [7, 8].

1.3.2 Embryonic versus adult stem cells

There are two basic categories of stem cells: embryonic stem cells and adult or somatic stem cells. Embryonic stem cells (ES cells) can divide and give rise to cells of all three germ layers, the ectoderm, the mesoderm and the endoderm [9]. One of their defining features is their potential to undergo symmetric cell divisions without differentiation, in order to produce identical progeny. This function is also known as self renewal. In contrast, tissue specific adult stem cells are lineage restricted, give rise to specific cell types and have only limited capacity for self renewal and differentiation [6, 10–12]. In many tissues the adult stem cells reside quiescently in so called stem cell niches, and are only activated in case of a lesion. These niches are specialized microenvironments, that keep the stem cell population from premature exhaustion [13]. The microenvironment is also responsible for the fate of the cells.

1.3.3 Asymmetric cell division

In addition to symmetric division, stem cells can also divide asymmetrically and form another stem cell and a second cell that will terminally differentiate as depicted in Figure 1.1. Theoretically this can be influenced in two ways, by the microenvironment of the cell or by the cell itself. An example for such a microenvironment is the basal layer of the epidermis. The cells in this niche only remain stem cells, if they have contact with the basal membrane [7]. Also Müller glia cells in culture only convert to the neuronal lineage in an aggregate culture under non-adhesive conditions [14]. The other possibility is the control by the cell itself. The division asymmetry can for example be determined by an asymmetric distribution of cell components.

1.4 Possible stem/progenitor populations in the eye

Different cell types have been suggested to act as neural progenitors in the adult mammalian retina. To better understand where these cell populations are located, a short description of the architecture of the neural retina and its surrounding tissues is given in the following.

1.4.1 The architecture of the neural retina and its surroundings

The retina has a common architecture in non-mammalian and mammalian species [15]. It consists of 6 types of neurons and 3 types of glial cells. Two types of these neurons are the light sensitive photoreceptor cells, so called rods and cones. Their nuclei are located in the outer nuclear layer, see Figure 1.2. The signal from the photoreceptors is processed through three types of interneurons: bipolar cells, horizontal cells and amacrine cells. Together with the nuclei of the Müller glia cells, their nuclei are located in the inner nuclear layer. In the outer plexiform layer the terminals of the rods and cones connect to the horizontal and bipolar

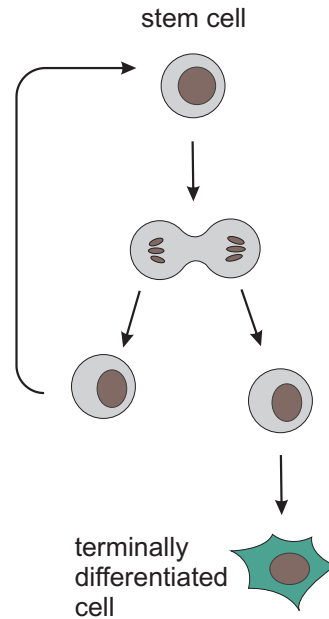


Figure 1.1: *Each daughter cell that is born when a stem cell divides can either remain a stem cell or go on and become terminally differentiated [7].*

cells. The cells modify the signals and transduce it to the dendrites of the amacrine cells and ganglion cells. The amacrine cells further process the incoming signal, whereas the ganglion cells transduce the signal to the brain.

The retina is separated from the choroid by the retinal pigment epithelium (RPE). The RPE is a single-layer epithelium of pigmented hexagonal cells. It is responsible for nourishing the photoreceptors and to recycling their disc membranes. The microvilli of the RPE ensheath the outer segments of the photoreceptors to do so.

At the anterior margin, the retina passes into the ciliary body, a structure responsible for the production of the aqueous humour of the eye. The outer pigmented layer is continuous with the retinal pigment epithelium, the internal layer is unpigmented and continuous with the retina.

Possible stem cells reside at three niches in the retina: the ciliary marginal zone, the retinal pigment epithelium and the Müller glia cells in the neural retina.

1.4.2 The ciliary marginal zone as a source of progenitor cells

The ciliary marginal zone or circumferential germinal zone is a zone on the anterior margin of the retina, see Figure 1.3. It exists in fish, amphibia and birds and allows for life long neurogenesis. The zone was searched for in mammals, and it has been claimed that retinal stem cells exist in the pigmented ciliary margin where the border of the iris is attached to the ciliary body. It was stated that stem cells from this region could be propagated *in vitro* [17] and form rod photoreceptors, bipolar neurons, and Müller glia, but the results are highly controversial [18]. According to Moshiri et al. this region does not appear to play a significant role in the regeneration of the majority of the retina in vertebrates [19].

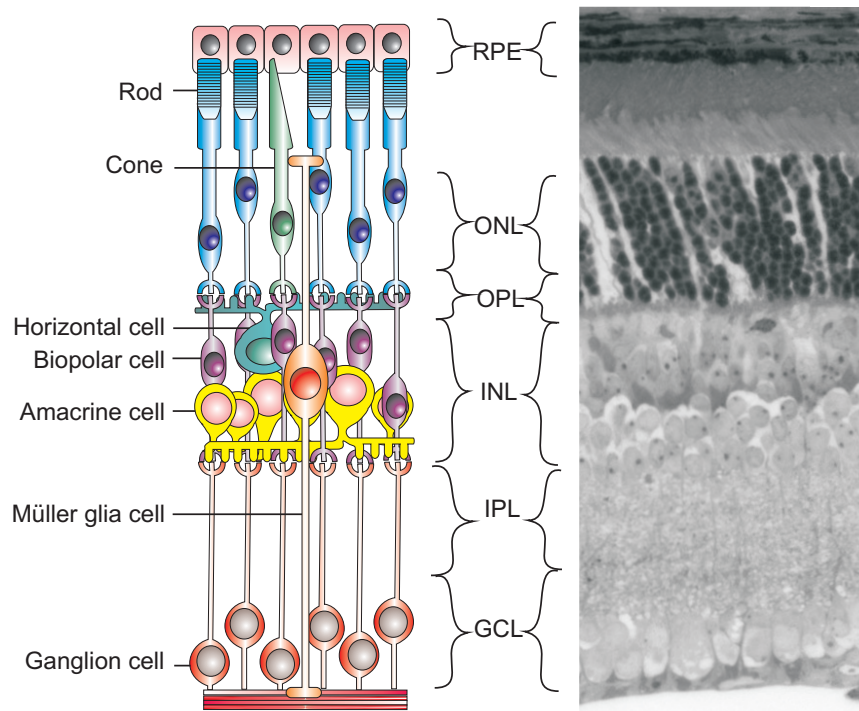


Figure 1.2: Schematic architecture of the retina (left): ONL = outer nuclear layer, INL = inner nuclear layer, GCL = Ganglion cell layer, IPL= inner plexiform layer, OPL = outer plexiform layer; RPE = retinal pigment epithelium; (drawing adapted from [16]); Micrograph of the layers of the retina (right).

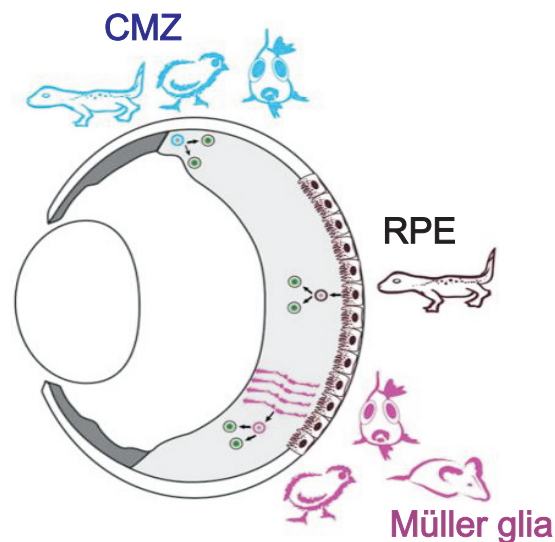


Figure 1.3: Progenitor cell populations can be found in the ciliary marginal zone, in the RPE and in the neural retina in the form of Müller glia cells. The species for which these cell types are considered to be stem/progenitor cells are shown as pictograms. As things are now, Müller glia cells are the most popular candidates for progenitor cells in the mammalian retina [15].

1.4.3 The retinal pigment epithelium as a source of progenitor cells

Urodeles (salamander) regenerate the retina after complete surgical removal from the retinal pigment epithelium, see Figure 1.3. The residing stem cells lose their pigmentation, form a new layer and recreate the whole retina, with all its layers, by recapitulating the sequence of normal histogenesis [20,21]. In chicken a similar process can be seen, but this is restricted to newborn animals [22].

1.4.4 Müller glia cells as progenitor cells

Müller glia as progenitor cells in fish and salamanders

In fish the retina can not regrow when everything but the RPE is removed. Accordingly, the stem cells appeared to be part of the neural retina [23]. Finally around 2005 several groups discovered that Müller cells were the primary source of regeneration in the fish retina, but rod precursors could also be making a contribution. In uninjured fish retina, the progeny of these progenitor cells are the rod photoreceptors, but after various lesions Müller glia in fish undergo a robust response and give rise to all types of cells including photoreceptors, see Figure 1.4.

In salamanders, on the other hand, Müller glia are not a source of regeneration. Unlike fish, they do not add new rods to the retina by slowly cycling Müller glia during their life. Due to this, their Müller glia may have lost their regenerative capacity and the RPE took over this task [15,24,25].

Müller glia as progenitor cells in chicken

In newborn chicken, Müller glia are also a source of regeneration. They are able to reenter the mitotic cycle after neurotoxic damage with NMDA, progressing through the S- and M-phase and generating two daughter cells. This process can be prolonged through the use of growth factors [26].

Unfortunately only a subset of the newborn cells express progenitor markers, and an even smaller number differentiates into cells that express neuronal markers. Most of these cells express markers of amacrine cells and of bipolar cells. Ganglion cells and horizontal cells are also rarely observed, see Figure 1.4, but to date there is no evidence that these cells are functional.

Just like in fish, retinal damage causes chicken Müller glia cells to proliferate and upregulate the expression of neural progenitor genes, but unlike fish cells they undergo only one round of division, whereas fish Müller glia undergo multiple rounds and form small neurogenic clusters [27–32].

Müller glia as progenitor cells in mammalia

In the mammalian retina the proliferative response is much more limited compared to fish or birds. After damage, Müller glia cells mainly get reactive and hypertrophic, but only few reenter the mitotic cycle [33]. Nevertheless Sahel et al. and Ooto et al. could show that in rats a subpopulation of Müller glia cells could reenter the cell cycle when treated with mitogens and after damage [15,34,35]. Ooto et al. even showed that 30% of the BRDU labeled cells persisted for at least 28 days.

The amount of damage appears to be important for the intensity of the regenerative response as well. After a heavy damage with MNU (methyl nitrosourea) a large number of Müller glia reentered the cell cycle in adult rats [15, 36, 37].

Beside lesions, growth factors influence the number of BRDU positive cells. For example Close et al. showed that the treatment of the eye with epidermal growth factor (EGF) injections increased the number of BRDU positive Müller glia after light damage in rats [15, 38, 39].

The types of neurons that can be generated is also limited in mammals. To allow for differentiation of Müller glia progeny into different cell types, Ooto et al. treated rat eyes with protein kinase C, neuron specific enolase, rhodopsin and the calcium binding protein - recoverin - after NMDA damage. In this experiment they could detect markers of bipolar cells and rods in the progeny of Müller glia cells [15, 35], see Figure 1.4. An amacrine cell fate could only be promoted in explant cultures by infecting cells with viruses expressing NeuroD1, Math3 and Pax6.

To get a regenerative response in mice is even more difficult than it is in rats, but Karl et al. were able to show that Müller glia cells in the mouse retina proliferate after NMDA injection if treated with EGF and fibroblast growth factor (FGF). In this experiment, a huge amount of Müller glia were recruited into the mitotic cell cycle 72 hours after injury and some of the Müller glia progeny showed markers of progenitor cells and even of amacrine cells [40]. Figure 1.4 shows which cells can be regenerated from Müller glia in different species. The variety of cells that can be formed from Müller glia declines from lower to higher developed animals.

1.5 A closer look at Müller glia cells

1.5.1 Architecture of Müller glia

Müller glia cells are radial glia (glia means 'glue' in Greek) spanning the whole retina, see Figure 1.2. They are one of three glia cell types in the eye, the other two are astrocytes - another type of macroglia - and the so called microglia, which are blood derived resident immune cells. The somata of the Müller glia cells lie in the inner nuclear layer. Their processes reach to the ganglion cell layer, where they border on the vitreous body, and to the outer nuclear layer, where they ensheath the photoreceptor cell bodies, see Figure 1.5. Each of the Müller glia cells is considered as the core of a micro-unit or columnar unit of about 15 retinal neurons. In this way it works as scaffold and anatomical link for the neurons to the compartments they exchange molecules with [41].

1.5.2 Müller glia in development

As the cells are born in the developing retina, single progenitor cells give rise to Müller glia cells and retinal neurons [43] in two phases. In the earlier phase, the cells in the apical margin of the neuroepithelium give rise to cone cells, horizontal cells and ganglion cells. In the second phase, rod photoreceptors, bipolar cells and Müller glia are born, see Figure 1.6. In mice, for example, the differentiation of Müller glia occurs approximately between postnatal day 1 and 8 [44].

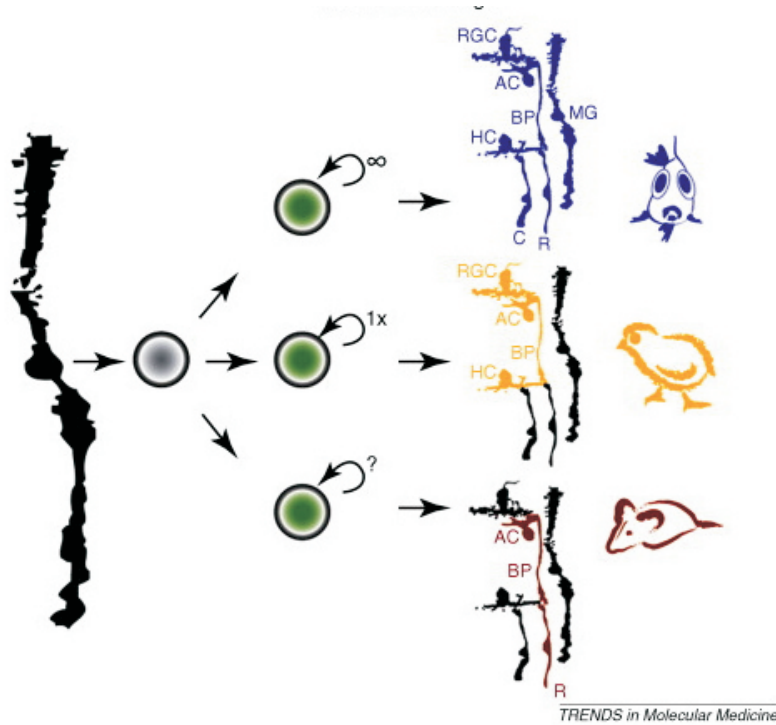


Figure 1.4: Cell types regenerated from Müller glia: The variety of cells that can be recovered from Müller glia as progenitor cells after injury declines in higher developed animals [15]. RGC = retinal ganglion cell; MG = Müller glia cell; BP = bipolar cell; AC = amacrine cell; HC = horizontal cell, C = Cone; R = Rod.

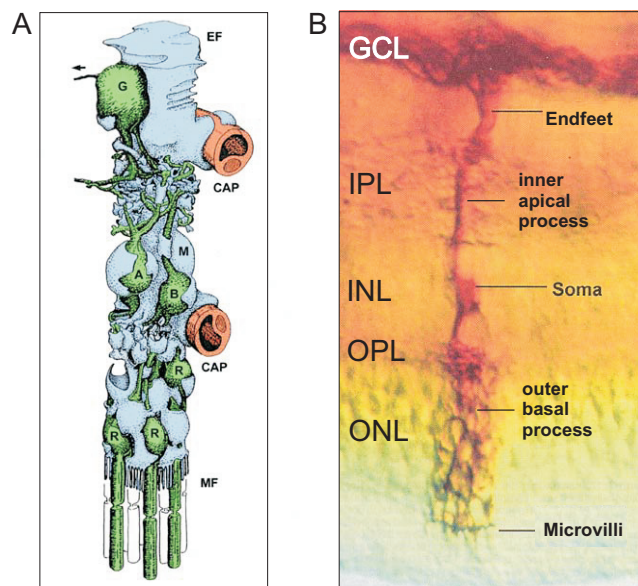


Figure 1.5: (A) Müller glia are the center of a so called microunit. They provide a scaffold and nutrition for about 15 neurons surrounding them. R = photoreceptor, B = bipolar cell, A = amacrine cell, G = ganglion cell, cap = capillary (Reichenbach, 1999). (B) Müller glia span the whole retina. Their soma lie in the inner nuclear layer. Their processes reach to the border of the vitreous body and ensheath the bodies of the photoreceptors with their microvilli [42].

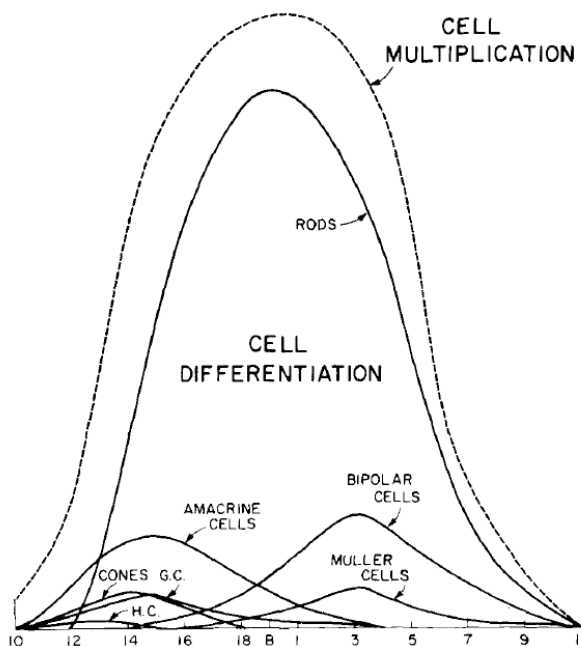


Figure 1.6: Time course of cell differentiation in the mouse retina. Cell in the retina differentiate in two phases. Müller glia and neurons are derived from the same progenitors in this process [44].

In a later phase of development the neurons have to migrate to their final positions. Müller glia cells are thought to guide much of this neuronal migration with their processes [45].

1.5.3 Functions of Müller glia

Müller glia cells have a variety of tasks in the retina, see Figure 1.7. They provide the metabolic support and nutrition of the neurons, like the delivery of lactate or pyruvate [46] or the storage of glycogen [47, 48]. They are responsible for potassium [49] and water homeostasis [50] as well as CO₂ buffering [51] and contribute to the neuronal signaling by transmitter uptake [52–54] and recycling [55, 56]. Additionally they are known to protect the retina against oxidative stress [57, 58], to recycle photopigments [59] and release growth factors [60]. Finally they were even found to act as optical fibers in the retina [61] and contribute to the B-wave of electroretinograms by regulation of potassium distribution [62–64].

1.5.4 Gliosis

In the event of lesions, Müller glia cells often react with a so called gliosis. Gliosis is an umbrella term for non-stereotypical responses by glia, associated with a pathological state [15]. In a gliotic reaction Müller glia cells can show cell hypertrophy, changes in gene expression, changes in morphology or even migration. Also the expression of glial fibrillary acidic protein (GFAP) is a hallmark of gliosis. Less often proliferation is part of this response [41].

Gliosis and regeneration are two different types of reaction of the Müller glia. This can be seen in the following experiment: Ciliary neurotrophic factor CNTF

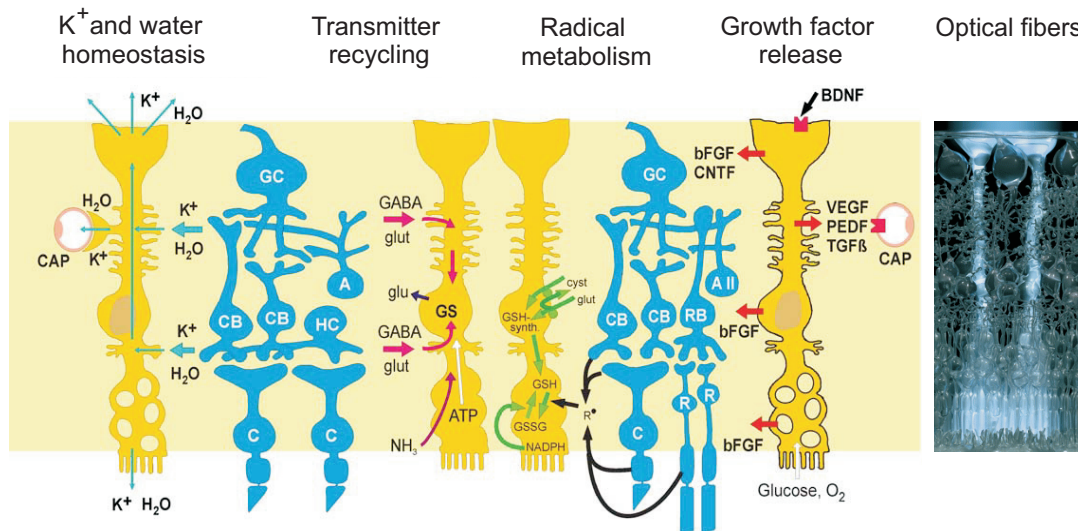


Figure 1.7: Some examples of the functions of Müller glia cells as mentioned in the text [60]. Müller glia cells can even act as optical fibers [61].

is a main factor triggering gliosis and is elevated after neuronal damage. Mouse models that overexpress CNTF even show gliosis without any damage. Interestingly in damaged chicken retina, the application of CNTF inhibits regeneration on the basis of Müller glia, but promotes gliosis [15, 41].

However, these two mechanisms are not exclusive reactions. In fish, for example, the retina regenerates completely and Müller glia show hypertrophy and express GFAP. All in all gliosis is an essential response of the glia in the event of damage. It provides rapid repair of the retina but is also responsible for the so called glial scar, which is a barrier for regeneration [15, 41].

1.6 The TGF- β pathway

As the purpose of this work was to evaluate the effects of an altered TGF- β pathway on the stem and progenitor cell populations in the retina, a short overview about this pathway and its functions are given in the following.

1.6.1 Functions of the TGF- β pathway

Ligands of the TGF- β pathway have multiple and sometimes opposite effects on cells. Because of this, TGF- β is often called janus-headed. Its effects depend on the cellular context, the stage of the target cell, the environment in the niche, and the identity and dosage of the ligand [65]. In embryogenesis it modulates proliferation, differentiation, developmental patterning and morphogenesis [66–69]. But it is also responsible for apoptosis, extracellular matrix formation and angiogenesis [70]. Additionally it plays an important role in disease pathogenesis. An inappropriate production of TGF- β for example leads to fibrosis, cancer and disorders relating to cartilage, bone, muscle fat, vessel walls, and the immune system [71–75].

1.6.2 TGF- β : a transforming growth factor

The TGF- β family consists of two subfamilies, one including bone morphogenic proteins (BMPs) and Müllerian inhibitory substance as well as many growth and differentiation factors (GDF), the other including nodal, myostatin, inhibin and TGF- β with its three highly homologous isoforms TGF- β 1, 2 and 3 [70, 76–78]. Each of the genes of the three isoforms encodes an inactive precursor protein.

Of the 391 amino acid precursors, the 112 C-terminal amino acids comprise the mature protein, whereas the N-terminal prodomain is called the latency associated peptide. In its biologically active form, TGF- β is a homo-dimer consisting of two peptides each with a size of 12.5 kDa, linked through disulfide bonds [79, 80]. Secreted TGF- β is composed of active TGF- β , covalently bound to the latency-associated peptide. Both are bound to the latent TGF- β binding protein (LTBP), which is linked to the extracellular matrix, and in this way stores the whole complex in the extracellular space and provides a source of readily available ligand [76, 81]. The latent TGF- β is activated by enzymatic proteolysis, executed by proteins like thrombin, integrin or plasmin [72, 78, 82].

1.6.3 The TGF- β /ALK receptors

The active members of the TGF- β family bind to heterometric transmembrane receptor complexes. The receptors belong to two families of serine/threonine kinases, known as Type I (TGF- β RI or ALK, 53-65 kDa) and Type II receptors (TGF- β RII, 70-95 kDa) [83–85]. As of now five Type II and eight Type I receptors, called activin like kinases (ALKs), are known [86]. The TGF- β receptor Type III (endoglin, betaglycan) is an indirect signaling mediator that influences the affinity of TGF- β RII for TGF- β 2, whereas TGF- β 1 and TGF- β 3 bind directly to TGF- β RII.

1.6.4 The TGF- β signaling

As shown in Figure 1.8 the binding of a ligand to the TGF- β RII leads to the recruitment of a Type I receptor kinase and phosphorylation of its cytoplasmic glycine serine domains. The phosphorylation activates the C-terminal kinase domain of the Type I receptor, which in turn phosphorylates and thereby activates the so called Smad-proteins [70, 76, 85]. These proteins are transcription factors and downstream mediators of the TGF- β pathway. Binding of TGF- β and activin to the receptor leads to phosphorylation of Smad 2,3 at C-terminal serin residues, whereas binding of BMPs leads to the phosphorylation of Smad 1,5,8. All these Smads are so called receptor-regulated- or R-Smads.

After phosphorylation R-Smads form a complex with Smad4, a so called Co-Smad, translocate to the nucleus and act as transcription factors in cooperation with co-activators and co-repressors to modulate specific genes.

The inhibitory Smads Smad6 and Smad7 modulate the TGF- β pathway and the BMP pathway via a negative feedback loop. They bind to the activated Type I receptor in a stable complex and block the phosphorylation of the R-Smads. By recruiting ubiquitin E3 ligases as Smurf 1 and Smurf 2, they also lead to an ubiquitination and degradation of the activated type I receptor. Aside from this, Smad6 and Smad7 also act in the nucleus. They interact with transcriptional

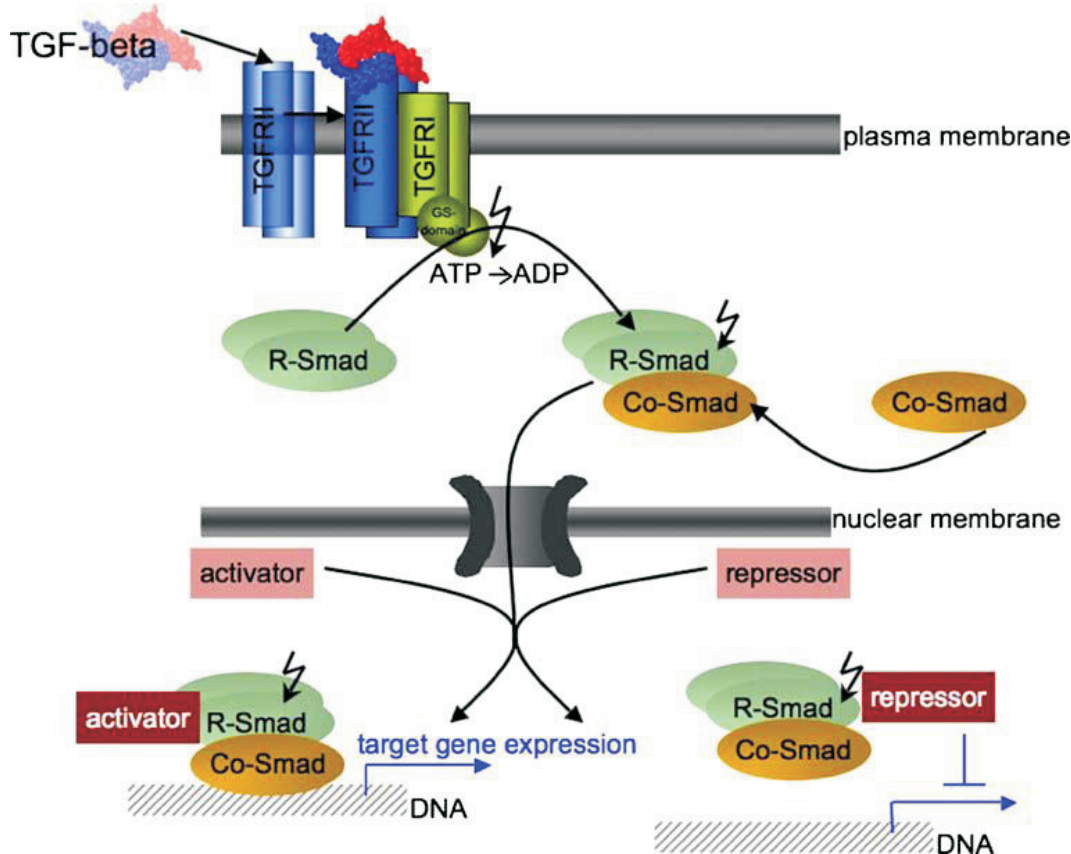


Figure 1.8: Receptor mediated TGF- β signaling: The TGF- β ligand binds to TGF- β RII that complexes with and activates TGF- β RI. This induces the downstream Smad-mediated signal transduction (Aigner and Bogdahn, 2008).

repressors like histone deacetylases and disrupt the formation of TGF- β induced R-Smad DNA complexes [78]. A deregulation of Smad7 is known to cause human diseases such as tissue fibrosis, inflammatory disease or carcinogenesis [78].

A thorough review of this issue can be found in [86].

1.6.5 Structure and regulation of the Smads

All Smads are structurally related proteins that act as transcription factors [84,87]. The Smad proteins possess two domains, Mad homology (MH) domain 1 and 2.

The MH1 domain is located on the amino terminus. It is responsible for the protein DNA interaction. The MH2 domain sits at the carboxy terminus and is responsible for the protein-protein interaction [88].

As the effector proteins of the TGF- β pathway, Smads are closely controlled by ubiquitination [89,90], changes in dynamics of cytoplasmic shuttling of Smads [91], and posttranscriptional modification like acetylation or phosphorylation [92,93].

1.6.6 TGF- β in embryonic and neural stem cells

Significant for our hypothesis is that the TGF- β pathway plays a major role in the self renewal of both human and mouse embryonic stem cells [94].

For example a dramatic decrease of proliferation in cultured mouse ES cells could be seen, when SB431542, an inhibitor of the type I receptor kinases, and therefore of the TGF- β signaling, was applied. The pluripotency of the cells was not influenced by the inhibitor. This suggests that activin, nodal and/or TGF- β signaling is indispensable for the proliferation of most embryonic stem cells [94].

TGF- β was also shown to have an effect on the differentiation of stem cells: TGF- β , activin or nodal signaling were observed in undifferentiated human embryonic stem cells and decreased upon early differentiation [95]. An inhibition of the TGF- β /activin/nodal signaling by SB431542 resulted in decreased expression of markers of undifferentiated cells [96–98]. This suggests that the TGF- β signaling keeps the cells from differentiating.

For neural stem cells TGF- β is important in maintenance and growth. Ablation of TGF- β receptor II gene in the mid/hind brain enhanced self renewal but not multipotency of stem cells, resulting in an enlargement of the mid brain [99] and Wachs et al. could show that in adult neural stem and progenitor cultures, as well as after cerebroventricular infusion, TGF- β 1 induced a long lasting inhibition of proliferation and a reduction of neurogenesis [100].

In vitro TGF- β 1 specifically arrested neural stem and progenitor cells in the G0/1 phase, but did not affect the self renewal capacity or the differentiation of the cells [70, 100].

Additionally TGF- β determines the fate of stem cells. The inhibition of TGF- β signaling directs commitment of ES cells to neuroectoderm lineages, resulting in the formation of embryonic neural stem cells [101].

1.6.7 TGF- β in the retina and in Müller glia

The TGF- β signaling is also an essential pathway in the retina. For example, TGF- β receptor I and II are expressed in the rodent retina and are located in the Nestin positive cells in early development. In later development, they are found in GLAST positive Müller glia. The most highly expressed ligand in the retina is TGF- β 2, which is expressed in inner retinal neurons [102].

Human Müller glia cells also show the expression of transcripts of TGF- β Type I and Type II receptors and of TGF- β 1 and 2 [103].

Not much further is known about the effect of the TGF- β pathway on Müller glia cells as progenitor cell population in the retina. To test the effect of TGF- β on Müller glia proliferation, Close et al. cultured retinal progenitors or Müller glia and added dissociated retinal neurons from older rats. This inhibited the proliferation of the progenitor cells and the Müller glia. In the presence of the inhibitor TGFbetaRII-Fc, proliferation was restored [102]. This points to an inhibitory effect of TGF- β on the proliferation of cultured Müller glia cells. Close et al. also showed that the injection of a TGF- β inhibitor into the eye at postnatal day 5.5 increased the proliferation in the central retina, and when co-injected with EGF at P10 stimulated the Müller glia. They conclude that retinal neurons produce a cytostatic signal that maintains mitotic quiescence in the postnatal retina [102].

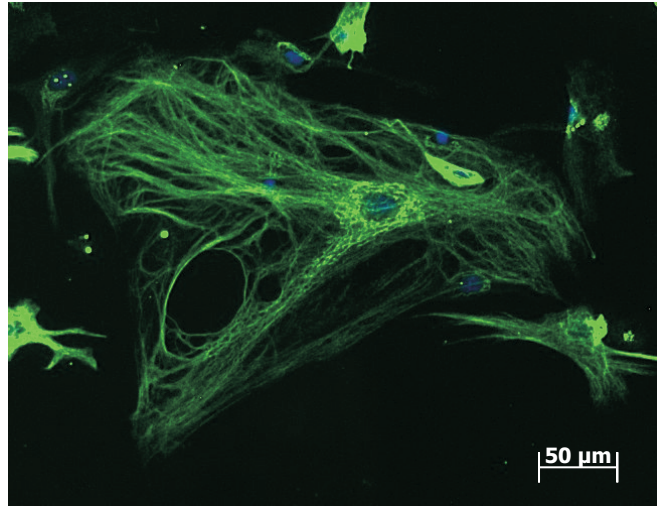


Figure 1.9: *Nestin filaments (green) in a cultured aged Müller glia cell.*

1.7 Nestin

As an important marker for stem and progenitor cells Nestin is often used in studies of regeneration. As the alteration of the TGF- β pathway influenced the Nestin expression in our studies, a short introduction to this interesting protein will be given in the following.

1.7.1 Nestin as a cytoskeletal protein

The cytoskeleton in an eukaryotic cell consists of actin filaments, microtubuli and intermediate filaments (IF).

Nestin is a member of a large family of more than 50 such intermediate filament proteins. These proteins belong to 6 classes, see Table 1.1 that divide them into acidic and basic keratins, lamins, neurofilaments, vimentin like proteins and Nestin. The structure of intermediate filaments, built by Nestin, can be seen in Figure 1.9 where a micrograph of the Nestin filaments in a cultured aged Müller glia cell is shown.

During the early stages of development Nestin is expressed in dividing cells of the central nervous system (CNS), the peripheral nervous system (PNS) and in myogenic tissues. When cells are differentiating, Nestin expression is downregulated, often combined with an upregulation of cell specific intermediate filaments like Glial fibrillary acidic protein (GFAP) in astrocytes, or alpha-internexin and neurofilaments in neurons [104].

Interestingly, for an intermediate filament, Nestin can not polymerize by itself. It prefers to interact with other intermediate filament proteins like vimentin or alpha internexin [105]. This inability to polymerize is due to a very short N-terminal 'head' domain, which in other IF proteins is essential for the assembly of filaments. The process of assembly and disassembly is closely regulated along with the cell cycle by the phosphorylation of Nestin [106,107]. The phosphorylation is placed by the cdc2 kinase which along with Cyclin B constitutes the MPF complex (maturation/M-phase promoting factor) [108].

Type	group	example
Type I and Type II	acidic and basic keratins	epithelial keratins
Type III	vimentin like proteins	GFAP, desmin, vimentin
Type IV	neuronal intermediate filaments	neurofilaments, alpha internexin
Type V	nuclear lamins	lamins
Type VI	Nestin	Nestin

Table 1.1: *Types of intermediate filaments.*

1.7.2 Nestin: a marker for neural stem cells

Nestin is widely used as a marker for neural stem/progenitor cells. There are several findings leading to this.

1. Nestin positive cells are observed in nervous tissue during ontogenesis [109] and most Nestin positive cells in early development are stem/progenitor cells engaged in active proliferation [104].
2. Nestin is expressed by neuronal [110] and glial [111] cells as well as by their common precursors [112–114].
3. Various forms of damage in the brain are followed by the appearance of, supposedly new, Nestin positive cells [115–118].
4. Stem cells that are transplanted into the nervous system start to express Nestin [116, 119].

1.7.3 Nestin and its role in proliferation and differentiation

Taking a closer look, Nestin appears to have more functions in the retina than just building the cytoskeleton. Aside from stabilizing cell structure as a cytoplasmic protein, Nestin is assumed to be involved in the asymmetric distribution of material like cytoskeletal proteins or cellular factors in dividing stem cells and in cytoplasmic trafficking [120], but despite many attempts being made, the in vivo physiological function of these proteins is widely unknown.

However, there is evidence that Nestin plays an important role in cell proliferation, survival and renewal. It is for example often found in tumors of the nervous system, like neuroblastomas [121] or gliomas [122]. Additionally a knock-down in vitro reduces cell growth in cultured neuroblastoma cells and astrocytoma cells [123, 124].

It also appears to play an important role in proper stem cell renewal of neural stem cells [125]. A knockout of Nestin in mice for example is lethal in the embryonic stage, and leads to the development of fewer neural stem cells in the neural tube. Surprisingly this role in self renewal is not coupled to its structural involvement in the cytoskeleton [125]. There are ideas how Nestin could be able to modulate the cell cycle, without necessarily being bound to the cytoskeleton: Nestin is known to constitute a dynamic scaffold for the Cdk5 signaling complex [107], a complex responsible for the withdrawal from the cell cycle. In myoblasts it could be shown that Nestin, interacting with the Cdk5/p35 complex

as a scaffold protein [126], has the ability to halt the differentiation of myoblasts *in vitro* when it is overexpressed. All in all the role of Nestin in controlling the behavior of stem cells remains to be clarified.

1.8 Aims of my work

The retina is often subject to degenerative diseases like Retinitis pigmentosa, AMD or glaucoma, leading to cell loss and severe visual impairment. Unlike fish or urodeles, the adult human retina has no regenerative capacities to compensate this loss. The control mechanisms of proliferation and regeneration in the retina are still only poorly understood. A better knowledge of the underlying signaling pathways would provide the basis for triggering regeneration in a lesioned eye, and to replacing lost cells by the body's own stem/progenitor cells.

One pathway involved in the control of progenitor populations is the TGF- β pathway. It plays a major role in controlling proliferation and neurogenesis in the brain. Based on this fact we state the hypothesis, that the TGF- β pathway may be involved in the control of proliferation and differentiation of the progenitor cells of the retina, especially of Müller glia cells, which are part of the stem cells in fish and birds.

Concordingly the aim of our work is to investigate the influence of the TGF- β pathway on the proliferation and differentiation in the developing and lesioned adult retina. To demonstrate effects of an alternated TGF- β pathway on the morphology of the retina and the proliferation and activation behavior of the progenitor cells, we use mice with a deficiency in Smad7, an inhibitor of the TGF- β pathway, and in the TGF- β receptor II. Additionally, with the help of NMDA lesions we want to examine the effect of the TGF- β pathway on Müller glia in case of a lesion in an adult animal.

Chapter 2

Materials and Methods

2.1 Materials

2.1.1 Chemicals and reagents

Chemical	Company
1,4-p-phenyldiamin	Sigma-Aldrich, Taufkirchen
2-mercaptoethanol	Roth, Karlsruhe
10x polymerase chain reaction (PCR)-buffer	Quiagen, Hilden
agarose	Biozym Scientific , Oldendorf
albumin fraction V bovine serum albumin (BSA)	Roth, Karlsruhe
ammonium peroxodisulfate (APS) 10% weight per volume (w/v)	Roth, Karlsruhe
Ampicillin	Serva, Heidelberg
bromophenol blue	Sigma-Aldrich, Taufkirchen
cacodylic acid sodium salt	Merck, Darmstadt
casyton	Roche/Innovatis, Bielefeld
CDP-Star	Roche, Mannheim
chloramphenicol	Roth, Karlsruhe
chloroform	Roth, Karlsruhe
Coomassie [®] BrillantBlueR-250	Sigma-Aldrich, Taufkirchen
corn oil	Sigma-Aldrich, Taufkirchen
disodium hydrogen phosphate dihydrate	Merck, Darmstadt
dimethyl sulfoxide (DMSO)	Roth, Karlsruhe
2'-deoxyribonucleotide- 5'-triphosphate (dNTP)	Bioline, Luckenwalde
sodium dodecyl sulfate (SDS)	Serva, Heidelberg
Dulbecco's modified eagle medium	PAA, Pasching, AT
epon	Serva, Heidelberg
glacial acetic acid	Merck, Darmstadt
ethanol, absolute	Roth, Karlsruhe

Chemical	Company
ethidium bromide	Serva, Heidelberg
fetal calf serum (FCS)	Biochrom AG, Berlin
fluorescein	Quiagen, Hilden
fluorescent mounting medium	DakoCytomation, Hamburg
formaldehyde	Roth, Karlsruhe
glutaraldehyde	Serva, Heidelberg
glycerin	Roth, Karlsruhe
glycine	Merck, Darmstadt
Immobilon TM western HRP-substrate	Millipore Corp., Billerica, USA
isopropanol	Roth, Karlsruhe
potassium dihydrogen phosphate	Roth, Karlsruhe
potassium ferricyanide (III)	Merck, Darmstadt
potassium ferrocyanide (II), trihydrate	Merck, Darmstadt
kanamycin	Roth, Karlsruhe
ketamine	Wirtschaftsgenossenschaft dt. Tierärzte (WDT), Garbsen
magnesium chloride (25mM)	Quiagen, Hilden
methanol	Merck, Darmstadt
skimmed milk powder	Roth, Karlsruhe
methylene blue	Roth, Karlsruhe
TEMED	
N,N,N',N',-tetramethylethylenediamine	Roth, Karlsruhe
sodium chloride	Roth, Karlsruhe
Na ₂ HPO ₄ x H ₂ O	Roth, Karlsruhe
sodium hydrogen phosphate monohydrate	Merck, Darmstadt
paraformaldehyde (PFA)	Sigma-Aldrich, Taufkirchen
phosphate buffered saline (PBS) 1x	PAA, Pasching, AT
Peqgold TriFast [®] -reagent	PeqLab, Erlangen
Penicillin-Streptomycin	PAA, Pasching, AT
protease-inhibitor-mix M	Serva, Heidelberg
proteinase K	Roth, Karlsruhe
Rotiphorese [®] Gel 30 (30 % acrylamide with 0.8 % Bi-sacrylamide 5:1)	Roth, Karlsruhe
hydrochloric acid 37 % (HCl)	Merck, Darmstadt
SYBR-Green I	Quiagen, Hilden
tergitol	Sigma-Aldrich, Taufkirchen
tris-(hydroxymethyl)-aminoethan (Tris) ultrapure, MB Grade	Usb Corp., Cleveland, USA
Tris/HCl	Roth, Karlsruhe
Trypsin/EDTA, 0.05 %	Invitrogen, Karlsruhe
Triton X-100	Sigma-Aldrich, Taufkirchen
Tween 20	Roth, Karlsruhe
Vectashield mounting medium for fluorescence with 4',6-diamidino-2-phenylindol (DAPI)	Vector Laboratories, Burlingame, USA

Chemical	Company
Water Rotisolv (RNase-free)	Roth, Karlsruhe
Xylazin	Serumwerk, Bernburg

Table 2.1: *Laboratory chemicals.*

2.1.2 Laboratory Consumables

Item	Company
3MM Whatman paper	Neolab, Heidelberg
96-well plates	Nunc, Roskilde, DK
adhesive PCR film	Peqlab GmbH, Erlangen
Biosphere filter tips	Sarstedt, Nümbrecht
CellScraper	Sarstedt, Nümbrecht
EasyFlasks Nunclon™ T25, T75	Nunc, Roskilde, DK
glass pipettes	Brand, Wertheim
glass ware	Schott, Roth, VWR
injection needles	VWR International GmbH, Darmstadt
multidishes Nuclon™ 6 well	Nunc, Roskilde, DK
micro test tubes 0.5 ml, 1.5 ml, 2 ml	Roth, Karlsruhe
nitril gloves	VWR International GmbH, Darmstadt
Omnifix sterile syringes	B. Braun, Wertheim
PCR plates, 96 well iCycler IQ	Biorad, Munich
pipette tips	Sarstedt, Nümbrecht
reaction tubes 15 ml, 50 ml	Sarstedt, Nümbrecht
Rotiprotect latex gloves	Roth, Karlsruhe
PVDF western blot membrane	Roche, Mannheim
Rotilabo 0.22 μm syringe filter	Roth, Karlsruhe
serological pipettes	Sarstedt, Nümbrecht
superfrost slides	Menzel-Gläser, Braunschweig
disposal bags for autoclavation	Sarstedt, Nümbrecht

Table 2.2: *Laboratory consumables.*

2.1.3 Laboratory Instruments

Equipment	Company
Aida Advanced Image Data Analyzer 4.06	Raytest, Straubenhardt
Axio Imager Z1	Zeiss, Göttingen
Axiovert 40 CFL	Zeiss, Göttingen
BioPhotometer	Eppendorf, Hamburg
centrifuges 5415D, 5415R, 5804R, 5810R	Eppendorf, Hamburg
Casy TT cell counting device	Innovatis, Reutlingen
Embedding station HMP 110 (Paraffin)	Microm, Waldorf
Hera Cell 150 incubator	Heraeus, Hanau
Hera Safe clean bench	Heraeus, Hanau
Inolab pH-meter	WTW GmbH, Weilheim
Inova 4200 shaker	New Brunswick, New Jersey, USA
IQ5 Multicolor Real-time PCR Detection System + iCycler	BioRad, Munich
Kern PJJ 2100-2M analytical balance	Kern & Sohn GmbH, Balingen-Frommern
LAS 3000 Intelligent dark box	Fujifilm, Düsseldorf
Mastercycler gradient	Eppendorf, Hamburg Wertheim
Mettler AE 163 precision scale balance	Mettler Toledo, Giessen
Microm HM 500 OM cryostat	Microm International, Walldorf
MilliQ Plus PF purification system	Millipore Corp., USA
Model 45-101-i class II electrophoresis system	Peqlab GmbH, Erlangen
NanoDrop-1000 spectrophotometer	Peqlab GmbH, Erlangen
Pipetman pipette	Gilson, Middleton, USA
Polymax 1040 shaker	Heidolph, Kelheim
Power Shot G5 digital camera	Canon, Krefeld
Power Supply	Consort, Turnhout, BE
Research pipettes	Eppendorf, Hamburg
Semidry electrophoretic transfer cell	Peqlab GmbH, Erlangen
Serva-E 25 pump	Serva, Heidelberg
Sunrise-Basic enzyme linked immunosorbent assay (ELISA)-Reader	Tecan Austria GmbH, Grodig, AT
Supercut 2050 microtome	Reihert-Jung, Kirchseeon
Systec V75 autoclave	Systec GmbH, Wettenburg
Thermomixer compact	Eppendorf, Hamburg
Vortex Genie 2	Scientific Industries Inc, New York USA
water bath	Memmert, Schwabach

Table 2.3: *Laboratory equipment.*

2.1.4 DNA and protein ladders

Item	Company
GeneRuler 100 bp ladder	Fermentas, St. Leon-Rot
1 kb Ladder	New England Biolabs, Frankfurt
PageRuler TM Prestained Protein Ladder	Fermentas, St. Leon-Rot

Table 2.4: *Protein and DNA - ladders.*

2.1.5 Reaction kits

Kit	Company
Cell Proliferation ELISA; BRDU (colorimetric)	Roche applied science
iScript TM cDNA synthesis kit	BioRad, Munich
DeadEnd TM Fluorometric TUNEL System	Promega

Table 2.5: *Reaction kits.*

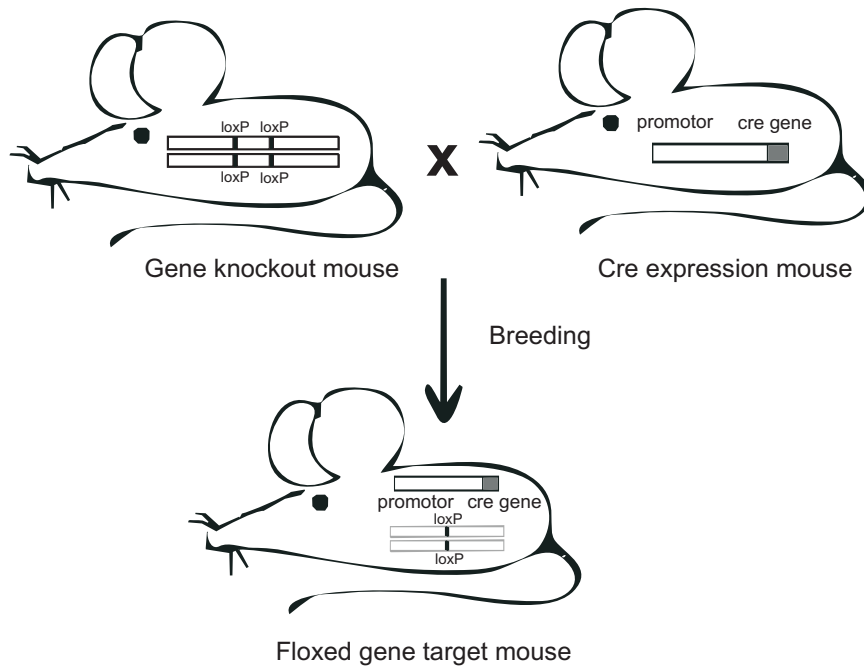


Figure 2.1: Schematic drawing of the function of the Cre/loxP System (adapted from [128]).

2.2 Animal models

2.2.1 Animal housing and maintenance

All animals were treated according to the 'ARVO Statement for the Use of Animals in Ophthalmic and Vision Research'. They were kept at a constant temperature of $23^{\circ}\text{C} \pm 2^{\circ}\text{C}$, a humidity of $55\% \pm 5\%$ and were allowed food (standard laboratory pellets) and water ad libitum. The day-night rhythm was kept at 12/12-hours.

2.2.2 Wistar rats

For primary Müller glia cell culture 8-12 day old Wistar rats were used.

2.2.3 The Cre/loxP recombination system

To achieve the heterozygous deletions needed to create Smad7 and TGF β RII deficient mice, the Cre-loxP system was used [127]. This system uses two components, see Fig. 2.1: A Cre recombinase that carries out a site specific recombination event, and the loxP recognition sites of this enzyme. The use of certain promoters for the Cre recombinase allows for tissue specific or inducible removal of the sequence flanked by the loxP sites. With mouse lines carrying a Cre recombinase and others carrying different genes flanked with loxP sites, genes and Cre recombinases can be combined freely by breeding.

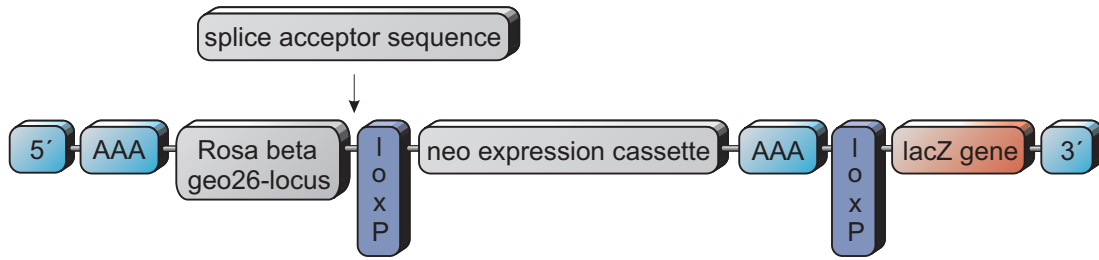


Figure 2.2: Schematic drawing of the *Rosa LacZ* mouse construct.

2.2.4 EIIa Cre mice

To achieve the deletion of the floxed sequences in *Smad7^{fl/fl}* and in *TGF- β RII^{fl/fl}* mice, EIIa Cre mice were used. This mouse line carries the Cre recombinase under the control of the adenovirus EIIa Cre promoter which targets the expression of the Cre in the early embryo. It was created by Heiner Westphal [129].

2.2.5 Rosa26 LacZ Reporter mice

This reporter mouse strain, purchased from Jackson labs, expresses β -Galactosidase in cells where a Cre recombinase is activated. The construct, see Fig. 2.2, contains a Stop sequence flanked by loxP sites. When this sequence is removed by an active Cre recombinase, β -Galactosidase is expressed and can be detected by a staining with x-gal in cells and tissue.

2.2.6 CAG Cre ERT - Tamoxifen inducible mice for the breeding of a TGF- β full knockout

The CAG Cre ERT mice have a Tamoxifen-inducible Cre-mediated recombination system. The Cre recombinase is expressed under the control of the CAG* promoter [130], which leads to a ubiquitous Cre expression in case of Tamoxifen induction. This is done by using a fusion product of the Cre recombinase and a mutant form of the mouse estrogen receptor. This receptor does not bind estrogen in physiological conditions but the synthetic ligand 4-hydroxytamoxifen. Before exposure to Tamoxifen the Cre/Esr1 fusion protein is restricted to the cytoplasm and can only enter the nucleus and induce the recombination when Tamoxifen is present. In this work the induction in the retina is achieved by using Tamoxifen eye drops.

Induction of Cre expression by Tamoxifen eye drops This technique was established by Sarah Leimbeck and Barbara Braunger (unpublished work). They could show that the induction of CAG Cre mice with Tamoxifen eye drops, leads to an activation of the Cre recombinase in all structures of the eye, by using the *Rosa LacZ* reporter mouse. The blue *LacZ* staining of an Tamoxifen treated eye is shown in Figure 2.3. For the induction of the Cre recombinase Tamoxifen is dissolved in corn oil in a concentration of 5 mg/ml. The mice are given the solution as eye drops for 5 days, three times a day, using 10 μ l for each eye. Figure 2.3 B shows

*cytomegalovirus immediate early enhancer-chicken beta-actin hybrid

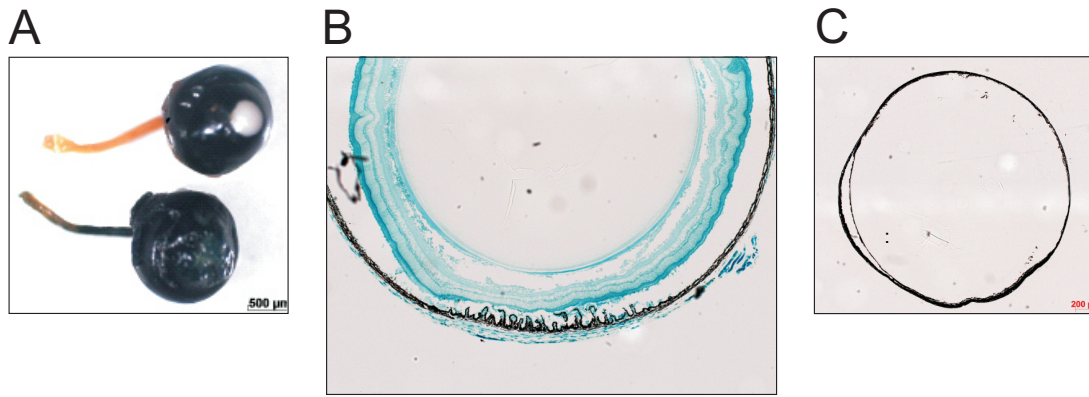


Figure 2.3: The induction with Tamoxifen eye drops leads to an expression of Cre recombinase in all structures of the eye. (A) The photo shows eyes of a CAG Cre positive and a Cre negative animal after LacZ staining. In the Cre positive eye, the lens, and even the optic nerve are LacZ positive, whereas the Cre negative control eye is unstained. (B) Section of a CAG Cre positive eye after Tamoxifen induction. Every cell in the retina of CAG Cre positive animals is LacZ positive after induction with Tamoxifen, the CAG Cre negative control can be seen in C (pictures by B. Braunger and S. Leimbeck).

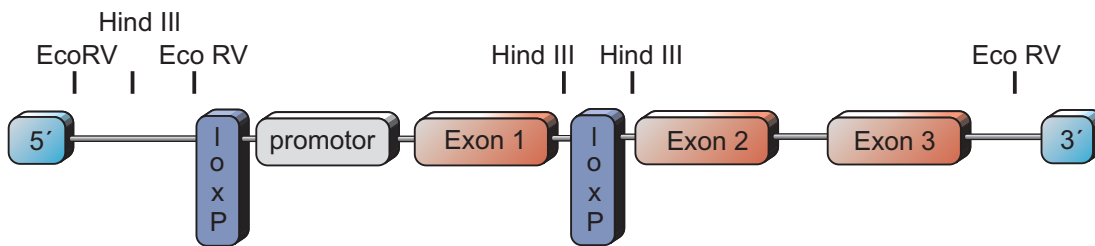


Figure 2.4: Schematic drawing of the $Smad7^{fl/fl}$ mouse construct.

that the induction with Tamoxifen eye drops leads to an ubiquitous Cre expression in the eye, that can be seen by the blue staining caused by the β -Galactosidase expression.

2.2.7 $Smad7^{fl/fl}$ mice

The $Smad7^{fl/fl}$ mouse strain was generated by Ingo Kleiter et al. [131]. In these mice the promoter region and exon I are flanked by loxP sites. Figure 2.4 shows a schematic drawing of the construct.

2.2.8 $TGF-\beta$ RII $^{fl/fl}$ mice

In the $TGF-\beta$ RII $^{fl/fl}$ mice, exon 2 of the $TGF-\beta$ type 2 receptor gene was flanked by loxP sites, see Fig. 2.5. These mice were created by the group of Harold L. Moses [132].

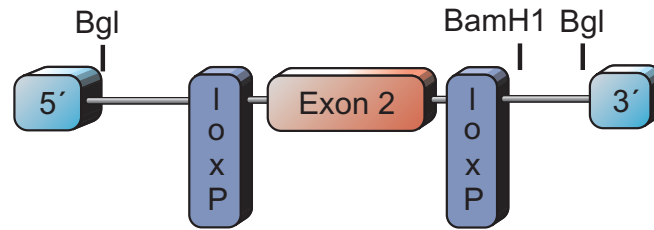


Figure 2.5: Schematic drawing of the $TGF-\beta$ $RII^{fl/fl}$ mouse construct.

2.2.9 β -B1 CTGF overexpressing mouse strains

These mouse strains, cloned by Junglas et al. [133] express CTGF (Connective Tissue Growth factor) in the fiber cells of the lens and secrete it into the aqueous humour. Three different strains were used for this work: Strain 1 with a low CTGF expression, strain 5 with a moderate CTGF expression and strain 6 with a high expression. To achieve wildtype littermate controls for the experiments, heterozygous mice are crossed with FVBN wildtype mice.

2.2.10 Breeding of $Smad7^{fl/-}$ and $TGF-\beta$ $RII^{fl/-}$ mice

Breeding of $Smad7^{fl/-}$ mice

To analyze the influence of an increased $TGF-\beta$ signaling, $Smad7$ deficient mice with a heterozygous deletion of the gene were used, as $Smad7$ is an inhibitor of the $TGF-\beta$ pathway. It was not possible to work with a mouse model with a homozygous deletion of $Smad7$ in this case, because this proved to be lethal at a late embryonic stage. Littermates without the deletion of $Smad7$, but homozygous for floxites served as a control.

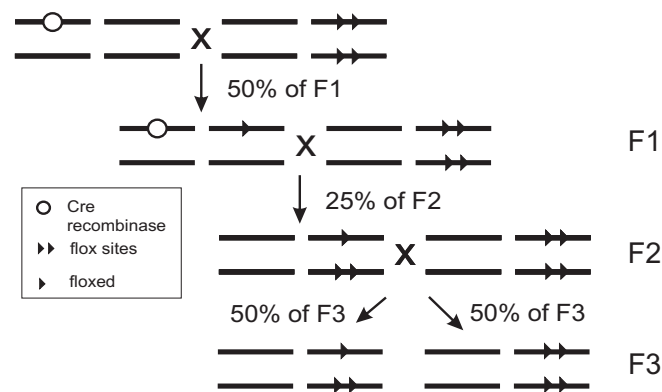


Figure 2.6: Breeding procedure for mice with a heterozygous deletion of $Smad7$ or $TGF-\beta$ RII ; The $EIIa$ Cre recombinase was eliminated during breeding. The heterozygous deletion is stably inherited.

To breed the animals, $Smad7^{fl/fl}$ mice were crossed with $EIIa$ -Cre mice, expressing Cre recombinase ubiquitously under the control of the $EIIa$ -Cre promoter. Figure 2.6 shows the detailed breeding procedure. In the F1 generation, the progeny was heterozygous for the floxed allele and about half of the progeny

was carrying the Cre recombinase. Because of the early activity of the recombinase, this leads to an ubiquitous heterozygous deletion of the floxed allele, including the germline cells of the mice. In this way, the deletion is inherited to the next generation. By crossing the mice with the heterozygous deletion with homozygous $Smad7^{fl/fl}$ mice it was possible to get rid of the Cre recombinase in the F2 generation. Subsequently mice without Cre recombinase and with a heterozygous deletion of Smad7 were crossed to mice homozygous for $Smad7^{fl/fl}$ in F3 and the following generations. All experiments were done with $Smad7^{fl/-}$ and the $Smad7^{fl/fl}$ littermates as a control. The latter are further referred to as wildtype or wildtype control.

By crossing EIIa Cre animals with the $Smad7^{fl/fl}$ mice, recombination and deletion of the exon I of Smad7 occurred. This deletion could be detected by the deletion PCR established by Ingo Kleiter [131], see section 2.3.6. During breeding, the genetic status was also confirmed by performing PCRs for EIIa Cre recombinase and for the flox sequences. After the initial phase of breeding, the animals did not carry the EIIa Cre recombinase anymore, but inherited the heterozygously deleted sequence.

Breeding of TGF- β RII $^{fl/-}$ mice

TGF- β RII $^{fl/-}$ mice were used as a model for reduced TGF- β signaling. To create a mouse line, comparable to the $Smad7^{fl/-}$ mice, the breeding was done analogously to that of the Smad7 mice, see above. This breeding lead to a heterozygous deletion of exon II of TGF- β RII. For the experiments, TGF- β RII $^{fl/-}$ mice and their littermates carrying floxsites on both alleles (fl/fl) were used. The latter are called wildtype or wildtype control in the following. For genotyping, the recombination PCR by Chytil et al. was used [132], see section 2.3.6.

2.3 Genotyping

2.3.1 Extraction of genomic DNA from mouse tails

To gain DNA from mouse tails, the mice were anesthetized with isoflurane. About 0.5 cm of the tip of the tail were cut off with a sterile pair of scissors and transferred to a 1.5 ml micro test tube. Proteinase K lysis buffer, shown in table 2.6, was mixed with fresh proteinase K (25 μ l per 1 ml lysis buffer) and 200 μ l of the mixture were added to each tail. The mouse tails were incubated at 55 °C over night in a shaker at about 750 rotations per minute (rpm). To inactivate the enzyme the cups were heated to 95 °C and afterwards centrifuged at 16.000 x g and 4 °C for 10 minutes (min). The supernatant was transferred to a fresh cup. The DNA was stored at -20 °C or directly used for PCR analysis.

2.3.2 DNA precipitation

To precipitate the DNA, mouse tail lysate was mixed with 150 μ l IRN buffer, see Table 2.7 and 375 μ l of pure ethanol. The mixture was kept at -20°C for a minimum of 30 min. After a centrifugation step at 4 °C and 14.000 rpm the supernatant was removed and the pellet was dried for 30 s. The DNA pellet was

Mouse tail lysis buffer	
KCl	50 mM
Tris HCl, pH 8.5	10 mM
MgCl ₂	2 mM
gelatin	0.1 mg/ml
nonidet P-40	0.45 % volume per volume (v/v)
tween 20	0.45 % (v/v)
add proteinase K before use	20 mg/ml

Table 2.6: *Mouse tail lysis buffer.*

solved in 50 μ l H₂O. If the pellet did not solve properly the sample was incubated at 37 °C and 500 rpm in a thermomixer.

IRN buffer	
Tris; 1 M; pH 8.0; 5 ml	50 mM
EDTA; 5 M; 4 ml	20 mM
NaCl; 3 M; 16.6 ml	0.5 M
add H ₂ O ad 100 ml	

Table 2.7: *IRN DNA precipitation buffer.*

2.3.3 PCR - polymerase chain reaction

The polymerase chain reaction is a method developed by K. Mullis [134] to amplify sequences of DNA. In this work the method is used to prove genetic alterations like deletions in knockout mouse models.

2.3.4 Genotyping EIIa Cre mice

To create mice with a heterozygous deletion, Smad7^{fl/fl} respectively TGF- β RII^{fl/fl} mice were bred with EIIa Cre mice. For the genotyping for the Cre recombinase during the breeding, protocols and programs shown in table 2.8 and 'EIIa cre' primers, see table 2.15 were used: The PCR shows a band at 700 bp when the Cre recombinase is present.

2.3.5 Genotyping the Smad7^{fl/fl} and TGF- β RII^{fl/fl} mice

To check for flox sites during breeding the protocols and programs shown in table 2.9 and 2.10 were used. The PCR gives different sized products depending on the presence of flox (fl) sites. For the Smad7 mice the wildtype allele gives a signal at 413 bp, the floxed allele at 568 bp. For the TGF- β mice the band for the wildtype allele has a size of 556 bp, for the floxed allele it appears at 711 bp. The glycerol mix needed for this PCR is shown in Table 2.11. The primers used are: 'TGF β RII^{fl/fl}' and 'Smad7^{fl/fl}', see Table 2.15.

genomic DNA (30 ng/ μ l)	1 μ l			
10x PCR-buffer	1.5 μ l	temperature	duration	
MgCl ₂ (25mM)	0.3 μ l	94 °C	1 min	
dNTPs (10mM)	0.75 μ l	94 °C	30 s	} 37 x
Primer forward (fw) (10 μ M)	0.6 μ l	57.3 °C	30 s	
Primer reverse (rev) (10 μ M)	0.6 μ l	72 °C	1 min	
Taq DNA polymerase	0.4 μ l	72 °C	1 min	
DMSO	0.75 μ l	4 °C	∞	
H ₂ O	9.1 μ l			

Table 2.8: PCR mix and program for *EIIa Cre* product: 700 bp.

genomic DNA (30 ng/ μ l)	1 μ l
10x PCR-buffer	1.5 μ l
MgCl ₂ (25mM)	0.3 μ l
dNTPs (10mM)	0.3 μ l
Primer fw (10 μ M)	0.3 μ l
Primer rev (10 μ M)	0.3 μ l
Taq DNA polymerase	0.3 μ l
5 x glycerol mix	3 μ l
H ₂ O	8 μ l

Table 2.9: PCR mixes for *Smad7 fl/fl*; *TGF- β RII fl/fl*; *Smad7* deletion; *TGF- β* deletion.

temperature	duration		temperature	duration	
95 °C	3 min		95 °C	3 min	
95 °C	45 s	} 35 x	95 °C	30 s	} 35 x
63 °C	30 s		61 °C	45 s	
72 °C	45 s		72 °C	1 min	
72 °C	5 min		72 °C	5 min	
4 °C	∞		4 °C	∞	

Table 2.10: Left: PCR programs for *Smad7^{fl/fl}* (wt: 413 bp fl/fl: 568 bp). Right: PCR programs for *TGF- β RII^{fl/fl}* (wt: 556 bp fl/fl: 711 bp).

5x glycerol mix (PCR)	
Cresol red	1 mM
glycerol	60%
fill with H ₂ O	40%

Table 2.11: 5x glycerol mix.

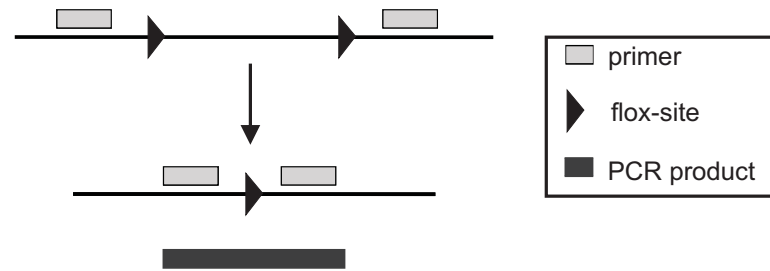


Figure 2.7: : The primers lie flanking the floxed region. The amplicon is only short enough to allow for a product when the region between the flox sites is deleted due to recombination by a Cre recombinase.

temperature	duration		temperature	duration	
95 °C	3 min		94 °C	3 min	
95 °C	15 s	} 37 x	94 °C	20 s	} 35 x
60 °C	45 s		60.5 °C	20 s	
72 °C	30 s		72 °C	1 min	
72 °C	5 min		72 °C	5 min	
4 °C	∞		4 °C	∞	

Table 2.12: PCR program for *Smad7* deletion product, 286 bp (left); PCR program for *TGF- β RII* deletion, 610 bp (right).

2.3.6 Genotyping the *Smad7*^{fl/-} and *TGF- β RII*^{fl/-} mice by deletion PCR

To detect the recombination in the *Smad7*^{fl/fl} mice and the *TGF- β RII*^{fl/fl} mice after crossing them to mice carrying a Cre recombinase, a deletion respectively recombination PCR was used. For the *Smad7* mice this PCR was established by Ingo Kleiter et al. [131] for the *TGF- β RII* mice by Chytil et al. [132]. The deletion PCRs for *Smad7* deficient mice and *TGF- β RII* deficient mice use the same principle. The primers are chosen flanking the region that is deleted by the recombination, when the Cre recombinase is active. As primers 'Smad7 recombinant' and 'TGF β RII recombinant' forward and reverse, see Table 2.15 were used. Only if the recombination has occurred, the size of the product that has to be amplified is short enough for the chosen elongation time of the PCR program, see Figure 2.7. For the deletion PCR the same PCR mix as for the flox PCRs was used, see section 2.3.5. The PCR program is shown in Table 2.12.

2.3.7 Genotyping Rosa LacZ mice

To genotype the Rosa26 LacZ reporter mice the protocol and program shown in Table 2.13 and the Rosa26 LacZ primer shown in Table 2.15 were used. The PCR results in a 315 bp product for transgenic mice. For the LacZ PCR Bioline Taq polymerase and Bioline PCR 10x buffer was used.

genomic DNA (30 ng/ μ l)	2 μ l	temperature	duration	
10x PCR-buffer	2.5 μ l	94 °C	3 min	
MgCl ₂ (25mM)	1.2 μ l	94 °C	30 s	} 34 x
dNTPs (10mM)	0.5 μ l	60 °C	30 s	
Primer fw (10 μ M)	0.5 μ l	72 °C	35 s	
Primer rev (10 μ M)	0.5 μ l	72 °C	5 min	
Taq DNA polymerase	0.3 μ l	10 °C	∞	
H ₂ O	17.5 μ l			

Table 2.13: PCR mix and cycler program for *Rosa LacZ*.

genomic DNA (500 ng; 1:20)	2 μ l	temperature	duration	
10x PCR-buffer	1.5 μ l	96 °C	2 min	
MgCl ₂ (25mM)	0.3 μ l	94 °C	30 s	} 37 x
dNTPs (10mM)	0.3 μ l	53 °C	45 s	
Primer fw (10 μ M)	0.3 μ l	72 °C	1 min	
Primer rev (10 μ M)	0.3 μ l	72 °C	5 min	
Taq DNA polymerase	0.15 μ l	10 °C	∞	
glycerol mix 5x	3.0 μ l			
H ₂ O	7.15 μ l			

Table 2.14: PCR mix and Cycler program for SV 40 (*CTGF* mice), the product size for transgenic animals is 300 bp.

2.3.8 Genotyping β -B1 CTGF mice

The SV40 primers used for genotyping the CTGF mice recognize the SV40 sequence which is inserted into the sequence and derived from Simian virus 40, a polyomavirus. Transgenic animals show a PCR product with a size of 300 bp. The PCR mix and cycler program used are shown in Table 2.14. To specify the sequence that is amplified, the oligonucleotide primer sequences 'SV 40 fw' and 'rev' shown in Table 2.15 were used.

2.3.9 Agarose gel electrophoresis

Following the PCR analysis, agarose gel electrophoresis was used to analyze the PCR products. In this method an electric field drags the DNA fragments through a molecular net, built by the agarose, to separate the DNA fragments according to their size. The gel contains ethidiumbromide which is a Phenanthridin-dye that intercalates in the DNA and fluoresces at 302 nm after excitation. Due to this the DNA is visible in the gel under UV light.

For the gel mixture 1 g agarose was solved in 100 ml TBE buffer by heating the solution in a microwave oven. After the solution was lukewarm 3 μ l of ethidium bromide were added, to an end concentration of 30 ng/ml and the gel was poured. PCR samples that did not contain glycerol mix were mixed with loading buffer, see table 2.16. Subsequently the gel was put into a buffer chamber filled with 1x TBE, see Table 2.16, and was loaded with 15 μ l of every sample. To allow a correct calculation of the PCR product sizes, a 100 bp DNA standard (NEB) was

name	sequence
Smad7 recombinant fw	5'tgcagacccggaaattagac 3'
Smad7 recombinant rev	5' ttgatcaccatgccaacta 3'
TGF β RII recombinant fw	5'taaacaaggtccggagccca 3'
TGF β RII recombinant rev	5'agagtgaagccgtggtaggtgagcttg 3'
EIIa Cre fw	5'atggtgtttgagtggttatg 3'
EIIa Cre rev	5'attgccctgtttcactatc 3'
TGF β RII ^{fl/fl} fw	5' gcaggcatcaggacctcagtttgatcc 3'
TGF β RII ^{fl/fl} rev	5' agagtgaagccgtggtaggtgagcttg 3'
Smad7 ^{fl/fl} fw	5'gtcaggttgatcaccatgcc 3'
Smad7 ^{fl/fl} rev	5' gactgcctggagaagtgtgtc 3'
SV 40 fw	5'gtgaaggaaccttacttctgtggtg 3'
SV 40 rev	5'gtccttggggctcttctacctttctc 3'
Rosa26 LacZ fw	5' atcctctgcatggtcaggtc 3'
Rosa26 LacZ rev	5'cgtggcctgattcattcc 3'

Table 2.15: *Genotyping primers.*

loading buffer		TBE 10x	
bromophenol blue	0.25 % (w/v)	TRIS	108 g
xylene cyanol FF	0.25 % (w/v)	borate	55 g
ficoll	15 % (w/v)	EDTA(0.5 M), pH 8	40 ml
		solve in H ₂ O distilled (dest.)	ad 1 l

Table 2.16: *Buffers for gel electrophoresis.*

loaded at one position in each row. Subsequently the gel was run at 120 V for 45 min and the detection was done by the use of an UV lamp.

2.4 Histology and Immunohistochemistry

2.4.1 Buffers and equipment for histology

Reagents	Company
acetone	Merck, Darmstadt
lead citrate	Merck, Darmstadt
Cacodylic acid sodium salt trihydrate	Merck, Darmstadt
2-Dodecenylsuccinic-acid-anhydride (DDSA)	Merck, Darmstadt
2,4,6-Tri(dimethylaminomethyl) Phenol (DPM-30)	Serva, Heidelberg
epon	Serva, Heidelberg
glutaraldehyde	Serva, Heidelberg
glycidic ether	Merck, Darmstadt
isopropanol	Roth, Karlsruhe
MNA	Carl Roth GmbH, Karlsruhe
osmium tetroxide	Merck, Darmstadt
paraffin	Engelbrecht, München
paraformaldehyde	Merck, Darmstadt
1,4-p-phenylendiamin	Sigma, Taufkirchen
Pioloform	Plano, Marburg
uranyl-acetate	Merck, Darmstadt
embedding station EM TP (Epon)	Leica, Wetzlar
embedding station HMP110 (Paraffin)	Microm, Waldorf
slotgrids	Plano, Marburg
Supercut 2050 (Paraffin)	Reichert-Jung, Kirchseeon
Ultracut E-ultramicrotome (Epon)	Reichert-Jung, Kirchseeon

Table 2.17: Chemicals and equipment for histology.

2.4.2 Tissue preparation

Perfusion To prevent artifacts in some immunostainings a perfusion through the left heart-ventricle was performed. This technique was used primarily for the BRDU immunostainings of adult mice because of artifacts to stained blood vessels. For this purpose a 10 ml syringe with a 23G butterfly needle ECOFLO[®] was used. Prior to perfusion the mice were deeply anesthetized with a mixture of xylazin (6 - 8 mg/kg bodyweight) and ketamin (90 - 120 mg/kg bodyweight) through intraperitoneal injection. For an easy access to the organs the mice's limbs were fixed with needles to a Styrofoam plate. Afterwards the abdomic and thoracic cavity was opened and the heart was exposed. The butterfly needle was inserted into the left ventricle and a cut into the vena jejunales or ileales was performed. Subsequently the animal was slowly perfused with about 8 ml room temperature PBS heparin solution, see table 2.18, until the fluid leaving the mesenterical veins was clear. Afterwards the syringe was changed and the animal was perfused with 8 ml ice-cold 4 % paraformaldehyde (PFA). After the perfusion was complete the eyes were removed and incubated in 4 % PFA for additional 4 h.

Heparin-solution	
PBS	50 ml
Heparin-Natrium 250000 IE	100 μ l

Table 2.18: *PBS heparin solution.*

Eye preparation for embedding and sectioning After an isoflurane anesthesia with isoflurane the mice were killed by cervical dislocation and eyes were enucleated by curved forceps without crushing the optic nerve. To allow the fixation medium to permeate the eye, the cornea was perforated by a small cut. Depending on the use of the material for paraffin-, epon- or cryo embedding, different fixation media were used for incubation.

Buffer I : 0.1 M $\text{Na}_2\text{HPO}_4 \times 2 \text{H}_2\text{O}$	35.6 g in 2 l H_2O
Buffer II : 0.1 M $\text{NaH}_2\text{PO}_4 \times 2 \text{H}_2\text{O}$	13.8 g in 1 l H_2O
phosphate buffer	Buffer I : Buffer II 5:1 pH 7.4
4% Paraformaldehyde fixation solution (4% PFA)	100 ml phosphate buffer 4 g formaldehyde
30% Sucrose solution	150 g sucrose 500 ml phosphate buffer

Table 2.19: *Buffers and solutions used for cryo embedding and immunohistochemistry.*

Cryo embedding and sectioning For cryo embedding, the enucleated eyes were fixated for 4 h in 4 % paraformaldehyde fixation solution (4 % PFA). The exact composition of the buffers used is shown in Table 2.19. Subsequently the eyes were washed 3 times for 5 minutes with phosphate buffer. To avoid cell damage by freezing, the eyes were incubated in sucrose solutions with ascending concentrations (10 %, 20 %, 30 %) each for 4 hours at room temperature or over night at 4 °C. The eyes were embedded in Tissue-Tek[®] and frozen directly on the sample holder in the cryostat to ensure the right adjustment of the sample. Sections, 12 μ m in thickness, were made with the Microm HM 500 OM. To mount the sections SuperFrost[®] slides were used. The sections were used directly for immunohistochemical staining or stored at -20 °C.

Paraffin embedding and sectioning For the paraffin embedding the eyes were fixated for 4 h with 4% PFA and washed 3 times for 5 minutes with phosphate buffer. To embed the tissue into paraffin it had to be dehydrated: The embedding was done by the embedding station HMP110 using the following protocol.

- 70% isopropanol ; 1 h
- 80% isopropanol ; 1 h
- 96% isopropanol ; 1 h

- 96% isopropanol ; 2 h
- 100% isopropanol; 1 h
- 100% isopropanol; 1 h
- 100% isopropanol; 2 h
- 100% xylene ; 1.5 h
- 100% xylene ; 2 h
- paraffin ; 4 h
- paraffin ; 8 h

Sagittal sections approximately 6 μm in thickness were produced using the Supercut 2050-Microtome.

Dewaxing and rehydration To prepare the paraffin sections for staining they were dewaxed and dehydrated as the following protocol shows.

- 2x 100% xylene; 10 min
- 2x 100% isopropanol; 10 min
- 2x 96% isopropanol; 5 min
- 2x 80% isopropanol; 5 min
- 1x 70% isopropanol; 5 min
- H₂O dest.; 5 min

Epon embedding and sectioning To measure retinal thickness and determine the number of axons in the optic nerve, epon semithin sections were used. For epon embedding the eyes had to be fixated for 12 h in EM fixation medium; see Table 2.20. After 4 x 20 min washing steps with cacodylate-buffer the eyes were fixated with 1 % osmium tetroxide. To remove the osmium tetroxide, eyes were washed with cacodylate-buffer and dehydrated using ascending alcohol-concentrations (ethanol 70%, 80%, 90%, 100%). The embedding was done with the help of an embedding station with the following protocol: Ethanol/acetone 1:1; 100 % acetone; epon/acetone 1:2; epon/acetone 2:1; To harden the samples they were incubated for 24 h at 60 °C and for 48 h at 90 °C. Epon itself is a 1:1 mixture of stock solution A and stock solution B containing 2 % DMP-30 as accelerator; see Table 2.20.

2.4.3 Histological stainings

The Richardson staining

Sections for measurement of retinal thickness were stained using the Richardson method [135]. The sections were incubated with Richardson's solution, see Table 2.21, for 15-30 seconds at 60 °C. The solution was removed by a washing step with H₂O dest..

buffer	compounds
cacodylate buffer	20.14 g cacodylic acid 0.5 l H ₂ O dest. pH 7.2
EM fixation medium	2.5 % paraformaldehyde 2.5 % glutaraldehyde in cacodylate buffer
stock solution A	62 ml glycidether 100 ml DDSA
stock solution B	100 ml glycidether 89 ml MNA

Table 2.20: *Buffers and solutions for Epon embedding.*

buffer	compounds
stock solution I	1 % Azur II in 500 ml H ₂ O dest.
stock solution II	1 % Methyleneblue in 500 ml 1 % Borax
Richardson's solution	1:1:2 stock solution I: stock solution II: H ₂ O dest.

Table 2.21: *Solutions for Richardson's staining.*

Paraphenyldiamin staining for axon counting of optic nerves

To stain optic nerves, 500 mg Paraphenyldiamin were dissolved in 50 ml ethanol. Three days at daylight lead to oxidation of the solution causing a brown color. The semithinsections were stained with this solution for 2-3 minutes followed by a washing step with ethanol. The sections were evaluated by light microscopy and the axons were counted manually using Photoshop CS3.

2.4.4 Measurement of retinal thickness

For the measurement of the retinal thickness, 3 week old mice were killed and their eyes were embedded in epon as shown in section 2.4.2. Sagittal sections, 1 μ m in thickness, containing the optic nerve and the papilla were stained with the Richardson method see section 2.4.3. The light microscopic images were used to measure the thickness of the retina with the help of the Axiovision software from Zeiss. For a comparable measurement of all eyes, the length of the retina was measured along the outer nuclear layer (ONL) and each side of the optic nerve was divided into 10 parts of equal length which leads to 9 measurement points along the retina as shown in Figure 2.8. The thickness of the retina at the optic nerve and the ora serrata was assumed to be zero. The measurements of both sides of the retina were averaged. For the detailed measurement of the inner nuclear layer (INL) the inner 10% (close to the optic nerve) of the retina were again divided into 10 parts and the thickness of the INL was measured.

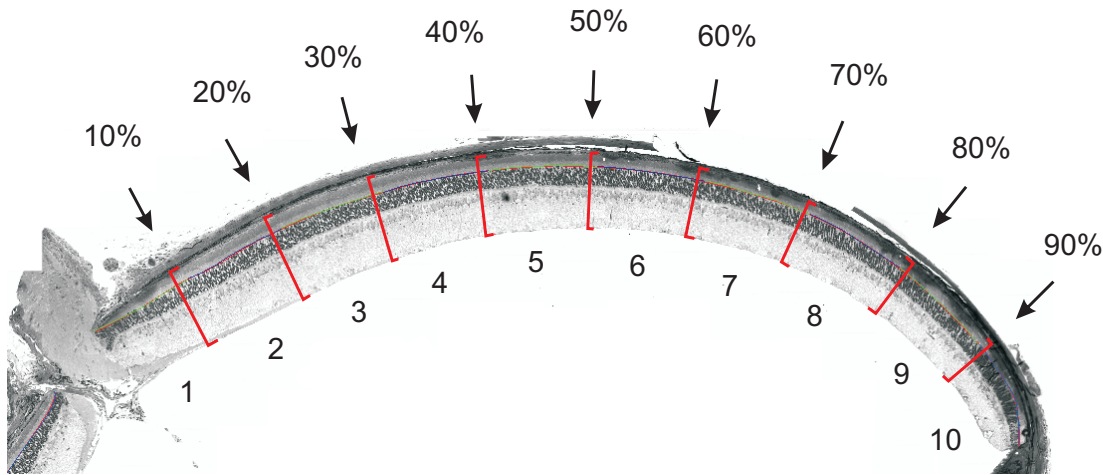


Figure 2.8: Example for a measurement on retinal thickness: For the measurement each side of the retina was divided into 10 parts of equal length, and the retinal thickness was measured for each part from the ganglion cell layer to the apical side of the RPE (red lines). For the measurement the program Axiovision from Zeiss was used.

2.4.5 Determination of axon number in optic nerves

To count the number of axons, mice that were treated with an NMDA injection (see section 2.4.6) in one eye and PBS in the partner eye at the age of 6 weeks were used. Three weeks after the injection the mice were killed, the optic nerves were embedded in epon, see section 2.4.2, and cross sections $1\ \mu\text{m}$ in thickness were made. The sections were stained with a paraphenyldiamin staining, see section 2.4.3. Afterwards microscopic images with 100 x magnification were used to count all axons of each nerve.

2.4.6 Intravitreal injection - the NMDA lesion model

The NMDA (N-methyl-D-aspartate) lesion is a method to damage retinal ganglion cells and cells of the inner nuclear layer. NMDA is a glutamate analogon and as such a synthetic agonist of the NMDA receptor, which is a ligand gated Ca^{2+} channel. In the model of exitotoxic damage, excess glutamate or NMDA binds to the NMDA receptor, triggering calcium influx, organelle stress and activation of pro-apoptotic pathways [136].

Prior to the intravitreal injection the animals were anesthetized with isoflurane. For the injection a 33 gauge (G) needle attached to a Hamilton pipet was used. NMDA ($3\ \mu\text{l}$ 10 mM) or PBS ($3\ \mu\text{l}$) as a control substance were injected into the vitreous body, through the sklera shortly behind the cornea, in the area of the ora serrata. After removing the needle the eyes were treated with an antiseptic substance (isomax-AS).

2.4.7 TUNEL staining

The TUNEL assay - a method to quantify apoptotic cell death The TUNEL method (TdT mediated dUTP-biotin nick end labeling) is a method to label apoptotic cells. The DeadEnd Fluorometric TUNEL system marks the fragmented DNA of

apoptotic cells by incorporating fluorescein-12-dUTP at 3'-OH ends. This is done by the enzyme Terminal Deoxynucleotidyl Transferase. During the experiment the tissue was permeabilized by Triton or Proteinase K and incubated with a mix of the enzyme and fluorescently labeled dUTP. The fluorescent cells can be evaluated and counted directly by fluorescence microscopy [137].

TUNEL - protocol for cryo sections

- Rinse slides three times with phosphate buffer see 2.19, 5 minutes each time
- Immerse slides in 4 % formaldehyde for 25 minutes at 4°C
- Immerse slides in 0.2 % Triton X-100 in phosphate buffer for 5 minutes
- Equilibrate slides with equilibration buffer (from the kit) at room temperature for 5-10 minutes
- Add TdT reaction mix to the slides. Incubate slides for 60 minutes at 37 °C in a humidified chamber; avoid exposure to light from this step forward
- Immerse slides in 2X SSC for 15 minutes
- Immerse slides three times in phosphate buffer, 5 minutes each time
- Mount slides with mounting medium containing dapi
- Detect localized green fluorescence of apoptotic tissue by fluorescence microscopy

Protocol for paraffin sections

- Dewax and rehydrate the slides ignoring the H₂O dest. step at the end; see 2.4.2 (Dewaxing and rehydration)
- Immerse slides in 50% isopropanol for 5 minutes
- Immerse slides in H₂O dest. for 5 minutes
- Immerse slides in 0.85% NaCl for 5 minutes.
- Rinse slides three times with phosphate buffer, 5 minutes each time
- Immerse slides in 4 % formaldehyde for 15 minutes at 4°C
- Rinse slides three times with phosphate buffer, 5 minutes each time
- Add 100 µl of a 20 µg/ml Proteinase K solution. Incubate at room temperature for 8-10 minutes.
- Immerse slides in phosphate buffer for 5 minutes
- Immerse slides in 4 % formaldehyde in PBS for 5 minutes
- Immerse slides in phosphate buffer for 5 minutes
- Equilibrate slides with equilibration buffer at room temperature for 5-10 minutes
- Add TdT reaction mix to the slides. Incubate slides for 60 minutes at 37 °C in a humidified chamber; avoid exposure to light from this step forward
- Immerse slides in 2X SSC for 15 min

- Immerse slides three times in phosphate buffer, 5 minutes each time
- Mount slides with mounting medium containing dapi
- Detect localized green fluorescence of apoptotic tissue by fluorescence microscopy

TUNEL - staining in newborn Smad7^{fl/-} mice The apoptosis rate in young Smad7^{fl/-} animals and their wildtype littermates was determined by carrying out a TUNEL assay on 8 day old mice. The enucleated eyes were embedded in paraffin for a better tissue preservation. After the TUNEL staining, the samples were evaluated with fluorescence microscopy and the TUNEL positive cell were counted on both sides of the optic nerve for every eye and averaged for the analysis.

TUNEL - staining after NMDA injection in Smad7- and TGF- β RII^{fl/-} mice Additionally to the axon count after NMDA injection, TUNEL stainings were made to show the effect of the genetic alterations on the apoptosis after a lesion. For the TUNEL assay 6 week old mice were killed 24 hours after the NMDA injection and the eyes were cryoembedded. For the staining the protocol for TUNEL assays with cryo sections was used, see section 2.4.7. After evaluation under the fluorescence microscope the cells in both halves of the retina were counted and averaged for each eye.

2.4.8 BRDU assays and stainings - methods to quantify cell proliferation

Injection of BRDU for in vivo experiments

Bromodesoxyuridine (BRDU) is a synthetic nucleoside analogon of thymidin. It is widely used to mark proliferating cells *in vivo* and *in vitro*. During the S phase of the cell cycle, cells incorporate the nucleotide analogon into the newly synthesized DNA. Special antibodies are used to detect the nucleoside within the nucleus and mark cells that proliferated since the injection of BRDU.

For *in vivo* experiments BRDU was injected intraperitoneally with a 34 gauge needle in a concentration of 10 mg/ml in PBS for adult animals and a concentration of 2 mg/ml for young mice. Prior to the injection the mice were weighed and 50mg BRDU per kilogram bodyweight was used. The mice were killed at different time points after the injection. The eyes were used for cryo- or paraffin embedding, see section 2.4.2.

BRDU staining for paraffin sections

This is the BRDU protocol for paraffin sections. To apply it for cryo sections, the first three steps have to be skipped. The protocol starts in this case from the washing step before the incubation with 1 M HCl (step 4).

- Immerse slides in aqua dest.
- Immerse slides in 0.05 M Tris HCl for 5 minutes
- Incubate slides with proteinase K (100 μ l in 47 ml 0.05 M Tris HCl) for 5 minutes

- Rinse slides with aqua dest.
- Incubate slides in 1 M HCl for 30 minutes
- Rinse slides with aqua dest.
- Wash slides two times in 0.1 M phosphate buffer; 5 minutes each time
- Incubate slides in 5 % skimmed milk powder in 0.1 M Php for 45 minutes
- Incubate slides with 1:50 BRDU antibody (Invitrogen) in 0.5 % skimmed milk powder over night at 4°C
- Wash slides three times in 0.1 M phosphate buffer; 5 minutes each time
- Incubate slides with anti-mouse Biotin 1:500 for 1 h
- Wash slides three times in 0.1 M phosphate buffer; 5 minutes each time
- Incubate slides with Streptavidin Alexa 488 1:1000 for 1 h
- Wash slides three times in 0.1 M phosphate buffer; 5 minutes each time
- Mount slides with mounting medium containing dapi

BRDU staining in newborn *Smad7^{fl/-}* mice The BRDU staining was used to evaluate the amount of proliferation in 4 day old *Smad7^{fl/-}* mice compared to their littermates. For this experiment the mice were injected with BRDU at P3 and killed 24 hours later. Their eyes were enucleated and embedded in paraffin; see section 2.4.2. After sectioning the protocol for BRDU staining in paraffin sections was applied.

BRDU staining after NMDA injection in *Smad7-* and *TGF- β RII^{fl/-}* mice To show the effect of an NMDA treatment on proliferation, BRDU was injected intraperitoneally right after the intraocular NMDA/PBS injection, see section 2.4.6. 24 hours later the BRDU injection was repeated. Again 48 hours after the first injection the mice were killed and their eyes were cryoembedded, sectioned and stained for BRDU. Furthermore for the *TGF- β RII^{fl/-}* mice the experiment was repeated by killing the mice 24 h after the first injection.

2.4.9 Apoptosis assays (TUNEL) and proliferation assays (BRDU) in newborn mice

To choose the appropriate point in development for proliferation and apoptosis studies in newborn mice the papers from R.W. Young were used [44, 138]. Figure 2.9 shows that the maximum of the ontogenetic cell death of Müller is glia lies about day 8. This time point was chosen for the TUNEL assays in newborn mice. The proliferation maximum of the central retina is at day 3 that of the peripheral retina at day 5, because of that day 4 was chosen for the proliferation studies.

2.4.10 LacZ staining of *EIIa Cre x Rosa LacZ*

To see where exactly the *EIIa Cre* recombinase is expressed in the retina, *EIIa Cre* mice were crossed with *Rosa LacZ* reporter mice. When the *Cre* recombinase is expressed in the same cell as the *Rosa LacZ* construct, a recombination in the

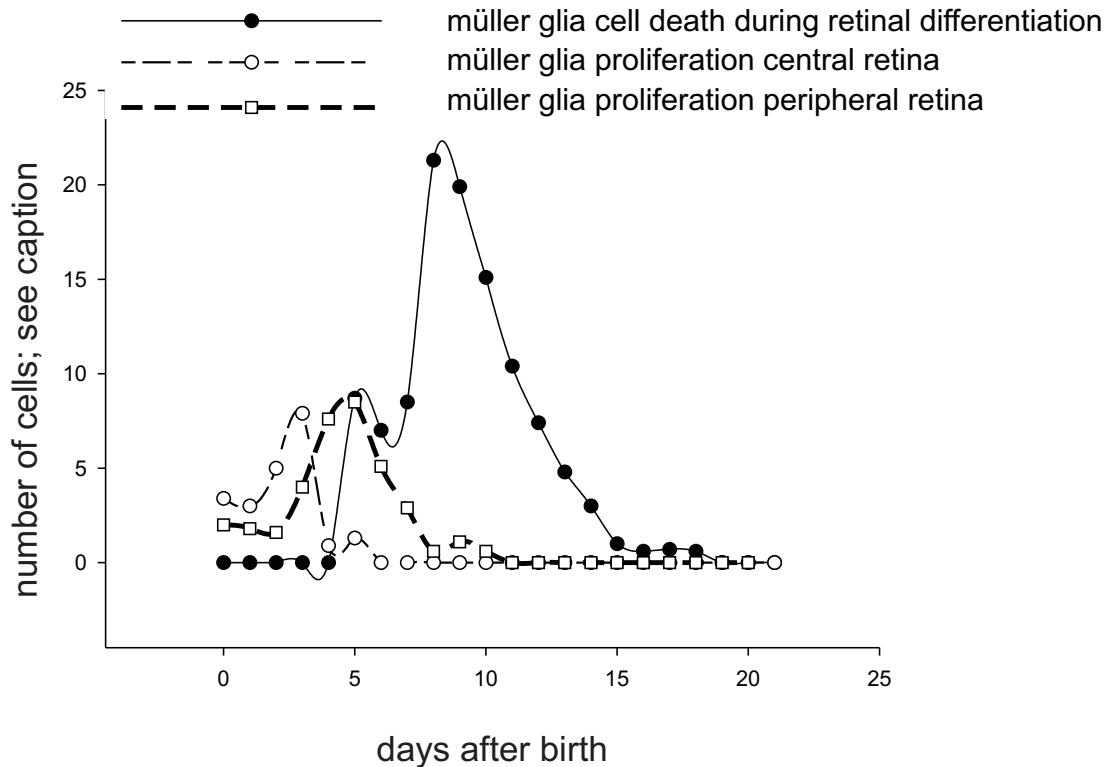


Figure 2.9: Müller glia proliferation and cell death in newborn mice: The graph with the solid circles shows all dead cells per $0.5 \mu\text{m}$ section from the optic nerve to the ora serrata; The curve for the proliferation for the retinal center shows all 3H -thymidine labeled cells within $500 \mu\text{m}$ from the optic nerve; The proliferation curve for the periphery shows all 3H thymidine labeled Müller glia cells within $500 \mu\text{m}$ from the ora serrata [44, 138]. The maximum of ontogenetic cell death for müller glia lies at P8, the maximum of proliferation between P3 and P5.

LacZ construct takes place causing the expression of β -Galactosidase in this cell. During a staining this enzyme cleaves the artificial substrate x-gal. This results in a blue color in the cell that carries the Cre recombinase. For the experiment 3 week old mice carrying the LacZ gene and the Cre recombinase were used. As a negative control mice free of the Cre recombinase but carrying the LacZ construct were chosen.

For the LacZ staining the eyes were enucleated and fixed for 30 min in LacZ fixation solution; see Table 2.22. Subsequently the eyes were washed 3 times for 15 min with LacZ washing buffer, see Table 2.23, followed by an over night incubation in LacZ staining solution, see Table 2.24. The following day the eyes were washed again 3 times for 15 min in LacZ washing buffer and were incubated for at least 10 min in Php prior to further handling. The LacZ stained eyes were treated with sucrose solutions following the protocol for paraffin embedding and sectioning shown in section 2.4.2.

2.4.11 Immunostaining of tissue

For immunostaining paraffin sections and cryo sections were used. Paraffin sections had to be dewaxed and rehydrated prior to staining as shown in section 2.4.2

LacZ fixation buffer	
glutaraldehyde 25%	0.4 ml
EGTA 250 mM pH 7.3	1 ml
MgCl ₂ 1 M	5 ml
sodium phosphate buffer (Php); pH 7.3; 0.1 M	43.5 ml

Table 2.22: *LacZ fixation buffer.*

LacZ washing buffer	
MgCl ₂ 1 M	1 ml
1% sodium desoxycholate	5 ml
2% tergitol	5 ml
phosphate buffer; pH 7.3; 0.1 M	489 ml

Table 2.23: *LacZ washing buffer.*

lacZ staining solution	
lacZ washing buffer	72 ml
X-Gal (25mg/ml in DMSO)	3 ml
K ₄ Fe(CN) ₆ x 3 H ₂ O	0.159 g
K ₃ Fe(CN) ₆	0.123 g

Table 2.24: *LacZ staining solution.*

and incubated in phosphate buffer prior to use. Cryo sections were washed 3 times for 5 minutes in phosphate buffer (Php) (see Table 2.19) to wash off the tissue tech. For blocking 3% BSA with 0.1% triton was used. The blocking solution was applied on the tissue and the slides were incubated for 1 h at room temperature. After 3 washing steps with Php the primary antibody see Table 2.25 was applied and the slides were incubated over night at 4 °C. Subsequently the slides were washed 3 times in phosphate buffer and the secondary antibody, see Table 2.26 was applied fo 1 h at room temperature. After three final washing steps with phosphate buffer the slides were mounted with mounting medium containing 1:10 dapi for a nuclear staining and stored at 4°C in the dark until use.

Primary antibody	Dilution	Source	Buffer	Company
Nestin	1:150	mouse	0.3% BSA 0.01% Triton	BD Pharmingen
Glutamine synthetase	1:500	rabbit	0.3% BSA 0.01% Triton	Sigma
GFAP	1:300	rabbit	0.3% BSA .01% Triton	Dako

Table 2.25: *Primary antibodies for immunostaining.*

Secondary/Tertiary antibody	Dilution	Company
goat anti mouse alexa 488	1:2000	Invitrogen
goat anti rabbit alexa 488	1:1000	Invitrogen
goat anti rabbit alexa 546	1:1000	Invitrogen
Biotinylated anti mouse	1:500	Vector
Biotinylated anti rabbit	1:500	Vector
Streptavidin Alexa 488	1:1000	Molecular probes
Streptavidin Alexa 555	1:1000	Molecular probes
Cy3 goat anti rabbit	1:1000	Jackson immuno research

Table 2.26: Secondary antibodies for immunostaining.

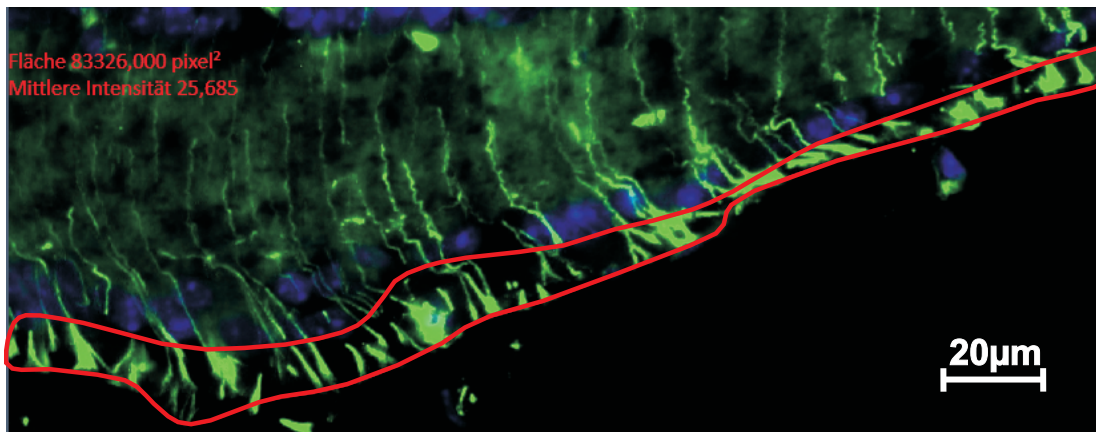


Figure 2.10: Example for intensity measurement.

2.4.12 Nestin and GFAP stainings

Nestin and GFAP staining as a control for Müller glia cell activation in untreated mice To see if a deficiency of Smad7 or TGF- β RII has any effect on the Nestin expression in untreated mice, 3 week old mice were used. The eyes were enucleated and cryo-embedded. The staining was done according to the protocol shown in section 2.4.11, using anti mouse or anti goat alexa 488 secondary antibodies.

Nestin and GFAP staining as a control for Müller glia cells activation after NMDA treatment After NMDA lesion, Müller cells are known to express more GFAP and Nestin. To see if a deficiency of Smad7 or TGF- β RII alters or enhances this reaction 6 week old mice were injected with NMDA. Three days after the injection the mice were killed and their eyes were cryo-embedded. The sections were stained with Nestin or GFAP according to section 2.4.11.

Measurement of Nestin fluorescence staining intensity with ZEN lite 2011 To determine the Nestin staining intensity in the Müller glia foot processes ZEN lite 2011 from Zeiss was used. To use a defined region for measurement the stained area between the nuclei of the ganglion cell layer and the vitreous humor of the eye was surrounded with a spline (red) as shown in Figure 2.10. The program calculates the average intensity of the staining. This intensity is already normalized to the area of the measurement.

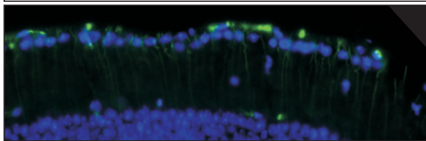
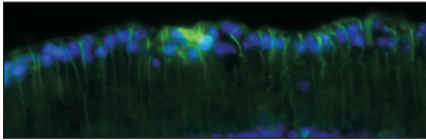
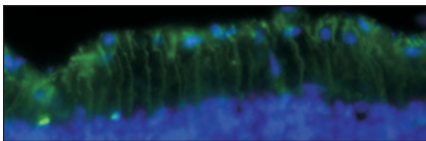
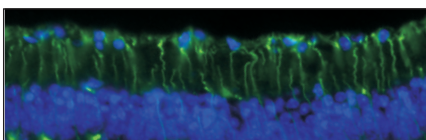
staining	description	score
	no nestin staining	0
	only tips of foot processes stained	1
	most parts of the foot processes are stained	2
	all foot processes stained; staining reaches into INL	3

Figure 2.11: *Scoring for Nestin staining intensity.*

Scoring of Nestin fluorescence staining intensity If it was not possible to use the program ZEN to measure the staining intensity, for example due to background staining, the stainings were examined by eye and scored with the system shown in Figures 2.11 and 2.12. To allow for further statistical analysis, the Mann-Whitney test was used. To present these results graphically, box plots are used.

2.4.13 Glutamine synthetase staining (GS) - Evaluation of the number of Müller glia cells in different mouse lines

For counting of the number of Müller glia cells in the retinae of the different mouse lines, 3 week old mice were used. The mice were killed, the eyes enucleated and cryo-embedded. Sagittal cryo sections through the papilla were stained with glutamine synthetase, a marker for Müller glia as Figure 2.13 A shows. For this staining the Biotin- Streptavidin system was used to get better results. Using the Axio Vision 40[†] program from Zeiss, three 200 μm sectors of the retina on each side of the optic nerve were determined: The first near the ora serrata (peripheral; 1), the second half way in between the ora serrata and the optic nerve (medial; 2) and the third close to the optic nerve (central; 3) as shown in Figure 2.13 B. The number of cellular bodies were determined, and for each eye the central, medial and peripheral counts of the the two sides were averaged.

2.4.14 Light- and fluorescence microscopy

The analysis of the paraffin-, cryo- and epon sections was done with the help of a Axio Imager Z1-microscope (Carl Zeiss, Göttingen).

[†]Release 4.8.2.0

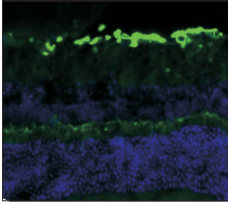
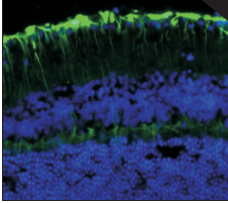
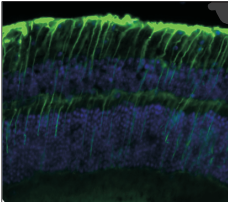
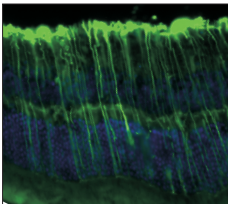
staining	description	score
	No müller cells GFAP stained	0
	Tips of müller glia processes stained	1
	Staining reaches into INL	2
	Staining spans whole retina	3

Figure 2.12: Scoring for GFAP staining intensity.

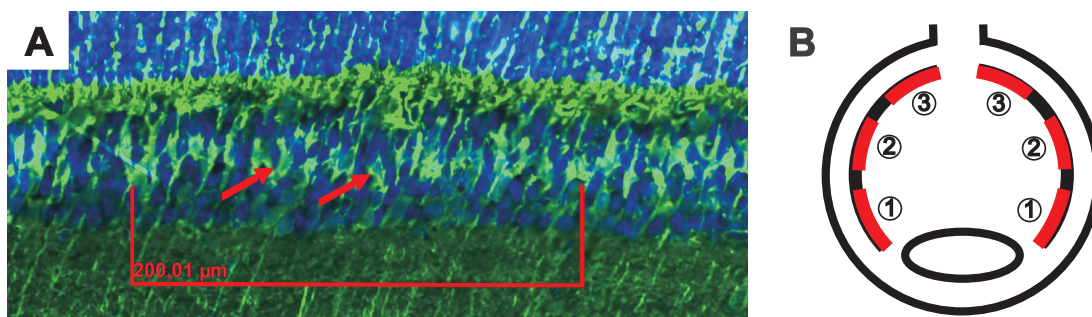


Figure 2.13: (A) Staining of Müller glia with glutamine synthetase. (B) Counting scheme.

2.5 Quantification of mRNA expression

Quantitative real-time (RT)-PCR is a method to determine the amount of a certain messenger ribonucleic acid (mRNA) present in a sample by monitoring the amplification process in real-time. For this method the mRNA has to be isolated and transcribed into complementary DNA (cDNA).

2.5.1 Retina preparation for mRNA isolation

To isolate the retinae, mice were killed, their eyes were enucleated and a circular cut was performed along the ora serrata to open the eye and remove the lens. The retina was brushed out of the remaining rear part of the eyeball with a pair of tweezers. The retinae of both eyes were pooled and immediately put into 200 μ l of peqGOLD TriFastTM. This fluid is a one phase solution of phenol and guanidine isothiocyanate that lyses the cells, inactivates RNAses and stabilizes the RNA. Subsequently the retinae in the Trizol were crushed with a pestle and either frozen at -20 °C until RNA isolation or immediately processed.

2.5.2 RNA isolation with TriFastTM

To isolate the RNA from the tissue the method by Chomczynski and Sacchi [139] was used. For this Chloroform was added to the lysed tissue and vortexed. Through centrifugation the mixture separated into three phases and the RNA could be precipitated from the upper aqueous phase with isopropanol. The exact protocol is shown below.

- Add Chloroform (1/4 of the sample volume) to the lysed tissue and vortex
- Incubate 2-3 minutes at room temperature
- Centrifuge 20 min at 4 °C at 12.000 x g
- Transfer the upper aqueous phase to a new cup
- Add isopropanol (1/1 of the sample volume) to the upper phase and vortex
- Freeze over night at -20 °C
- Centrifuge 20 min at 4 °C at 12.000 x g
- Remove supernatant
- Add 700 μ l 75 % ethanol
- Centrifuge 5 min at 4 °C at 7.500 x g
- Let the pellet dry
- Add 10 μ l RNase free H₂O

RNA can be stored at -80 °C.

2.5.3 RNA-quantification

The RNA concentration was determined measuring the UV absorption in a NanoDrop-1000 Spectrometer. Using the optical density (OD) of the sample at 260 nm, the

Reaction mix	sample	control
RNA	0.5 μg	0.5 μg
5x iScript TM reaction Mix	2 μl	2 μl
iScript TM reverse transcriptase	0.5 μl	-
H ₂ O	fill to 10 μl	fill to 10 μl

Table 2.27: Reaction mixture for cDNA synthesis.

temperature	duration
25 °C	5 min
42 °C	30 min
85 °C	5 min
10 °C	∞

Table 2.28: Cyclor program for cDNA synthesis.

absorption peak of nucleic acids, the RNA concentration was calculated as equation 2.1 shows.

$$\text{RNA concentration } [\mu\text{g/ml}] = OD_{260} \cdot 40 \mu\text{g/ml} \quad (2.1)$$

The purity of the RNA was determined by the the OD_{260}/OD_{280} ratio, where the OD_{280} is proportional to the the concentration of proteins in the sample. A ratio between 1.8 and 2.0 indicates pure RNA.

2.5.4 cDNA synthesis

To perform a quantitative real-time (RT)-PCR, a stable form of the extracted mRNA was needed. To achieve this, cDNA (copy DNA or complementary DNA) was synthesized in vitro from the mRNA template using the enzyme reverse transcriptase. Due to the use of oligo dT primers only the poly A tailed mRNA is transcribed in this method. To exclude that any signal in the real-time PCR originated from cDNA as template and not from DNA, a negative control without the reverse transcriptase (-RT control) was prepared in this step. For the reaction the "iScript cDNA Synthesis kit" by Biorad was used. The composition of the reaction mixture is shown in Table 2.27. The reaction was performed in a thermocycler using the program shown in Table 2.28

The synthesis of the cDNA takes place during the 42°C step the reverse transcriptase is inactivated at 85°C. The cDNA was stored at -20°C until use. By determining the amount of a certain cDNA in the sample the amount of the corresponding mRNA can be evaluated.

2.5.5 Quantitative real-time (RT)-PCR

All real-time analysis were carried out with the RNA (transcribed to cDNA) of the retinae of three week old mice. To get enough RNA, the retinae of the two eyes per mouse were pooled.

The quantitative real-time RT-PCR is a method to determine the concentration of a certain mRNA/cDNA in a sample [140]. During RT-PCR an amplification re-

name	sequence
GNB2L1 fw	5'gctactacccccgcagttcc3'
GNB2L1 rev (Guanidine nucleotide binding protein 2 like 1)	5'cagtttccacatgatgatggtc 3'
mSmad7 RT fw	5'cccaatggattttctcaaacc 3'
mSmad7 RT rev (Mothers Against Decapentaplegic homolog 7)	5'gggccagataattcgttcc 3'
m TGFbr2 Ex2 fw	5'agaagccgcatgaagtctg 3'
m TGFbr2 Ex3 rev (Transforming growth factor receptor II)	5'ggcaaaccgtctccagagta 3'
Nestin fw	5'ctgcaggccactgaaaagtt 3'
Nestin rev	5'tctgactctgtagaccctgcttc 3'
CTGF fw	5'tgacctggaggaaaacattaaga 3'
CTGF rev (Connective tissue growth factor)	5'agccctgtatgtcttcacactg 3'

Table 2.29: *Q-PCR primers.*

Reaction mix	
cDNA	0.15 μ l
10x PCR-buffer	1.5 μ l
MgCl ₂ (25 mM)	0.6 μ l
dNTPs (25 mM)	0.12 μ l
Sybr-Green I	0.19 μ l
Fluorescein	0.015 μ l
Taq DNA polymerase (5U/ μ l)	0.06 μ l
H ₂ O	7.37 μ l
Primer mix	5 μ l

Primer mix	
H ₂ O	60.5 μ l
Primer forward (1 μ M)	1 μ l
Primer reverse (1 μ M)	1 μ l

Table 2.30: *Reaction mixture for real-time PCR.*

action is performed and the amount of the PCR product is continuously measured during the reaction.

For the amplification reaction the master mix and the Taq polymerase of the HotStart Taq Kit (Quiagen) were used. The reaction mix was prepared as shown in Table 2.30. The primers (see Table 2.29) were constructed by using the Universal probe library[‡] and ordered from Invitrogen.

As cyciler a iQ5 Multicolor Real time-PCR Detection System iCycler was used. Table 2.31 shows the standard cyciler program. The reaction was carried out in 96-well-format plates with every sample measured as triplicate and for every sample a -RT control as described in sec. 2.5.4.

[‡]www.roche-applied-science.com

step	temperature	duration
step 1 (1x)	95 °C	15 min
step 2 (40x)	95 °C	10 s
	60 °C	40 s
step 3 (1x)	95 °C	1 min
step 4 (1x)	55 °C	1 min
step 5 (81x)	55 °C	6 s
melting curve	+ 0.5 °C per cycle	

Table 2.31: *Cycler program for quantitative RT-PCR.*

To track the amplification in real-time, the fluorescent dye SYBR green is incorporated into the DNA and fluoresces strongly when the DNA is in double stranded conformation. The fluorescence is excited by a laser and the amount of fluorescence is equivalent to the amount of PCR product present in the sample. Knowing the cycle when the fluorescence PCR product reaches a defined concentration threshold lying in the exponential phase of the amplification (C_T ; cycle threshold), the original amount of mRNA in the sample can be calculated.

For the concentration of any amplified gene $c_{\text{gene}}(C_T)$ versus the cycle count C_T holds the following relation:

$$c_{\text{gene}}(C_T) = c_{\text{gene}}(0) \cdot 2^{C_T} \quad (2.2)$$

In the used method, the amount of fluorescence was not directly calibrated to a certain cDNA concentration. Because of this, the C_T value of the gene of interest had to be compared to the C_T value of a housekeeping gene that is not affected by the treatment or genetic modification. In this way the relation between the housekeeper gene and the gene of interest could be calculated. With this form of normalization the mRNA amount of the gene of interest in different samples could be compared.

Assuming the concentration of the housekeeping gene passes the threshold at cycle $C_{T,hk}$, while the concentration of the amplified gene of interest does so at cycle $C_{T,g}$, the ratio of the starting concentrations is

$$\frac{c_g(0)}{c_{hk}(0)} = 2^{C_{T,hk} - C_{T,g}} \quad (2.3)$$

with c_{hk} being the concentration of the housekeeper cDNA and c_g the concentration of the gene of interest cDNA. To exclude a signal that is caused by unspecific products like primer-dimers a melting curve was produced at the end of the amplification. The data was evaluated with the iCycler IQ Optical System software.

2.6 Protein biochemical techniques

2.6.1 Protein isolation with the trizol method

For protein isolation the organic phase from the phenol-chloroform extraction of the RNA was used, see 2.5.2. All samples used for western blots were taken from

washing buffer	
guanidine HCl	0.3 M
solve in 95 % ethanol	

Table 2.32: *Washing buffer for protein isolation.*

the retinae of three week old mice. To isolate the proteins from the organic phase following protocol was used.

- Add 900 μ l isopropanol to the remaining phenol-chloroform phase
- Incubate for 10 min at room temperature
- Centrifuge for 10 min at 16.000 x g
- Remove supernatant
- Wash pellet with washing buffer (see Table 2.32) for 3 times and with 95% ethanol the fourth time; centrifuge after each washing step 5 min at 4 °C and 7500 x g
- Add about 150-200 μ l of 1% SDS with protease inhibitor 1:1000 and phosphatase inhibitor 1:100
- Incubate at 50 °C over night
- Centrifuge 10 min at 10000 x g and use supernatant

2.6.2 Sodium-dodecyl-sulfate polyacryl-amid gel electrophoresis: SDS PAGE

To separate the proteins according to their size the method of discontinuous SDS page by Laemmli [141] was used. In this method the proteins are completely denaturated and brought to a negative charge proportional to their size by binding SDS to their hydrophobic regions. The separation of the proteins is done by gel electrophoresis. Due to a two part gel- and buffer system, that is different in pH, acrylamide- and ion concentration, the proteins are focused in a stacking gel between the leading Cl⁻ ions and the following Glycine⁻ ions and resolved by their size in the resolving gel. Table 2.33 shows the gel composition of both components and Table 2.34 the buffer needed to pour and run the gel. According to the protein size a different acrylamide concentration of the resolving gel can be chosen.

To pour the gels, the vertical gel casting system by PeqLab Biotechnology GmbH was used. The casting chamber was set up according to protocol. To cast the gel, the resolving gel solution was filled between the two glass plates and overlaid with isopropanol. After polymerization the isopropanol was removed, the stacking gel solution was poured between the glass plates. A comb was inserted into the fluid stacking-gel to form the gel pockets. When the stacking gel is solid the gel casting device was inserted into the electrophoresis chamber according to protocol. The comb was removed and the chamber was filled with electrophoresis buffer. Prior to loading 15 μ l of protein were mixed with 4x Laemmli buffer, see Table 2.34 and heated for 5 min to 100 °C in a water bath to denaturate the protein. To run the gel 5 μ l of marker (PageRuler™ Prestained Protein Ladder;

Gels for SDS-PAGE	Stacking gel (1 ml)	Resolving gel 10 % (5 ml)
H ₂ O dest.	0.68 ml	1.9 ml
Rotiphorese [®] Gel 30	0.17 ml	1.7 ml
Tris/HCl, 1 M, pH 6.8	0.13 ml	-
Tris/HCl, 1.5 M, pH 8.8	-	1.3 ml
10 % SDS	0.01 ml	0.05 ml
10 % APS	0.01 ml	0.05 ml
TEMED	0.001 ml	0.002 ml

Table 2.33: Gel composition for SDS gel electrophoresis; Buffers are shown in Table 2.34.

Buffer	Composition
SDS-solution, 10 % (w/v)	10 g SDS solve in H ₂ O dest. ad 100 ml
SDS-Laemmli buffer, 4x	0.25 M Tris/HCl, pH 6.8 30 % glycerin 8 % (w/v) SDS 0.02 % (w/v) bromophenol blue 10 % β-mercaptoethanol
10 x SDS electrophoresis buffer	250 mM Tris/HCl 400 mM Glycine 1 % (w/v) SDS solve in H ₂ O dest. ad 1 l
Tris/HCl, 1.0 M, pH 6.8	121.14 g Tris solve in H ₂ O dest .ad 1 l adjust pH
Tris/HCl, 1.5 M, pH 8.8	181.71 g Tris solve in H ₂ O dest .ad 1 l adjust pH

Table 2.34: Buffers for SDS gel electrophoresis.

Fermentas) and all of the protein solution were loaded into the gel pockets and the power supply was set to 45-60 min at 20 mA.

2.6.3 Western blot protein transfer

To transfer the separated proteins from the resolving gel to the Polyvinylfluoride (PVDF)- membrane (Roche, Mannheim) a Semidry Blotting device (Pierce and Warriner, Erlangen) was used. The PVDF membrane was cut to the size of the resolving gel and incubated for 15 s in methanol to activate the surface. Subsequently the membrane was washed for 1 minute in distilled water and equilibrated for 5 minutes in transfer buffer. The whatman papers were equilibrated in transfer buffer as well, see Table 2.35. The stacking of the blot was done as shown in Table 2.36. Blotting was done for 1.5 h at 25 V.

10x transfer-buffer	
Tris	5.8 g
glycine	2.9 g
methanol	200 ml
SDS	3.7 ml 10 % (w/v)
solve in H ₂ O dest., ad 1 l	

Table 2.35: *Transfer buffer for western blotting.*

cathode (-)
3 layers whatman-paper
resolving gel
PVDF-membrane
2 layers whatman-paper
anode (+)

Table 2.36: *Stacking scheme for western blotting.*

TBS, 10x, pH 7.4	
Tris/HCl	30 g
NaCl	80 g
KCl	2 g
fill with H ₂ O dest. ad 1 l	

TBST, 1x	
10x TBS	100 ml
Tween 20	0.05 % (v/v)
fill with H ₂ O dest. ad 1 l	

Table 2.37: *TBS and TBST buffer for immunostaining.*

2.6.4 Western blot immunostaining

To detect the protein of interest on the PVDF membrane after blotting, an antibody against the protein was used. To prevent the antibody from binding un-specifically, the membrane was incubated in 5% BSA in TBST or 5% skimmed milk (SM) powder in TBST (see Table 2.37) prior to the antibody treatment. After blocking, the membrane was incubated in the primary antibody solution (see Table 2.38) over night at 4°C. For that, the antibody was solved in TBST with 10% blocking solution. After washing the membrane 3 times for 5 minutes with TBST, the secondary antibody (see Table 2.39) was applied for 1 hour. This antibody carried horseradish peroxidase (HRP), an enzyme that can convert luminol to a fluorescing product.

Prior to detection the membrane was again washed 3 times for 5 minutes with TBST and 1 ml of HRP Substrate Luminol Reagent mixed with HRP Peroxidase Solution (1:1) was applied. After 5 minutes incubation time the fluorescence was detected by the LAS 3000 digital intelligent dark box and analyzed by Aida Advanced Image Data Analyzer Version 4.06.

Primary antibody	dilution	source	buffer (in TBST)	company	protein size
TGF- β RII C16	1:200	rabbit	0.5% SM	Santa cruz	70 kDa
pSmad3	1:200	rabbit	0.5% BSA	Cell signaling	52 kDa
CTGF	1:5000	rabbit	0.5% BSA	Gene Tex	38 kDa
pERK	1:500	rabbit	0.5% BSA	Cell signaling	44.42 kDa
Akt	1:1000	rabbit	0.5% BSA	Cell signaling	60 kDa
pAkt	1:500	mouse	0.5% BSA	Cell signaling	60 kDa
GAPDH HRP conjugate	1:10.000	rabbit	0.5% BSA	Santa Cruz	37 kDa

Table 2.38: Primary antibodies; SM = skimmed milk powder, BSA = bovine serum albumin.

Secondary antibody	dilution	company
chicken anti rabbit HRP	1:2000	Santa cruz
chicken anti mouse HRP	1:2000	Santa cruz

Table 2.39: Secondary antibodies.

Coomassie-staining	
methanol	40 ml
acetic acid	2 ml
Coomassie-Brilliant Blue R250I	0.2 g
fill with H ₂ O dest.	ad 100 ml

Coomassie-destainer	
Methanol	500 ml
acetic acid	1 ml
fill with H ₂ O dest.	ad 1 l

Table 2.40: Solutions for Coomassie staining and destaining.

2.6.5 Coomassie staining for loading control

The protein dye triphenylmethan Coomassie-brilliant blue R 250 is used to stain proteins on the PVDF membrane unspecifically. It binds to basic sidechains of proteins. To stain the membrane it was put into the staining solution, see Table 2.40, for 10 minutes. To remove the excess dye the membrane was incubated in Coomassie destaining solution (see Table 2.40) over night. Subsequently the membrane was dried.

reagents, media and equipment	company
BrdU Cell proliferation ELISA (colorimetric)	Roche, Mannheim
Dulbecco's modified eagle medium (DMEM) 4500	PAA, Pasching, AT
ethanol, absolute	Roth, Karlsruhe
fetal bovine serum	Invitrogen, Karlsruhe
collagenase A	Sigma, Taufkirchen
Gentamycin (5 mg/ml)	Invitrogen, Karlsruhe
Penicillin-Streptomycin	Invitrogen, Karlsruhe
phosphate buffered saline (PBS)	Invitrogen, Karlsruhe
Trypsin/EDTA (0.05 %)	Invitrogen, Karlsruhe
Sunrise-basic ELISA-Reader	Tecan Austria, Grodig, AT
cell culture flasks, well plates	Nunc, Roskilde, DK
Petri dishes	Sarstedt, Nurnbrecht
Julabo SW20 water bath	Julabo Labortechnik, Seelbach
Hera Cell 150 incubator	Heraeus, Hanau
Hera Cell 150 clean bench	Heraeus, Hanau
serological pipettes	Sarstedt, Nurnbrecht

Table 2.41: *Reagents, media and equipment for cell culture.*

Müller cell medium	
DMEM medium	500 ml
FCS (serum)	50 ml
penicillin streptomycin mixture	5 ml
gentamycin	1 ml

Table 2.42: *Müller cell medium.*

2.7 Cell culture

2.7.1 Cell culturing techniques

All cells were cultured and treated under sterile conditions. All single use items were wrapped in sterile packaging, the glassware used was autoclaved. All media and buffer were sterile and mixed under the clean bench if necessary. Cell cultivation was carried out in Hera Cell 150 incubators at 37 °C and 5 % CO₂. During culture the medium was changed every two to three days. For splitting, the cells were washed with sterile PBS and treated with trypsin-ethylene-diamine-tetraacetic-acid (EDTA) for about 2 min at 37 °C. The enzymatic reaction was stopped with Müller glia medium, see Table 2.42 and the cell suspension was centrifuged at 1000 rpm for 5 min. Depending on the experiment the cell were seeded in different concentrations for treatment or further cultivation.

2.7.2 Cell counting with the CASY Cell Counter

To evaluate the number of cells per ml prior to seeding a CASY Cell Counter and Analyzer TT was used. The cells were washed with PBS and detached from

digestion solution	
serum free Müller cell medium	2 ml
trypsin	500 μ l
collagenase I	70 U/ml

Table 2.43: *Müller cell digestion solution.*

the flask using trypsin-EDTA. To stop the reaction Müller glia cell medium with serum was used. Subsequently 50 μ l of cell suspension were mixed with 10 ml of sterile Casy-ton (from OLS) and used for the measurement.

2.7.3 Enrichment of rat Müller glia cells for cell culture

The enrichment of rat Müller glia cells was done by the method of Hicks and Courtois [142]. To achieve an enriched culture, Wistar rats were killed between P8 (postnatal day) and P12 and the eyes were enucleated. After piercing them with a needle they were incubated in serum free Müller cell medium over night at room temperature. To digest the cells the eyes were incubated for 20 min in digestion solution, see Table 2.43, at 37 °C and digestion was stopped by removing the solution and adding medium with serum. To isolate the retinae a circular cut was performed along the ora serrata to open the eye and remove the lens. The retina was brushed out of the remaining rear part of the eyeball with a pair of tweezers and transferred to a 2 ml petri dish containing PBS solution on ice. For one small flask the retinae of 8 to 10 eyes were needed. By pipetting up and down with a 1 ml eppendorf pipette the retinae in the PBS solution were homogenized and subsequently centrifuged at 1000 rpm for 5 min. The cell pellet was dissolved in DMEM medium and seeded in small cell culture flasks containing 5 ml Müller cell medium, see Table 2.42, flasks were incubated at 37°C and not moved for the following 3-4 days. When cells started to grow from the retina debris the cell layer was washed by pipetting the overlaying medium on it and by changing the medium afterwards. The remaining cells are considered as Müller glia to a high percentage confirmed with stainings and expression analysis [143].

2.7.4 Colorimetric cell proliferation ELISA

The thymidin analogon bromodesoxyuridine is incorporated into the DNA during the amplification of the DNA in cell proliferation. The more proliferation, the more BRDU is incorporated into the cells. BRDU can be detected in cell culture by an antibody carrying a Peroxidase (POD). This enzyme catalyzes the conversion of the chromogen substrate 3,5,3',5'-tetramethylbenzidine into a the chromatic complex 3,5,3',5'-tetramethylbenzidine semiquinone-imine. The reaction is stopped by adding H₂SO₄. This also changes extinction of the molecule from 450 nm (blue) to 690 nm (yellow). The extinction of each well caused by this reaction product is proportional to the BRDU incorporated and to the proliferation in the well.

To test the effect of TGF- β 1 on the proliferation of rat Müller glia cells the colorimetric cell Proliferation ELISA from Roche was used. Primary Müller glia cells (P1; passage 1) were seeded in Müller cell medium with serum in a density of $2 \cdot 10^4$ cells per well using a 96 well plate (P2). Two wells were left without cells

to act as a blanc. After the cells had settled they were washed with PBS, and 100 μl /well serum free Müller glia cell medium containing 1:1000 BRDU (10 μl final concentration) labeling reagent was applied. In one third of the wells no TGF- β 1 was added to the medium as a control. For another third 2 ng/ml TGF- β 1 and for the last third 4 ng/ml TGF- β 1 were added. The well plates were incubated for 24 h at 37 °C. After the treatment the supernatant medium was tapped off and 200 μl of Fix denat solution were added to each well. After 30 minutes the solution was tapped of and the anti BRDU POD working solution was applied and incubated for 90 minutes. After removing the antibody solution by tapping, the plates were rinsed for three times with washing solution 200-300 μl /well (PBS). For the detection substrate solution (100 μl /well) was applied and after 5 minutes the reaction was stopped by adding 25 μl /well of 1M H₂SO₄. The absorbance was measured with a Sunrise-Basic ELISA-Reader (Tecan) at 690 nm. After the measurement the average value of the blank wells (without cells) was subtracted from all measured values.

2.7.5 TGF- β 1 treatment and RNA isolation from Müller glia cells

For RNA isolation P0 primary Müller glia grown from the seeded retinae, were split from a small 5 ml flask to two 6 well plates for treatment. As soon as the cell layer was about 80 % dense the cells were washed with sterile PBS and 3 of the wells of each plate were treated with serum free Müller cell medium containing 2 ng/ml TGF- β 1. Three of the wells served as a control and were treated with serum free medium only. To harvest the cells 200 μl of trizol were added to each of the wells and the 600 μl were used pooled for RNA isolation.

2.8 Diagrams and Statistics

In all diagrams beside the box plots values are shown as mean \pm SEM. In box plots used to show ordinal (score) data, the boundary of the box closest to zero indicates the 25th percentile, a line within the box marks the median, and the boundary of the box farthest from zero indicates the 75th percentile. Whiskers (error bars) above and below the box indicate the 90th and 10th percentiles. For the statistical analysis of numeric data the student T test, for ordinal data (scores) the Mann - Whitney test was performed. A p-value < 0.05 was considered significant and marked with an asterisk (*) in diagrams.

Chapter 3

Results

3.1 Aims and ideas

The aim of this work was to evaluate the effect of the TGF- β pathway on precursor cell populations in the mouse retina, especially on Müller glia cells. To influence the TGF- β pathway, mainly two mouse models were used: One with a heterozygous deletion of exon II of TGF- β RII (Transforming growth factor beta receptor II), to investigate the effects of reduced TGF- β signaling; the other with a heterozygous deletion of the promoter and exon I of Smad7, an inhibitor of the TGF- β pathway, to study an increased TGF- β signaling. Additionally CTGF overexpressing mice, as a target protein for the TGF- β pathway, and mice with a Tamoxifen inducible TGF- β RII homozygous deletion in the retina were examined. With the help of these mouse models we evaluated if the TGF- β pathway had any effect on proliferation, cell death, activation or the reaction of retinal precursor cell populations to lesions.

3.2 Expression of EIIa Cre recombinase - EIIa mice x Rosa LacZ

To create TGF- β RII or Smad7 deficient mice with the help of the Cre LoX system, EIIa Cre mice were used for breeding. This mouse strain expresses a Cre recombinase under the adenoviral EIIa promoter with an early ubiquitous onset.

To see in which retinal cells the EIIa Cre recombinase actually leads to a recombination, we bred EIIa Cre mice to Rosa LacZ mice. This reporter mice are used to label regions where the Cre recombinase is active. In cells where the recombination occurs, β -Galactosidase is expressed and can be detected in sections by β -Galactosidase staining.

Interestingly the Cre recombinase under the control of an EIIa Cre promoter leads to a strong mosaicism in the first generation of breeding. Only some cells carry the recombination in the very beginning, but as the recombination occurs very early in the embryo, it is inherited to all cells that originate from this progenitor. In the retina this leads to a stripe pattern, where supposedly so called columnar units are stained (Figure 3.1 A). Columnar units are retinal units where

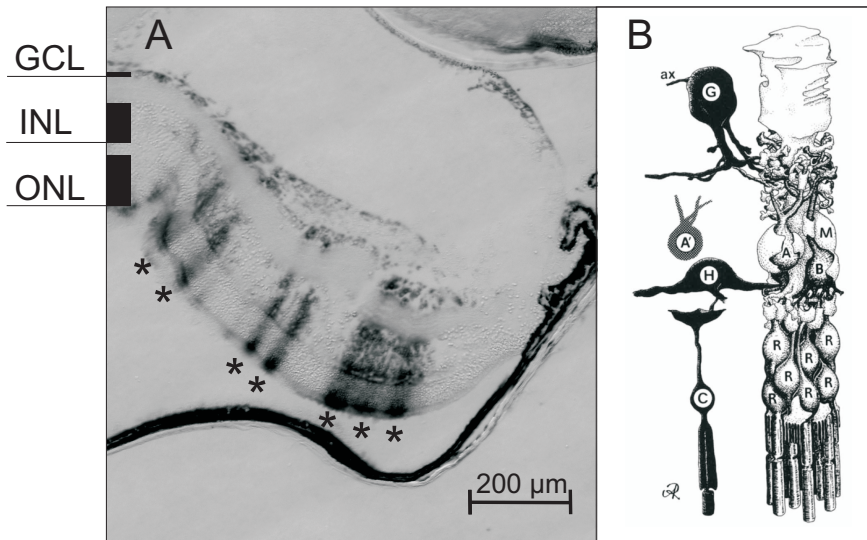


Figure 3.1: Mosaicism of *EIIa Cre* recombinase expression after breeding with *EIIa Cre*: (A) The *LacZ* staining shows regions with active *Cre* recombinase where the recombination took place. It depicts a stripe pattern in the retina - marked with an asterisk - that is possibly formed by so called columnar units. (B) Schematic drawing of a columnar unit: The structures in the retina originate from a single progenitor cell and are assembled as shown in the Semi-schematic drawing (taken from [151]). ONL = outer nuclear layer, INL = inner nuclear layer, GCL = ganglion cell layer.

cells originating from a single progenitor cell are arranged in a column like structure around one central Müller glia cell [144–151] (Figure 3.1 B). The feature of marking related cells makes the *EIIa Cre* x *Rosa LacZ* mouse an interesting model for clonal analysis of tissues.

For our purpose the mosaicism was a problem, solved by the elimination of the *Cre* recombinase during breeding and by establishing a stable heterozygous inheritable deletion. The breeding of these mouse models is shortly described in the following.

3.3 Effects of an altered TGF- β pathway

3.3.1 Breeding of *Smad7^{fl/-}* and TGF- β *RII^{fl/-}* mice

To analyze the influence of an increased TGF- β signaling, *Smad7^{fl/-}* mice were used, as *Smad7* is an inhibitor of the TGF- β pathway. It was not possible to work with a homozygous mouse model in this case, because the homozygous deletion proved to be lethal at a late embryonic stage.

By crossing *EIIa Cre* animals with the *Smad7^{fl/fl}* mice, recombination and deletion of the exon I of *Smad7* occurred. This deletion could be detected by the deletion PCR established by Ingo Kleiter [131], see section 2.3.6. During breeding, the genetic status was confirmed by performing PCRs for *EIIa Cre* recombinase and for the flox sequences. After the initial phase of breeding, the animals did not carry the *EIIa Cre* recombinase anymore, but inherited the heterozygously deleted sequence. Littermates without the deletion of *Smad7* but homozygous for

floxsites ($Smad7^{fl/fl}$) served as a control. Additionally TGF- β RII $^{fl/-}$ mice were used as a model for reduced TGF- β signaling. To create a mouse line, comparable to the $Smad7^{fl/-}$ mice, the breeding was done analogously to that of the $Smad7$ mice. For the exact breeding procedure, see section 2.2.10. The procedure for genotyping can be found in section 2.3.6.

3.3.2 Confirmation of gene deletion and gene product deficiency

Confirmation of the heterozygous deletion in $Smad7^{fl/-}$ mice

First, it had to be confirmed that the applied breeding procedure (section 2.2.10), lead to a ubiquitous heterozygous deletion on DNA level in the $Smad7^{fl/-}$ mice. To show that the recombination had occurred, a $Smad7$ deletion PCR [131] was performed for mouse tail DNA and for retina DNA.

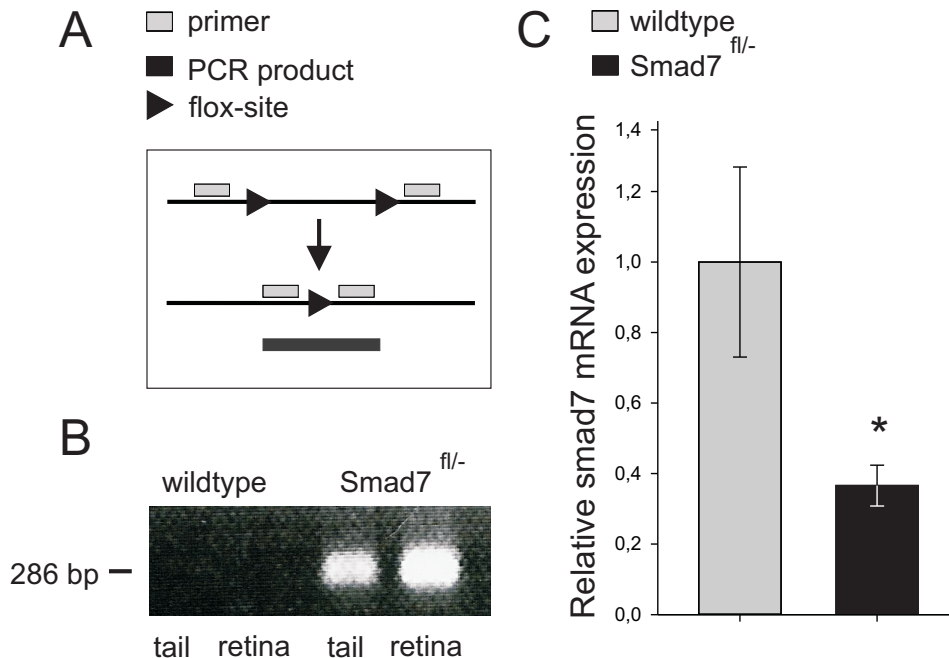


Figure 3.2: Confirmation of gene deletion and RNA deficiency in $Smad7^{fl/-}$ mice: (A) Scheme of $Smad7$ deletion PCR: Only DNA with a deletion of exon I results in a product in PCR. (B) Gel picture of deletion PCR: $Smad7^{fl/-}$ mice show deletion in mouse tail and retina DNA ($n = 3/2$ (wt/het)). (C) $Smad7$ expression on RNA level in retinae of $Smad7^{fl/-}$ mice and their wildtype littermates: The $Smad7$ level in the $Smad7^{fl/-}$ mice is reduced significantly to about 40% of the wildtype level ($n = 6$; $p = 0.044$).

The PCR only generates a product when the recombination took place, because the product for the non recombined DNA is too long for amplification (Figure 3.2 A). In a gel picture (Figure 3.2 B) bands can be seen for the retina and mouse-tail of the $Smad7^{fl/-}$ animal, but not for its wildtype littermate ($n = 3/2$ (wt/het)).

Confirmation of the Smad7 deficiency on mRNA level

After demonstrating the deletion on DNA level, the deficiency of Smad7 on mRNA level had to be confirmed. Quantitative real-time PCR was used to test RNA samples from retinæ of Smad7^{fl/-} mice and their wildtype littermates for their Smad7 mRNA levels (n = 6). Figure 3.2 C shows the normalized Smad7 expression in heterozygous Smad7-deficient mice and their wildtype littermates. In heterozygous Smad7-deficient mice, the Smad7 expression is significantly reduced to about 40% of the level observed in wildtype mice. This is in good agreement with the expected level after a mouse with a heterozygous gen deletion.

Confirmation of the TGF- β RII deletion on DNA and deficiency on protein level

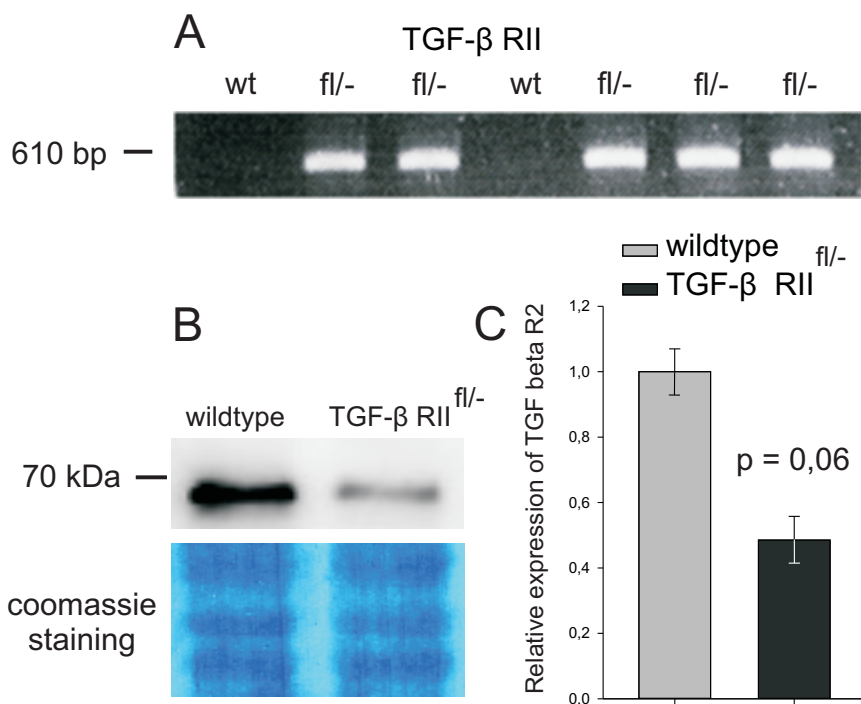


Figure 3.3: (A) TGF- β RII^{fl/-} mice carry the deletion in the retina: The DNA gel shows a positive reaction of the deletion PCR for the retina DNA of all heterozygous mice (n= 2/5 (wt/het)). (B) The TGF- β RII protein level is reduced markedly in TGF- β RII^{fl/-} mice: The western blot was done with the retina protein of 3 week old mice (n=4/5). (C) In real-time data a trend to a decreased TGF- β RII level can be seen (n=6).

For the TGF- β RII mice the confirmation of the recombination on DNA level was done analogously to the Smad7 mice. The deletion PCR, also used for genotyping the animals, was performed with retina DNA of 3 week old genotyped mice. Like the deletion PCR used for the Smad7 mice, this PCR only shows bands if the target gene is deleted. All animals positive for the heterozygous deletion in the tail DNA were also positive for the deletion in the retina, whereas the wildtype animals did not carry the deletion (Figure 3.3 A).

Additionally to the deletion on DNA level a TGF beta RII deficiency could be shown on protein level. Western blot analysis for TGF- β RII, done with retina

protein of 3 week old mice, showed that the level of protein in the heterozygous animals was markedly lower than in wildtype mice (Figure 3.3 B). In Figure 3.3 C real-time data of the TGF- β RII mRNA level in the retinae of TGF- β RII $^{fl/-}$ mice and their wildtype littermates is shown. In this case a trend to a decreased mRNA level in TGF- β RII $^{fl/-}$ mice can be seen.

3.3.3 Phenotype analysis

Histological phenotype of $Smad7^{fl/-}$ mice

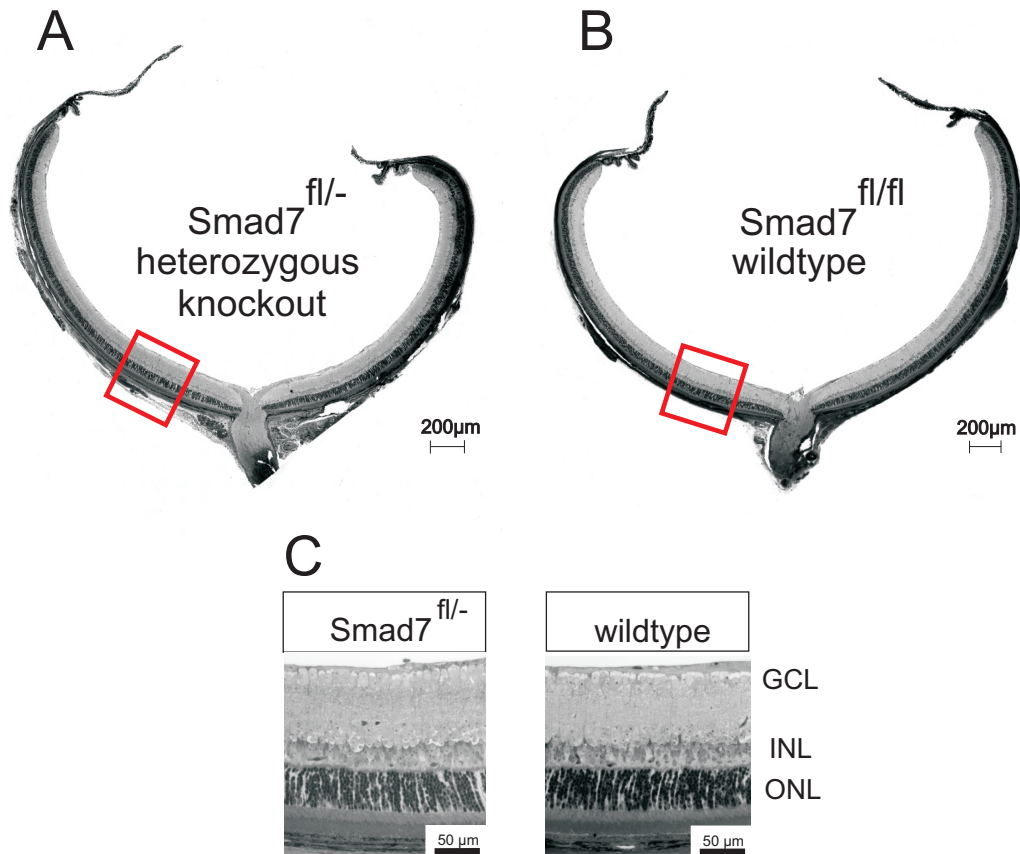


Figure 3.4: Phenotype analysis in 3 week old $Smad7^{fl/-}$ mice: The eyes of heterozygous $Smad7$ -deficient mice (A) show no apparent morphological differences compared to their wildtype littermates (B). Micrographs in higher magnification (C), taken close to the optic nerve head, show no difference in the organization and structure of the retinal layers. GCL = ganglion cell layer, INL = inner nuclear layer, ONL = outer nuclear layer, ONH = optic nerve head.

To evaluate any morphological changes in the retina, eyes of 3 week old $Smad7^{fl/-}$ mice and their wildtype littermates were enucleated and embedded in epon. Sagittal semithin sections through the papilla, 1 μ m in thickness, were stained with Richardson's stain and evaluated by light microscopy. Figure 3.4 shows light micrographs of the eye of a heterozygous $Smad7$ -deficient mouse (A) and its wildtype littermate (B). Higher magnifications are shown in C.

The structure of the eye of the $Smad7$ -deficient mouse and the retinal cell layers appear to be regular defined. No apparent changes in retinal thickness are visible.

The size of the eyes is normal and the higher magnifications show no difference in the organization and structure of the retinal layers. Nevertheless, through detailed measurements distinct morphological changes in the central retina can be detected, as will be shown in section 3.3.4.

Phenotyping TGF- β RII^{fl/-} mice

Analogous to the Smad7 mice, epon sections of 3 week old mice were examined. Figure 3.5 shows micrographs of TGF- β RII^{fl/-} mice (A) and their wildtype littermates (B). Comparing the eyes of TGF- β RII^{fl/-} and wildtype mice, no phenotypic changes were found. The size of the eye and the thickness of the retina remained unchanged. Higher magnifications showed no changes in the different layers of the retina as well (Fig. 3.5 C).

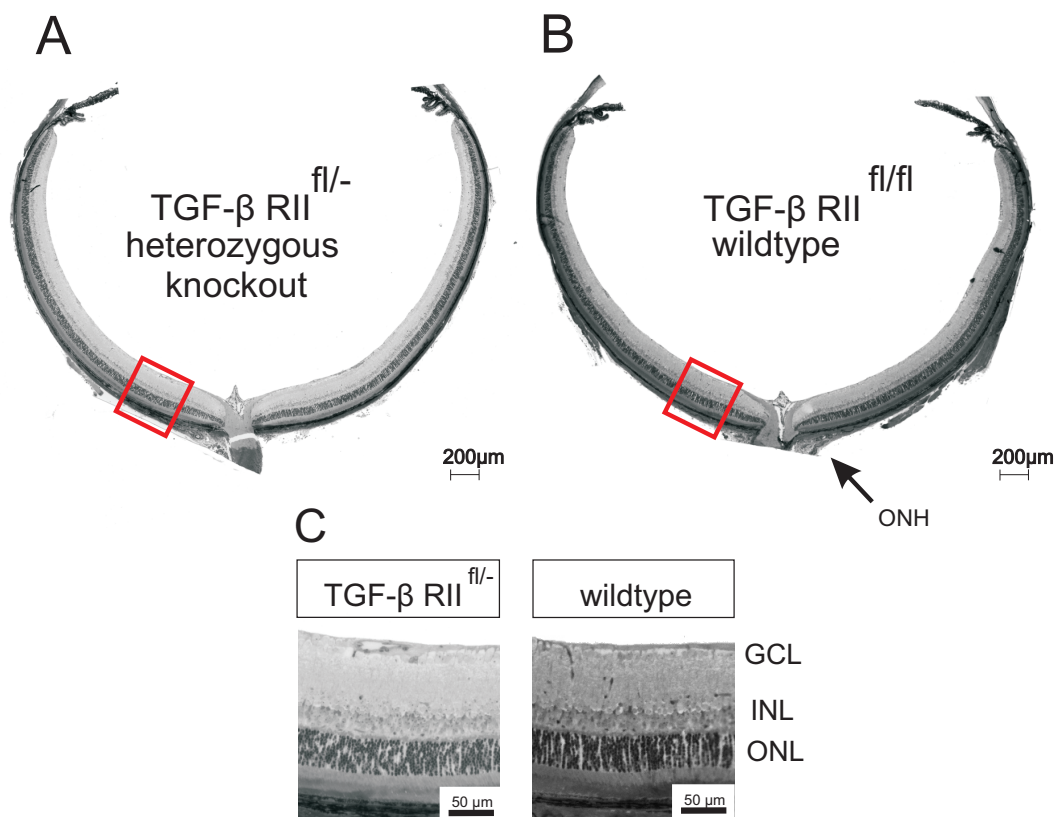


Figure 3.5: Micrographs of 3 week old TGF- β RII^{fl/-} mice (A) and their wildtype littermates (B). The structure of both eyes appears to be regular. No morphological changes could be found. Neither were changes detected in the structure of the retinal layers (C). GCL = ganglion cell layer, INL = inner nuclear layer, ONL = outer nuclear layer, ONH = optic nerve head.

3.3.4 Measurements of retina thickness

Increased retinal thickness in $Smad7^{fl/-}$ mice

As we were interested in any changes in proliferation or cell death, thickness measurements of the retinae of 3 week old mice were conducted. For the measurements, the epon semithin sections referred to in section 3.3.3 were used. Looking at the retina thickness of $Smad7^{fl/-}$ mice, morphological changes in the central retina can be seen. As figure 3.6 shows, the inner 10% of the retina of the $Smad7^{fl/-}$ are thickened significantly compared to their wildtype littermates. The change in thickness amounts to about 10 μm , which is about 5% of the thickness of the whole retina.

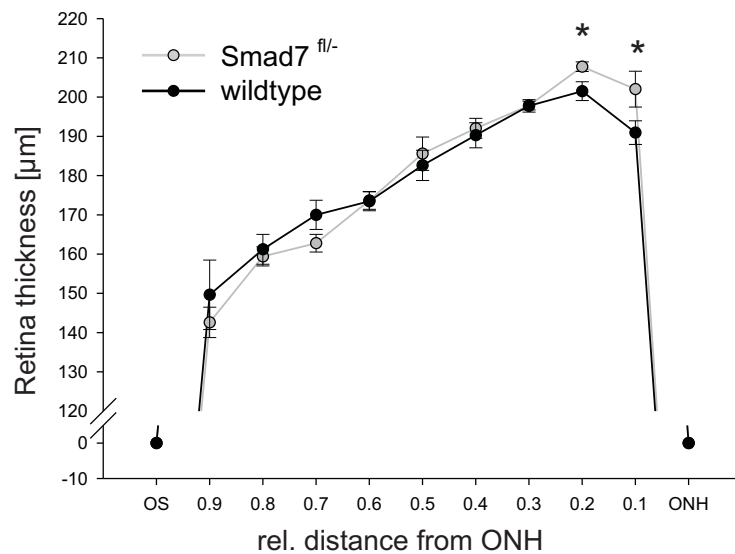


Figure 3.6: Measurement of retina thickness in $Smad7^{fl/-}$ mice: Next to the Optic nerve head (ONH) the retina of the $Smad7^{fl/-}$ mice is thickened significantly compared to their wildtype littermates ($n=5/7$ (wt/het), $p \approx 0.03$). The change in thickness amounts to about 5% of the thickness of the whole retina. ONH = optic nerve head; OS = ora serrata.

Increased thickness of inner and outer nuclear layer in $Smad7^{fl/-}$ mice

Figure 3.7 shows a compilation of pictures from the optic nerve head of 3 week old $Smad7^{fl/-}$ mice and their wildtype littermates. For a better visualization, the inner nuclear layer was colored digitally. Taking a closer look, the inner nuclear layer and the outer nuclear layer appear to be thickened. The measurement of the outer nuclear layer, and the inner 10% of the inner nuclear layer reveals that both layers are slightly, but nevertheless significantly thickened around the optic nerve head (Figure 3.8). The change in thickness amounts to up to 20% for the inner nuclear layer and up to 10% for the outer nuclear layer of $Smad7$ deficient mice compared to their littermates.

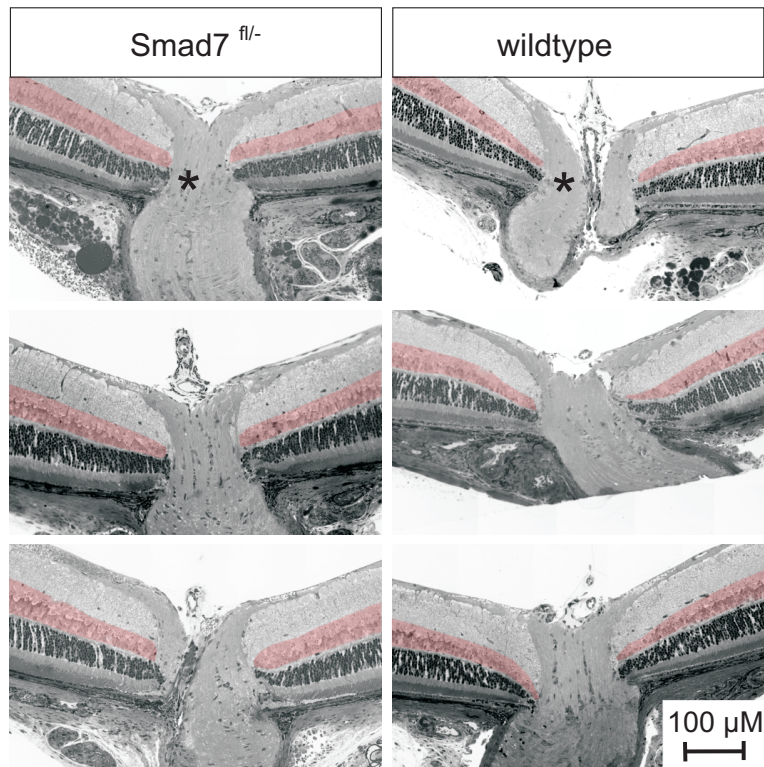


Figure 3.7: Micrographs taken at the optic nerve: Inner and outer nuclear layer of the $Smad7^{fl/-}$ mice appear to be thickened where they reach the optic nerve head, marked by an asterisk (*) in the first row. For a better visualization the inner nuclear layer was colored digitally.

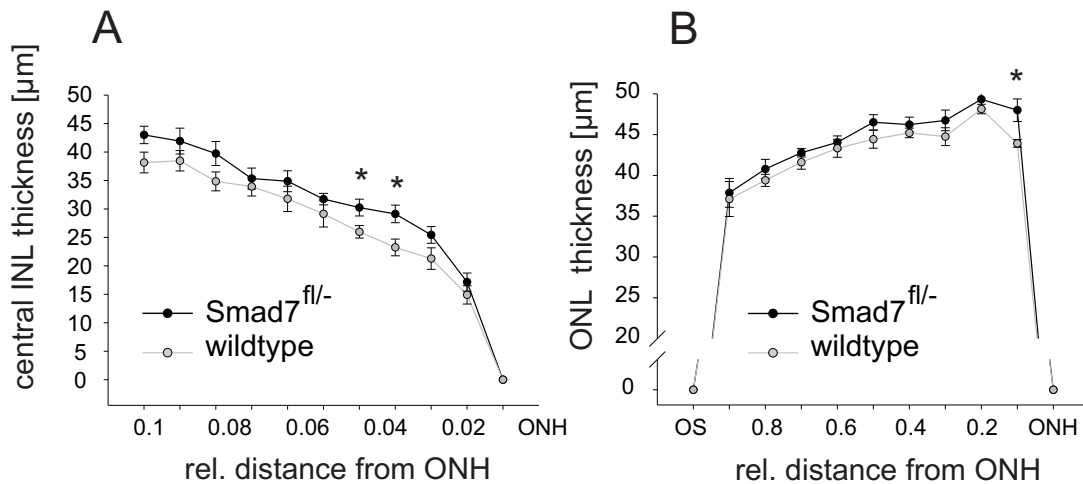


Figure 3.8: Measurement of the inner and outer nuclear layer thickness in $Smad7^{fl/-}$ mice: (A) Thickness of the inner 10% of the inner nuclear layer is increased significantly: In the inner 10% of the retina, an up to 20% thickening of the inner nuclear layer is visible ($n = 5/5$, $p = 0.042/0.023$).

(B) Thickness of the outer nuclear layer is increased significantly: Close to the optic nerve head, the outer nuclear layer is about 10% thicker than in the wildtype littermates ($n = 5/6$ (wt/het), $p = 0.03$).

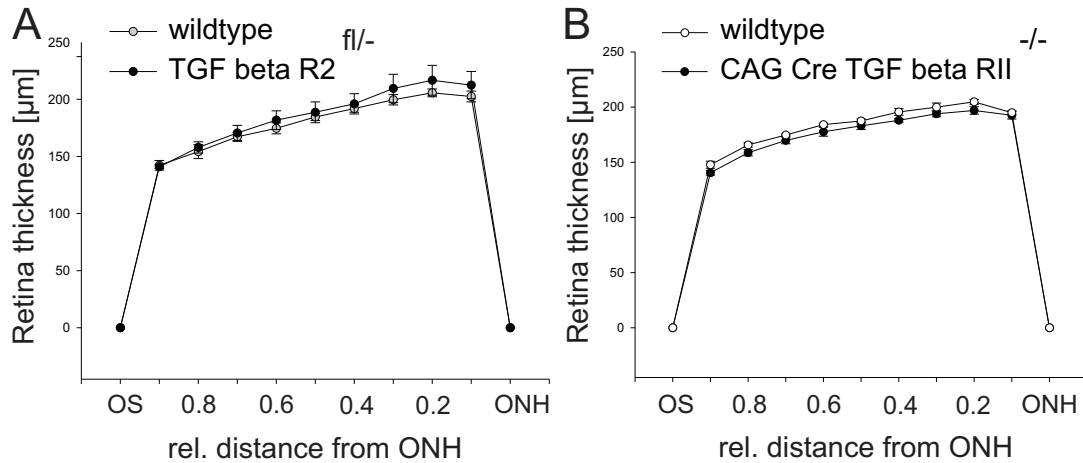


Figure 3.9: (A) Measurement of the retina thickness of TGF- β RII $fl/-$ mice: No change in the thickness of the retina could be found comparing TGF- β RII $fl/-$ mice and their wildtype littermates ($n = 5$). (B) Retina thickness of Tamoxifen induced CAG Cre x TGF- β RII fl/fl mice and their wildtype littermates: It is noteworthy that the average retina thickness of the mice with the conditional homozygous deletion of TGF- β RII is significantly smaller than in the wildtype mice, which is the contrary effect to the Smad7-deficient mice ($n = 5/6$ (wt/kn), $p=0.047$). OS = ora serrata; ONH = optic nerve head.

Influence of TGF- β RII heterozygous deletion and conditional homozygous deletion on retina thickness

To see if the heterozygous deletion of TGF- β RII has a contrary effect on the retina thickness compared to the Smad7-deficient mice, measurements on both sides of the optic nerve were conducted and averaged for every eye. The TGF- β RII $fl/-$ mice showed no change in retina thickness compared to their wildtype littermates. Even close to the optic nerve, where the heterozygous deletion of Smad7 showed an effect on the retina thickness, no differences could be seen (Figure 3.9 A). It is noteworthy that an inducible homozygous deletion of TGF- β RII in the eye by the Tamoxifen induced CAG Cre x TGF- β RII fl/fl model shows an effect on the retina thickness. If the average thickness of the whole retina is taken into account the retina of these mice is significantly thinned (Fig. 3.9 B).

3.3.5 Evaluation of the number of Müller glia

Increased number of Müller glia cells in Smad7 $fl/-$ mice

Our special interest lies in Müller glia cells as potential progenitor cells in the retina. To see if the thickening of the retina and the inner nuclear layer was also accompanied by a raised number of Müller glia cells, cryo sections of 3 week old mice were stained with glutamine synthetase, a Müller cell marker (Figure 3.10 A). Cells were counted in 200 μ m segments in the peripheral (1), medial (2), and central (3) retina as described in section 2.4.13 and depicted in Figure 3.10 B. In Figure 3.11 the numbers of Müller glia in the central, medial and peripheral retina are shown. The number of Müller glia is significantly increased in the

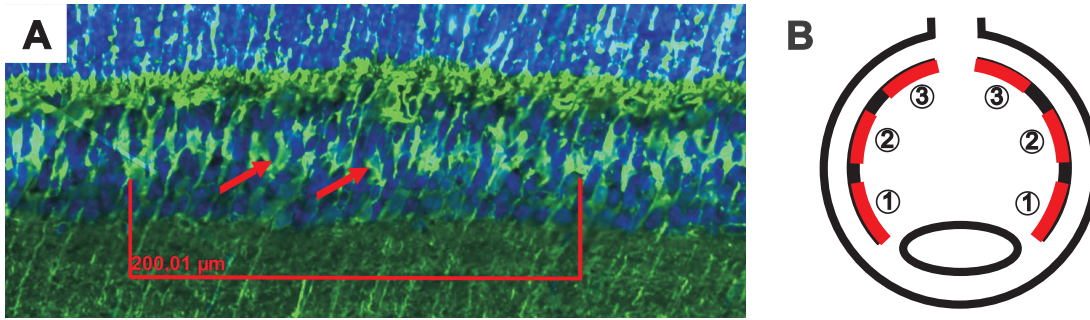


Figure 3.10: (A) Counting of the Müller glia was done by performing a glutamine synthetase staining (green) on sagittal eye sections. The arrows point out two examples of cell somata of the Müller glia in the inner nuclear layer (green). (B) Counting was performed in 200 μm segments in the peripheral (1), medial (2) and central (3) retina and averaged for both sides of the retina.

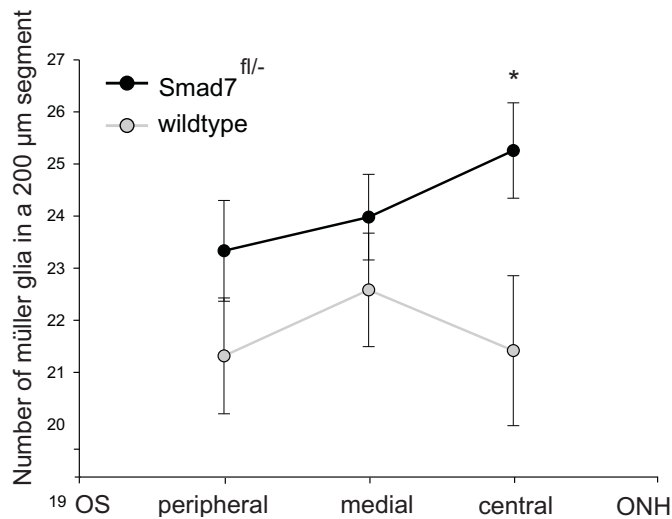


Figure 3.11: Number of Müller glia in the retina in *Smad7*-deficient mice: The number of Müller glia is significantly increased near the optic nerve head by almost 20% compared to the wildtype littermates ($n=9/6$, $p=0.049$).

central retina of *Smad7*-deficient mice by almost 20 % compared to the wildtype number.

Number of Müller glia cells in *TGF- β RII^{fl/-}* mice

To see if the *TGF- β RII* heterozygous deletion also has an influence on the number of Müller glia, the cells were counted with the help of a glutamine synthetase staining as described previously. As can be seen in figure 3.12 the number of the Müller glia cells does not vary between the *TGF- β RII^{fl/-}* and the wildtype mice. This is consistent with the result of the retina thickness measurement. The heterozygous *TGF- β RII* deletion does not appear to influence the cell number in the retina.

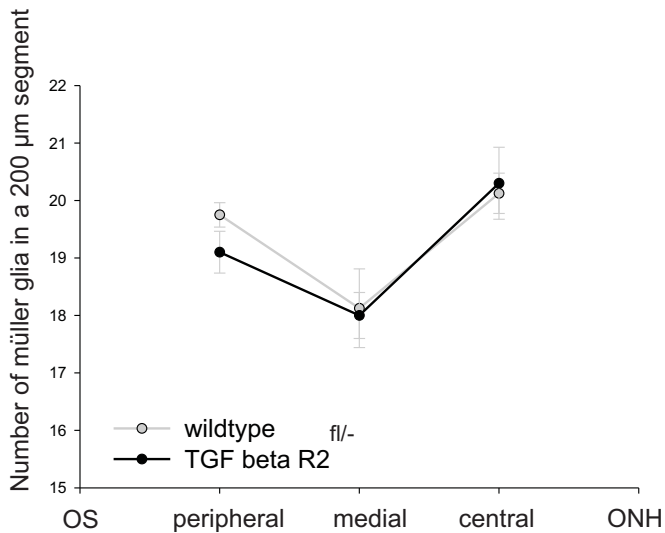


Figure 3.12: Number of Müller glia in the retina of TGF- β RII $fl^{-/-}$ and wildtype mice: The figure shows the number of Müller glia in a 200 μm segment in the peripheral, medial and central retina of TGF- β RII $fl^{-/-}$ and wildtype mice. The number of Müller cells is not affected by the heterozygous deletion of TGF- β RII ($n = 5$). OS = ora serrata; ONH = optic nerve head.

3.3.6 Proliferation and Apoptosis in newborn Smad7 mice

There are two possibilities why the retina of the Smad7 $fl^{-/-}$ mice could be thickened; a decrease in cell death or an increase in proliferation. To decide which effect is dominant we conducted further experiments.

Increase in the number of BRDU positive cells in newborn Smad7 $fl^{-/-}$ mice

To test for increased proliferation as a possible cause of the thickened retina, 3 day old Smad7 $fl^{-/-}$ mice and their wildtype littermates were injected with BRDU and killed 24 h after injection. The eyes were paraffin embedded and the sections were stained with an anti-BRDU antibody.

Figure 3.13 shows pictures of the BRDU stained retinae with the BRDU positive nuclei in green. For quantitative evaluation, the number of BRDU positive cells in the whole retina was counted. The graph shows the number of BRDU positive cells per 100 μm in the peripheral, the medial and the central third, and in the innermost 200 μm of the retina. The number of BRDU positive, and supposedly proliferating cells, is increased significantly in the innermost 200 μm of the retina. This is the same area where the retina in the 3 week old mice appears thickened. We suppose therefore that an increase in proliferation causes the thickening of the retina.

No increase in TUNEL positive cells in newborn Smad7 $fl^{-/-}$ mice

To exclude a decrease in cell death as a cause for the thickened retina, TUNEL stainings were performed. Retinal paraffin sections of 8 day old animals were simultaneously stained with TUNEL (green staining) and glutamine synthetase (red staining) (Figure 3.14 A). This way, not only the number of cells undergoing ontogenetic cell death, but also the ratio of Müller glia undergoing this process could be evaluated. The graph in Figure 3.14 B shows that there is no difference in the number of cells undergoing ontogenetic cell death in Smad7 $fl^{-/-}$ mice and their wildtype littermates at day 8. Also the number and percentage of Müller glia undergoing apoptosis stays the same at a percentage of 25-30% of all TUNEL positive cells. We suppose that the heterozygous deletion has no effect on the ontogenetic cell death in this stage.

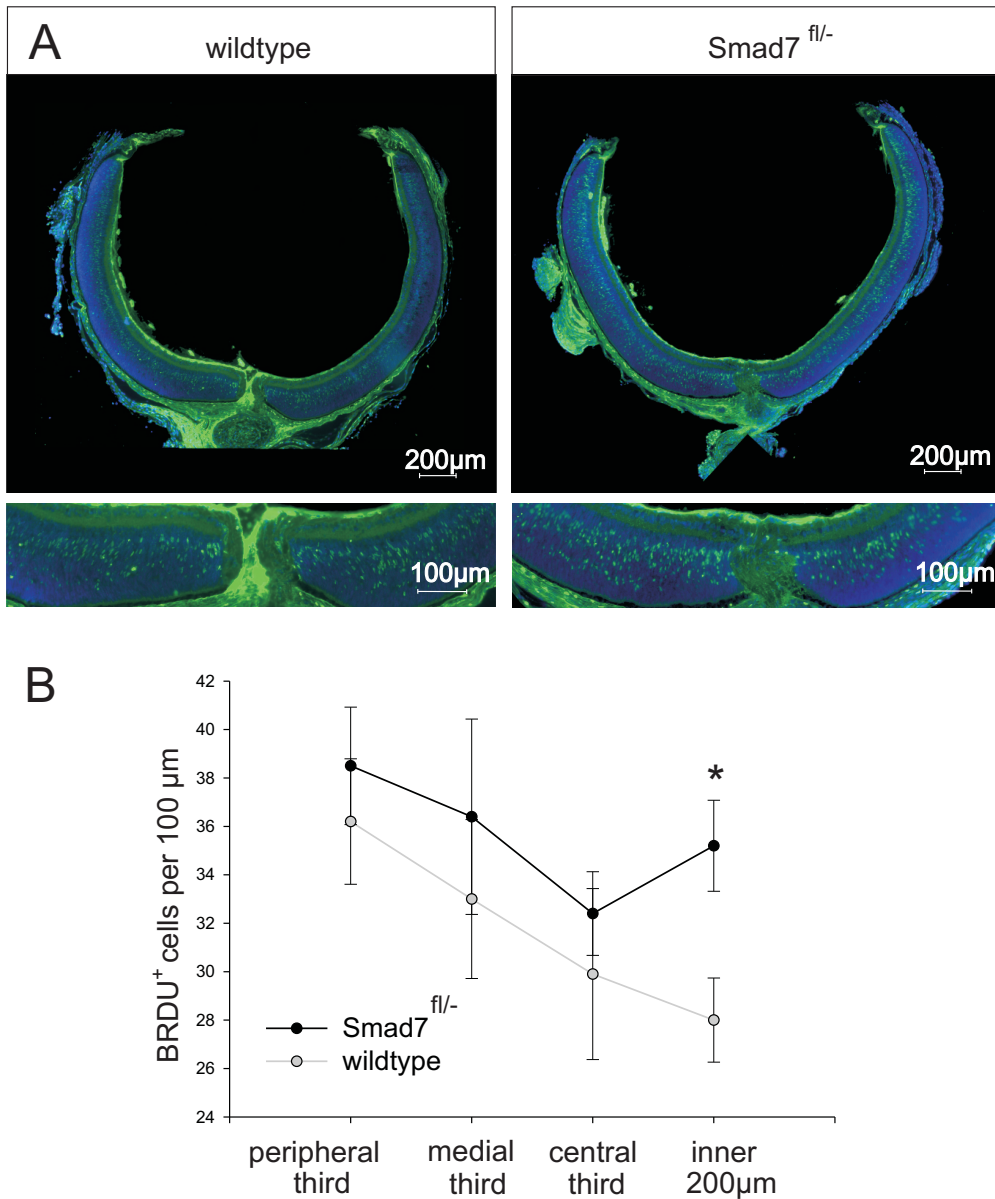


Figure 3.13: Proliferation in 4 day old Smad7-deficient mice: (A) Micrographs of BRDU stainings (green) in 4 day old Smad7-deficient mice and their wildtype littermates. At this stage of development the inner nuclear layer is not yet separated from the outer nuclear layer. Close to the optic nerve head the number of BRDU positive cells appears to be elevated. (B) The counting reveals a significant increase in the number of BRDU positive cells in the inner 200 µm of the retina, close to the optic nerve head. This is the region where the retina of the 3 week old Smad7-deficient mice was thickened. In the more peripheral parts of the retina no significant elevation in the number of BRDU positive cells was found ($n=5$; $p=0.024$).

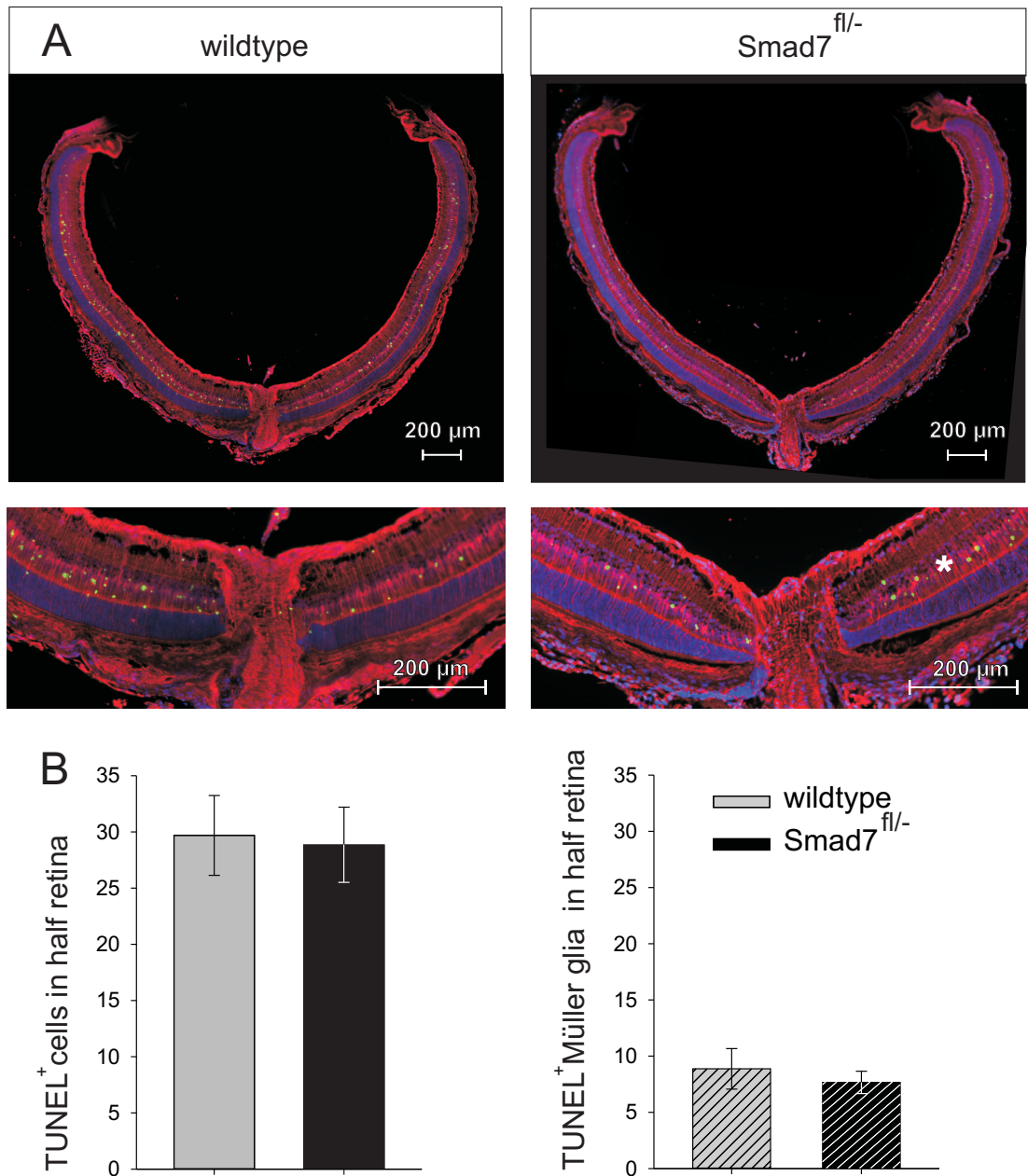


Figure 3.14: TUNEL staining in 8 day old $Smad7^{fl/-}$ mice and wildtype controls: (A) The micrographs show a staining for glutamine synthetase (red cell somata) as Müller glia marker, and a TUNEL staining to mark apoptotic cells (green nuclear staining) in sagittal eye sections of $Smad7^{fl/-}$ mice and their wildtype littermates. Most of the TUNEL positive cells are found in the inner nuclear layer, marked with an asterisk (*). (B) After counting the TUNEL positive cells in the whole retina and the TUNEL and glutamine synthetase double positive Müller glia, no change in the number of TUNEL positive cells can be seen comparing $Smad7^{fl/-}$ mice to their littermates ($n = 8/9$ (wt/het)). The percentage of Müller glia cells undergoing apoptosis stays at 25-30% in both, heterozygous and wildtype animals.

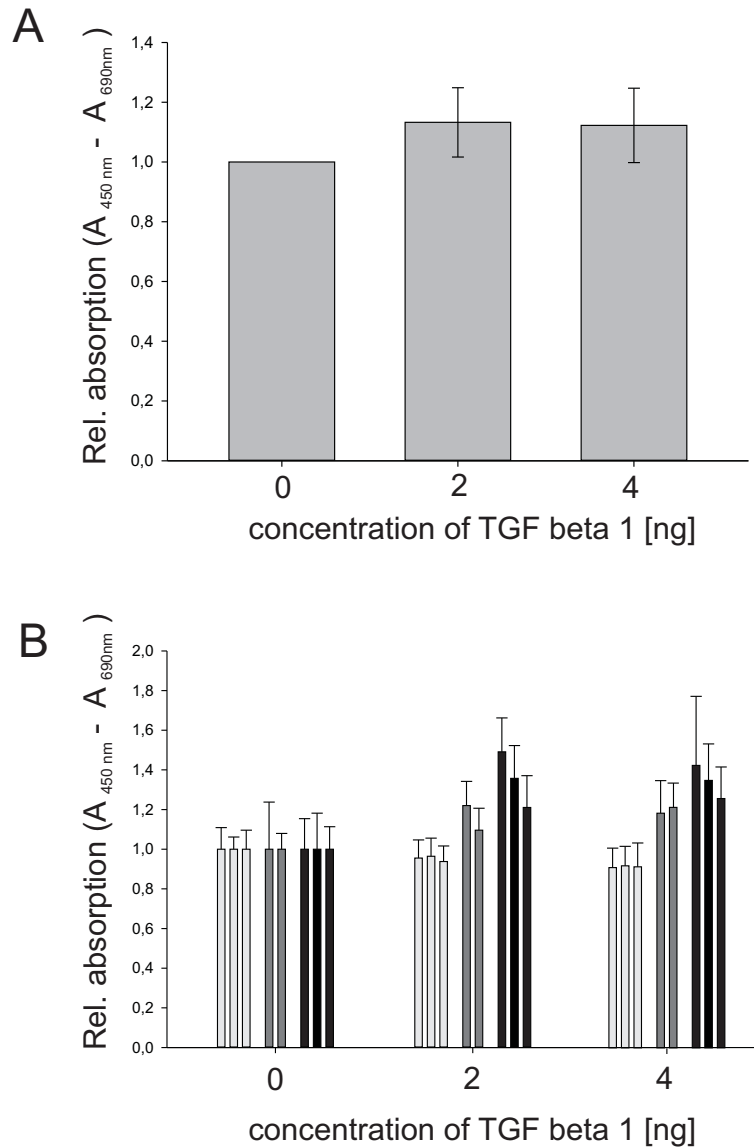


Figure 3.15: Relative proliferation rate of rat Müller glia cells after 24 h TGF- β 1 treatment: (A) Figure A shows that there is no significant difference in proliferation between treated and untreated cells. (B) In Figure B the results of the single experiments are shown. Here it can be seen that the 3 different cell isolations show very different reactions to the TGF- β treatment. While the cells of the first isolation (bars shown in light gray) show no reaction to the treatment, the third isolation (bars shown in black) react with a significant elevation in proliferation.

Influence of TGF- β 1 on proliferation in a Müller glia primary cell culture

Trying to reproduce the proliferative effect of the Smad7 heterozygous deletion in the young retina *in vitro*, we worked with Müller glia primary cell cultures taken from 8-12 day old rats as described in section 2.7.3. With the help of a cell proliferation ELISA (section 2.7.4) the effect of a 24 h TGF- β 1 treatment on the cells was evaluated. The experiment was repeated 3 times with different primary cultures using two to three 96 well plates for each experiment. As shown in figure 3.15 A there is no significant difference in the amount of cell proliferation

between TGF- β 1 treated and untreated cells. Taking a look at the results of the single experiments (figure 3.15 B), it can be seen that the different cell isolations show very different reactions to the TGF- β 1 treatment. While the first isolation showed no reaction, the third showed a significant proliferative effect. All in all, in this case the primary cell culture does not appear to be a reliable system.

3.3.7 Nestin and GFAP expression

Increased expression of Nestin in Smad7^{fl/-} mice

Increased Nestin expression on protein level in Müller glia foot processes: As Nestin is a marker for activated Müller glia, and stem cells in general, we were interested in the Nestin expression of Smad7^{fl/-} mice. For the experiment, eyes of 3 week old mice were used, and sagittal cryo sections were stained with a Nestin antibody. The Nestin staining (green) was mainly visible in the foot processes of the Müller glia covering the ganglion cell layer (Figure 3.16 A). Comparing the intensity of the staining in Smad7^{fl/-} mice with the staining in wildtype mice, an increase in intensity was visible mainly in the central retina. To demonstrate this, the staining intensity was measured with the program ZEN from Zeiss in the foot processes beneath the nuclei of the ganglion cell layer (section 2.4.12). The measurement data in Figure 3.16 B shows a significant increase in staining intensity in the central and medial areas of the retina.

The micrographs in Figure 3.16 C show an example of a double staining of Nestin (green) and glutamine synthetase (red) in the retina of 3 week old mice. This was done to demonstrate that the Nestin positive stained processes above the ganglion cell layer are the foot processes of the Müller glia cells. The glutamine synthetase staining (red) of the ends of the foot processes is extremely bright compared to that of the nuclei of the Müller glia cells. Because of this, the staining of the nuclei of the Müller glia cells is hard to distinguish in the glutamine synthetase staining. All in all the staining shows that the same cells are stained with both Nestin and glutamine synthetase and accordingly the Nestin positive cells and their foot processes are Müller glia.

Increased Nestin expression on mRNA level in Smad7^{fl/-} mice: To further confirm this finding, a real-time PCR for Nestin, using the retinae of 3 week old mice was performed (Figure 3.16 D). Similar to the result of the staining, a significant increase of Nestin mRNA in the Smad7^{fl/-} mice compared to their wildtype littermates was found.

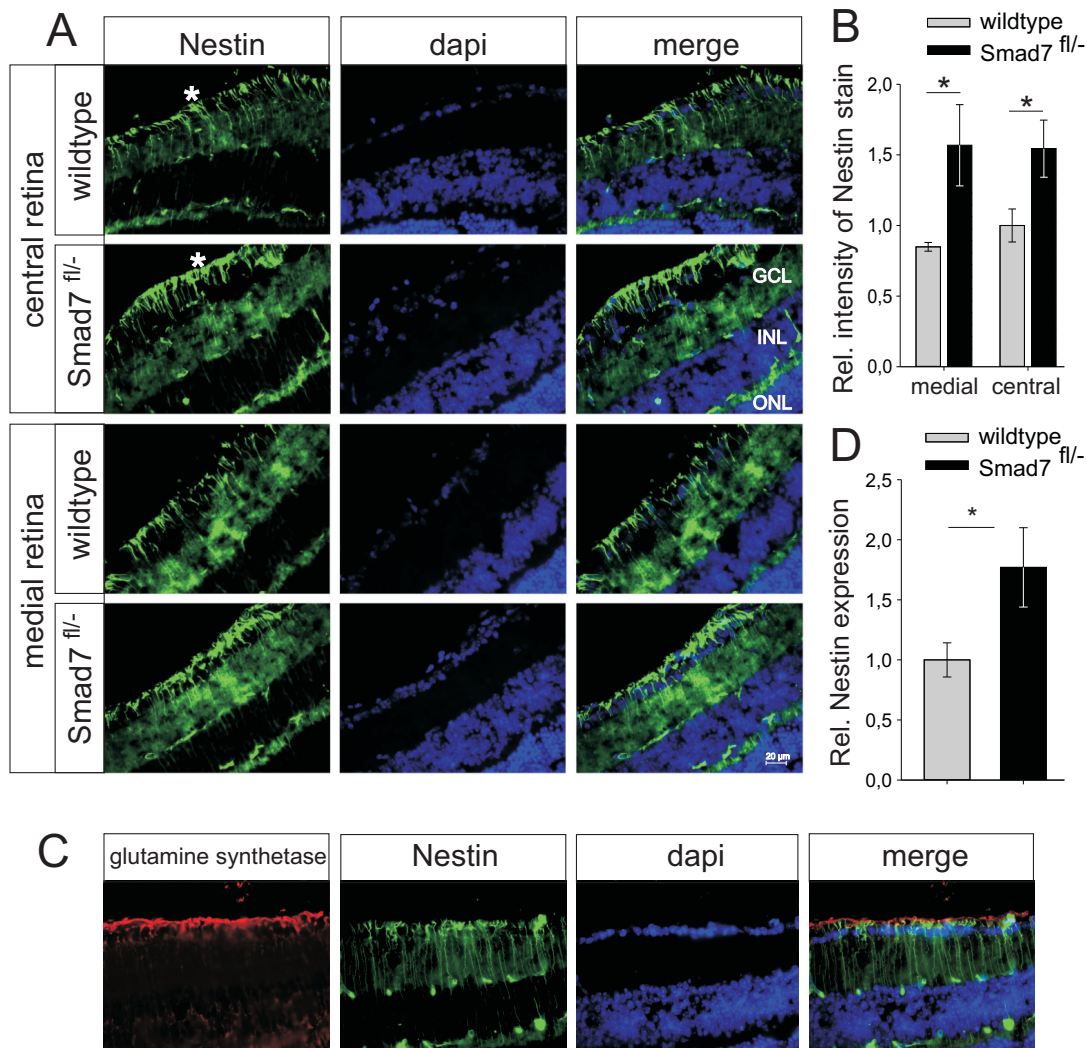


Figure 3.16: (A) Nestin staining of the central and medial retina of 3 week old mice. The Nestin staining (green) can be seen in the foot processes of the Müller glia that border on the vitreous humor. In the figure they are marked with an asterisk (*). (B) Measurement of Nestin staining intensity with ZEN ($n = 6$, $p = 0.041$, $p = 0.032$). The Nestin staining is significantly stronger in the Müller glia foot processes in the central and medial retina of $Smad7^{fl/-}$ mice than in their wildtype littermates. (C) Double-staining of glutamine synthetase (Müller cell marker, red) and Nestin (green). The stainings overlap in the processes and foot process tips of the Müller glia. Consequently the Nestin positive cells are Müller glia. (D) Nestin real-time data shows a significant increase in the Nestin level of retinal mRNA of 3 weeks old $Smad7^{fl/-}$ mice ($n = 11/9$ (wt/het), $p = 0.034$). ONL = outer nuclear layer, INL = inner nuclear layer, GCL = ganglion cell layer.

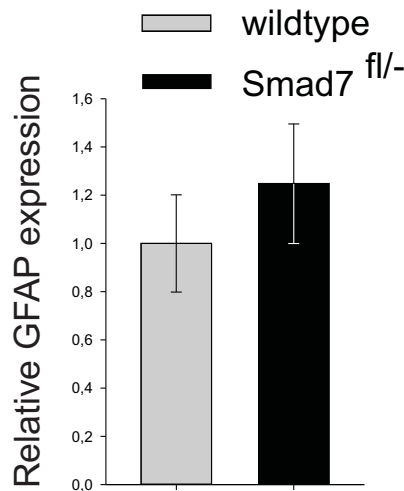


Figure 3.17: *GFAP real-time data: In untreated mice there is no significant difference in the GFAP levels on mRNA level of Smad7^{fl/-} mice and their wild-type littermates. (n = 12, p = 0.44).*

No increase in GFAP in Smad7^{fl/-} mice: To control if the rise in the Nestin level is due to a general activation, caused by an irritation in the retina, the GFAP level of the eyes was checked by real-time PCR. GFAP (glial fibrillary acidic protein) is a marker of activated Müller glia and astrocytes. This marker rises for example during inflammation, lesion gliosis or any irritation of the retina. For the experiment the retinal RNA of 3 week old mice was used.

As Figure 3.17 shows, there is no significant change in the GFAP mRNA level in the Smad7^{fl/-} mice. We conclude that there appears to be no general irritation of the retina.

Expression of Nestin in Müller glia cells of TGF- β RII^{fl/-} mice

Evaluation of Nestin expression by immunohistochemistry: The influence of a TGF- β RII heterozygous deletion on the activity of the Müller glia cells was tested by a Nestin staining in 3 week old mice. In unlesioned wildtype mice only the tips of the foot processes of the Müller glia facing the vitreous humor are Nestin positive (Figure 3.18 B). This is not altered by the TGF- β heterozygous deletion. The measurement data of the staining intensity, depicted in Figure 3.18 A, gave evidence that there is no difference in Nestin expression between TGF- β RII^{fl/-} and wildtype mice (n=5).

Evaluation of Nestin and GFAP mRNA level in vivo: To demonstrate the findings of immunohistochemistry, real-time measurements of the Nestin level in TGF- β RII^{fl/-} were done. Here, also no significant change in Nestin expression was found (Figure 3.19 A). Controlling the GFAP level to look for a general activation in the retina, a tendency to an increased GFAP level was found in TGF- β RII^{fl/-} mice. This could point to a general activation or irritation caused by the deficiency of TGF- β RII.

Nestin expression in vitro after TGF- β 1 treatment

As an *in vitro* test system primary rat Müller cell cultures were used. We were interested to see if a 24 h TGF- β 1 treatment could have the same effect on the Nestin expression as the Smad7 deficiency had. As can be seen in figure 3.20 the Nestin mRNA level does not rise *in vitro* after 24 h TGF- β 1 treatment. As the

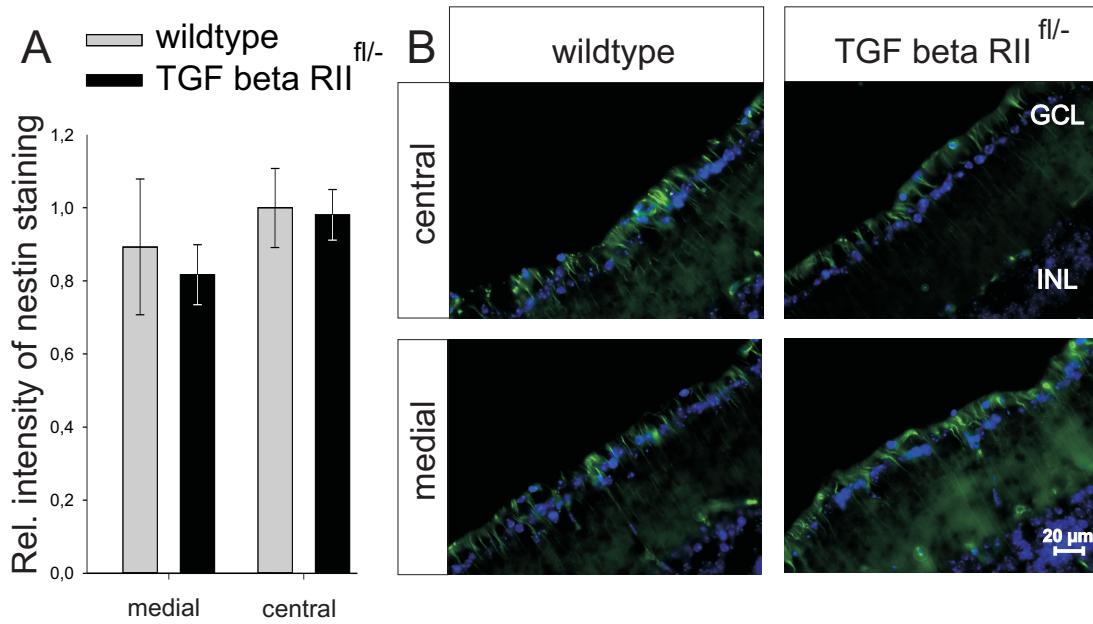


Figure 3.18: Nestin expression in untreated TGF- β RII^{fl/fl-} mice: (A) The relative Nestin expression in the Müller glia foot process tips was measured with the program ZEN from Zeiss in the medial and central retina. (B) The micrographs show the nuclei of the ganglion cell layer (blue) with the Müller glia foot processes (green) that border on the vitreous humor. The micrographs as well as the measurement in Figure A reveal no difference in Nestin expression in the foot processes of the Müller glia cells ($n = 5$). INL = inner nuclear layer, GCL = ganglion cell layer.

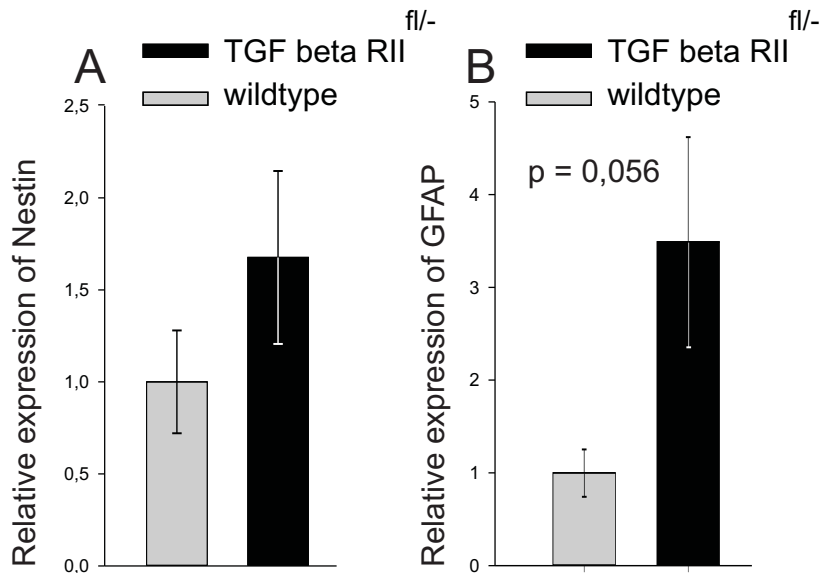


Figure 3.19: Figure A shows the real-time data of the Nestin and GFAP expression in TGF- β RII^{fl/fl-} mice and their wildtype littermates. Supporting the findings of the immunohistochemistry experiments, no alteration in the Nestin levels was found ($n = 5$). The GFAP real-time data in Figure B reveals a trend to an increased GFAP level in the TGF- β RII^{fl/fl-} mice. This could point to a general activation or irritation of the retina ($n = 6$, $p = 0.057$).

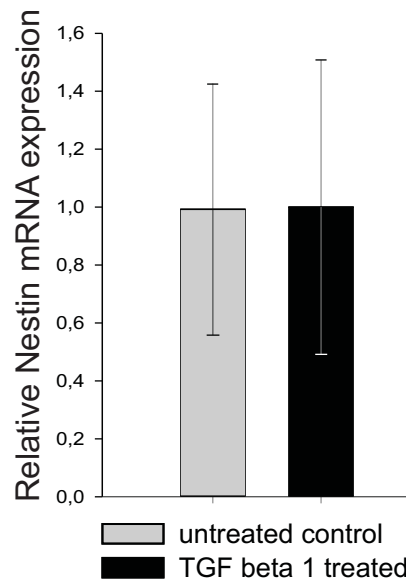


Figure 3.20: Nestin mRNA level in primary rat Müller glia culture after 24 h TGF- β 1 treatment: No change in Nestin level between TGF- β 1 treated and untreated Müller cells was found.

Nestin levels react to every lesion, it is possible that the levels in isolated Müller cells are already elevated, and can not be stimulated any further.

3.3.8 Activated pathways in Smad7^{fl/-} mice

As recent publications showed, a Smad7 deficiency could not only modulate the TGF- β pathway, but also the EGF pathway [152]. An increased EGF signaling would be a reasonable cause of increased proliferation in the retina. With this in mind, experiments were conducted to show if the TGF- β pathway is activated and if the EGF pathway plays a role causing the shown phenotype.

Activation of the TGF- β pathway - increase of pSmad3 in Smad7^{fl/-} mice

To examine the activation of the TGF- β pathway, western blot analysis for pSmad3, a receptor regulated Smad of the TGF- β pathway, was performed. The proteins used for the experiment were isolated from the retinae of 3 week old mice. The level of pSmad3 was markedly raised in the Smad7^{fl/-} mice ($n = 4/5$) (Figure 3.21). This indicates an activation of the TGF- β pathway. The housekeeper gene GAPDH was used as a control.

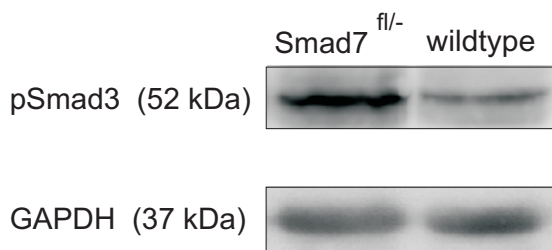


Figure 3.21: Western blot analysis of pSmad3: The protein pSmad3 was increased in Smad7^{fl/-} mice compared to their wildtype littermates ($n = 4/5$ (wt/het)).

No alterations in the EGF pathway in Smad7^{fl/-} mice

To examine an activation of the EGF pathway western blot experiments were conducted. As the experiments show, important proteins involved in the EGF

signaling like ERK, Akt are not altered in expression respectively phosphorylation (figure 3.22). Most likely the EGF pathway is not influenced by the Smad7 deficiency.



Figure 3.22: Western blot for pERK, Akt and pAkt on retina protein of 3 week old Smad7^{fl/fl} mice and wildtype littermates: None of the components of the EGF signaling is altered in expression or phosphorylation ($n = 5/4$).

3.4 NMDA lesions in Smad7 and TGF- β RII deficient mice

It is well documented, that under certain conditions retinal lesion models like NMDA lesions or light damage lead to an activation of retinal progenitor cells and even promote proliferation. Accordingly we performed lesion experiments in Smad7^{fl/fl} and TGF- β RII^{fl/fl} mouse models.

3.4.1 Axon number after an NMDA lesion

No effect on axon count after NMDA injection in Smad7^{fl/fl} mice

Before any experiments concerning the proliferation in the retina were conducted, we wanted to examine an eventual influence of the heterozygous deletion on cell death in the retina.

To analyze the influence of a lesion on cell death in Smad7^{fl/fl} mice, the axon number in the optic nerve after a lesion with NMDA was evaluated. For the experiment 6 week old mice were injected with NMDA in one eye and PBS, as a control, in the other eye. 3 weeks after the injection the mice were killed and epon semithin sections of the optic nerve were stained to count the number of axons via light microscopy. At this time after the lesion, most of the apoptotic ganglion cells and accordingly most of the killed axons were abolished. Examples for micrographs of PBS and NMDA treated nerves can be seen in Figure 3.23. As shown in Figure 3.24, no significant difference in axon number could be found between the Smad7^{fl/fl} mice and the wildtype littermates, neither after NMDA injection nor after PBS Injection. Smad7^{fl/fl} mice as well as wildtype animals react to the NMDA injection with loss of about 60% of axons.

No effect of TGF- β RII heterozygous deletion on axon number after NMDA lesion

By counting the axon number in the optic nerve after NMDA lesion, we also evaluated the influence of the heterozygous TGF- β RII deficiency on apoptosis in the retina.

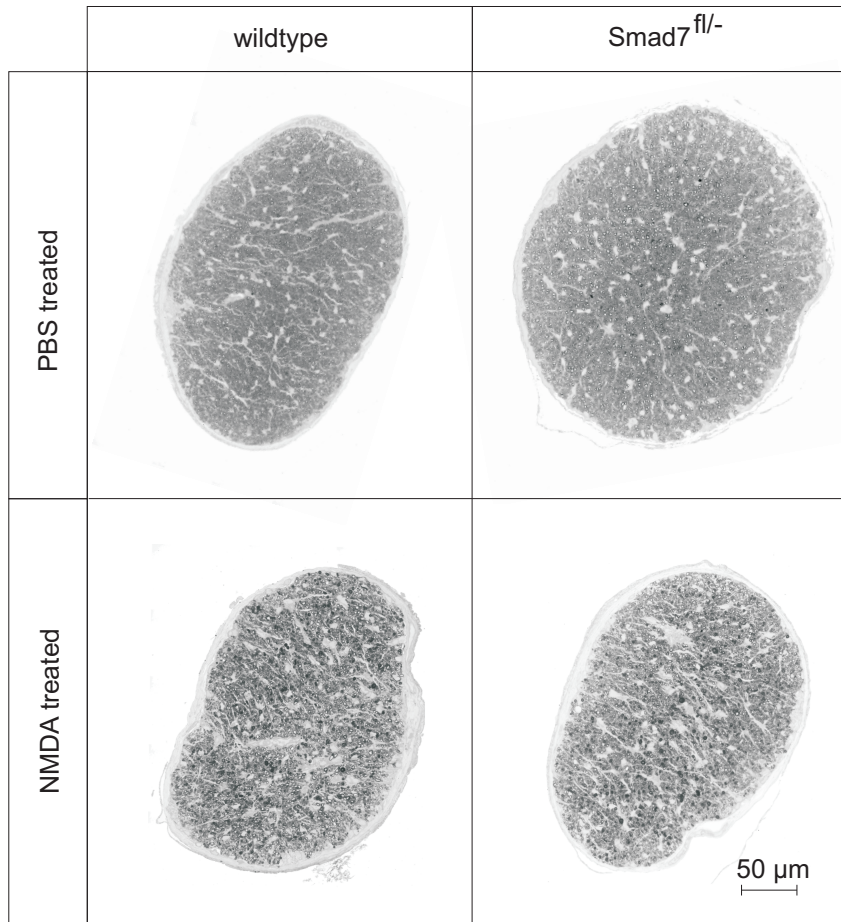


Figure 3.23: Morphology of a cross section of the optic nerve in Smad7^{fl/-} mice: Smad7^{fl/-} mice and their wildtype littermates show no apparent difference in the morphology of PBS and NMDA treated optic nerves (PBS n = 3, NMDA n = 3).

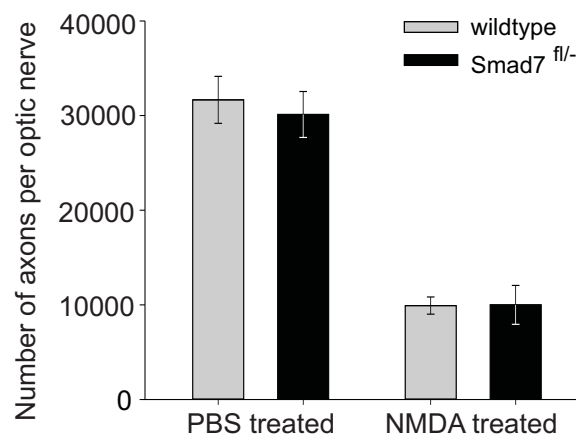


Figure 3.24: Axon count in NMDA treated Smad7^{fl/-} mice: Smad7^{fl/-} mice and their wildtype littermates show no difference in axon number in the optic nerve in PBS and NMDA treated eyes. In Smad7^{fl/-} and wildtype mice after NMDA injection about 60% of the axons are lost (PBS n = 3, NMDA n = 3).

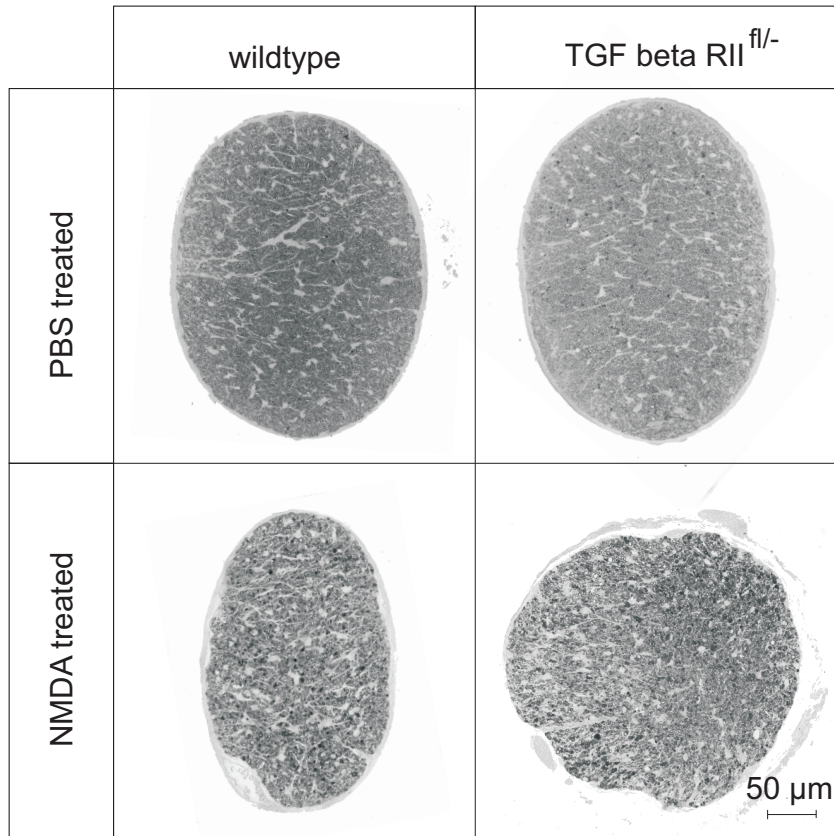


Figure 3.25: The micrographs of the optic nerve of TGF- β RII and wildtype mice show no morphological differences, neither in the PBS treated nor in the NMDA treated nerves (PBS $n = 3$, NMDA $n=3$).

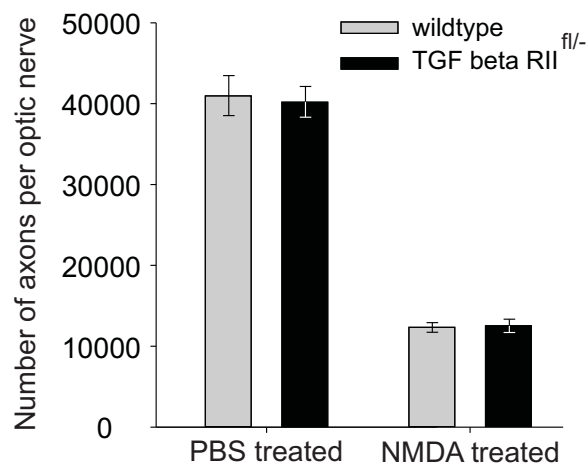


Figure 3.26: Total axon count of the optic nerves: In both genotypes, TGF- β RII^{fl/-} and wildtype, the axon number is about 75 % lower after the NMDA lesion. The TGF- β RII deficiency has no influence on the axon count, neither in PBS treated nor in NMDA treated optic nerves (PBS $n = 3$, NMDA $n=3$).

As in the $Smad7^{fl/-}$ mice, the eyes were injected with NMDA respectively PBS at an age of 6 weeks and were killed 3 weeks later. Epon sections of the optic nerve were used to count all axons in the PBS and NMDA treated nerves. The micrographs of TGF- β RII $^{fl/-}$ mice and wildtype mice show no difference in the morphology of the optic nerves, neither in PBS treated nor in the NMDA treated nerves (Figure 3.25). Figure 3.26 reveals the actual axon numbers. The axon number in TGF- β RII $^{fl/-}$ mice and wildtype littermates is at the same level in PBS treated eyes and is reduced by about 75% in NMDA treated eyes for both, TGF- β RII $^{fl/-}$ and wildtype mice. We conclude that the heterozygous deletion of TGF- β RII has no influence on the axon number after a lesion.

3.4.2 Retinal apoptosis after an NMDA lesion

Smad7 deficiency does not influence the amount of apoptosis after an NMDA lesion.

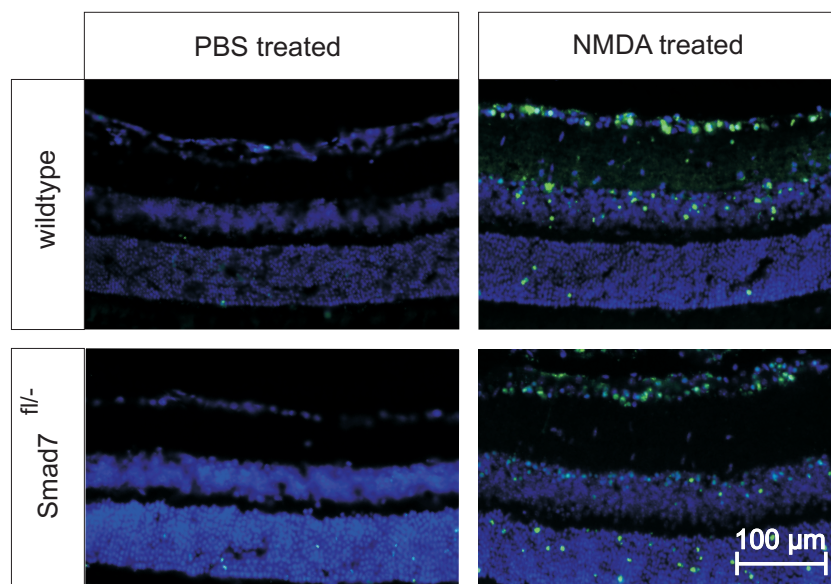


Figure 3.27: TUNEL staining (green) in NMDA treated retinæ: As expected the NMDA lesion causes apoptosis in ganglion cells and also in the inner nuclear layer. Comparing $Smad7^{fl/-}$ mice and their wildtype littermates there are no obvious differences in the amount or distribution of TUNEL positive nuclei (green). ONL = outer nuclear layer, INL = inner nuclear layer, GCL = ganglion cell layer.

To back up the result of the axon counting, and to see the effect of the $Smad7$ deficiency on apoptosis in the retina after a lesion, TUNEL assays were performed. These immunohistochemical assays stain the nuclei of apoptotic cells and were performed on sagittal retina sections, an example is shown in Figure 3.27. The TUNEL stained nuclei appear in green. For the sections, 6 week old mice were killed 24 h after NMDA injection. The sagittal cryo sections were TUNEL stained and TUNEL positive cells in both halves of the retina were counted and averaged for each eye. Figure 3.28 A shows a diagram with the number of TUNEL positive cells in half a retina, 3.28 B depicts the TUNEL positive cells of outer nuclear layer, inner nuclear layer and ganglion cell layer.

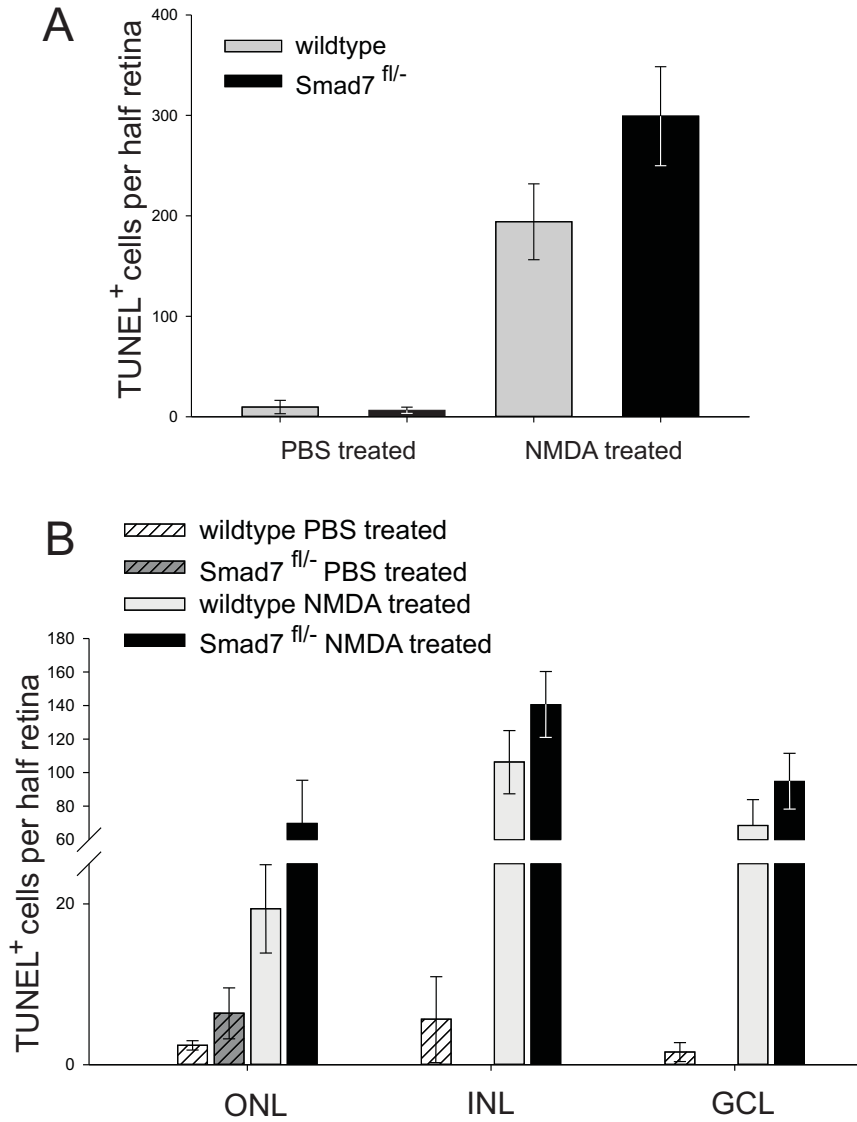


Figure 3.28: *TUNEL* positive cells after NMDA injection in *Smad7^{fl/-}* mice and their wildtype littermates. (A) Number of *TUNEL* positive cells in half of a retina: No significant difference in the number of *TUNEL* positive cells between the wildtype littermates and the *Smad7* deficient mice is visible. (B) Number of *TUNEL* positive cells in different layers: ONL = outer nuclear layer; INL = inner nuclear layer; GCL = ganglion cell layer. There is no obvious difference in the number of *TUNEL* positive cells in the different retinal layers comparing the *Smad7* deficient with the wildtype mice (PBS $n=6$, NMDA $n=5$).

The number of TUNEL positive cells in the whole retinae of the Smad7 deficient mice, as well as in the single retinal layers, showed no significant difference to the wildtype animals. It appears that the heterozygous deletion has no effect on the apoptosis after a lesion in the eye. Remarkably the NMDA lesion does not only damage the ganglion cell layer, but also the inner nuclear layer and even the outer nuclear layer, see Figure 3.28 B.

TGF- β RII deficiency does not influence the amount of apoptosis after an NMDA lesion

The apoptosis rate after NMDA lesion was also checked for TGF- β RII deficient mice, using TUNEL stainings like for the Smad7 deficient mice.

In Figure 3.29 A the data for TUNEL positive cells of the whole retina for the TGF- β RII deficient mice and the wildtype mice is shown. The data reveals no difference in apoptosis caused by the heterozygous deletion. The data for the different layers, see Figure 3.29, shows that not only the ganglion cell layer but also especially the INL is heavily damaged after an NMDA lesion. The more detailed data still reveals no difference between the TGF- β RII^{fl/-} mice and the wildtype.

3.4.3 Proliferation after NMDA treatment

No proliferation after NMDA injection in Smad7^{fl/-} mice

Karl et al. demonstrated that proliferation in mice can be induced by a lesion in the eye under special conditions [40]. To provoke a possible proliferative reaction in the retinae of Smad7^{fl/-} mice, 6 week old animals were lesioned with NMDA. To test for a possible proliferative reaction, BRDU was injected intraperitoneally at the time of the NMDA eye injection. After 24 h the mice were again injected with BRDU and killed 24 h after this last BRDU injection as depicted in Figure 3.30. Sagittal cryo sections of the cryo embedded eyes were stained for BRDU. Despite the high animal number of 9 mice per group no BRDU positive cells could be found in the mice retinae. We conclude that there appears to be no influence of the Smad7 deficiency on the proliferative reaction after lesion.

No proliferation after NMDA lesion in TGF- β RII^{fl/-} mice

To see if the heterozygous deletion of TGF- β RII allows a proliferative reaction after lesion, experiments were conducted with two different time delays between injection and killing of the mice.

For the first experiment the mice that had been used for the TUNEL experiment (3.4.2) were additionally injected with BRDU at the day of NMDA injection and killed 24 h later. This way the reaction after 24 h and a possible connection with the ongoing apoptosis could be tested, as the sections of the mice were also stained for TUNEL positive cells.

As the retinae of the mice killed 24 h after NMDA injection were examined for BRDU positive cells, only three of eleven animals (6 wt/5 het) showed sporadic positive cells in the outer nuclear layer. Examples are shown in Figure 3.31. These were the same animals that revealed the strongest lesion in the outer nuclear layer in the TUNEL experiment, but the reaction did not depend on the genotype. In

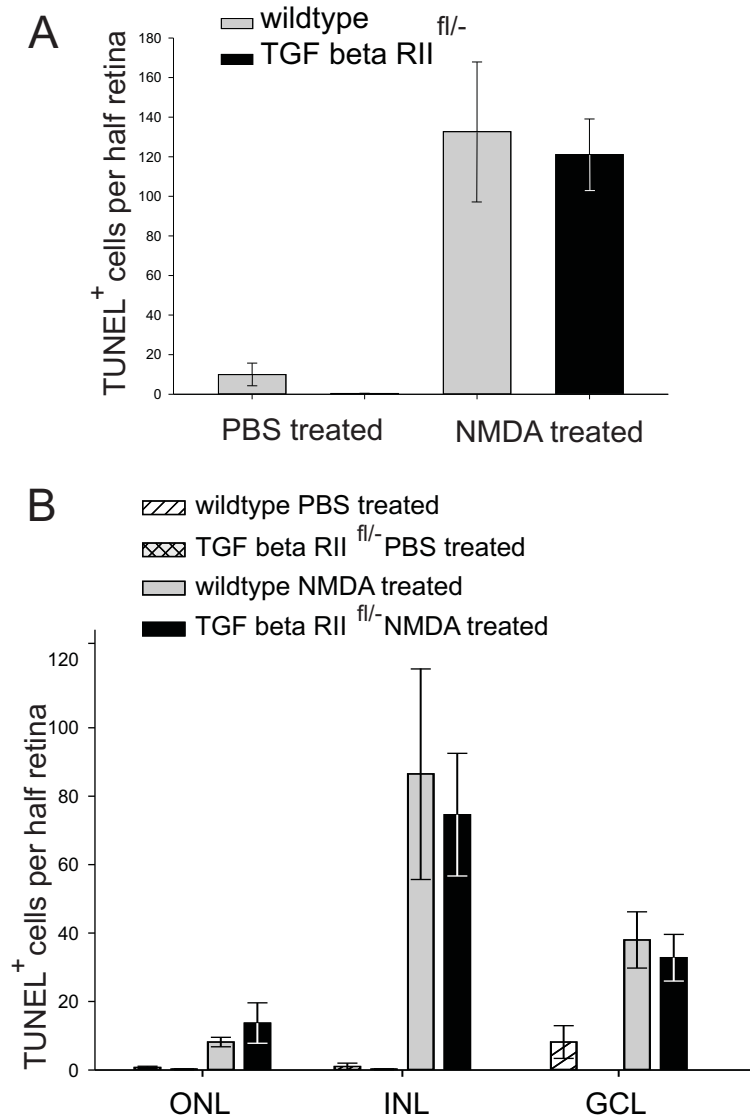


Figure 3.29: Figure A shows the number of TUNEL positive cells in TGF- β RII deficient mice after NMDA/PBS injection averaged over both halves of the retina. There are no significant differences in the number of TUNEL positive cells comparing TGF- β RII to wildtype mice, neither in the PBS, nor in the NMDA treated retinae. In Figure B the detailed number of TUNEL positive cells in different layers of the retina is shown. Besides the expected lesion on the ganglion cell layer, the NMDA lesion causes a vast lesion in the inner nuclear layer, but the TGF- β RII heterozygous deletion has no influence on the number or distribution of dying cells ($n = 6/5$ (wt/het)). ONL = outer nuclear layer; INL = inner nuclear layer; GCL = ganglion cell layer.

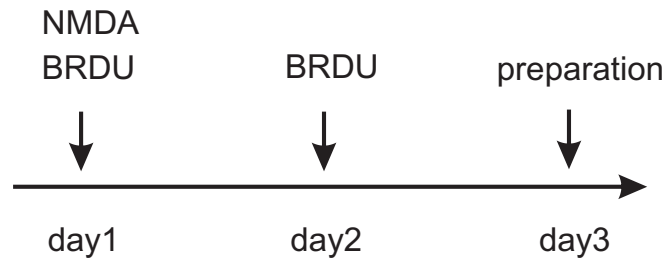


Figure 3.30: Scheme of NMDA and BRDU injections.

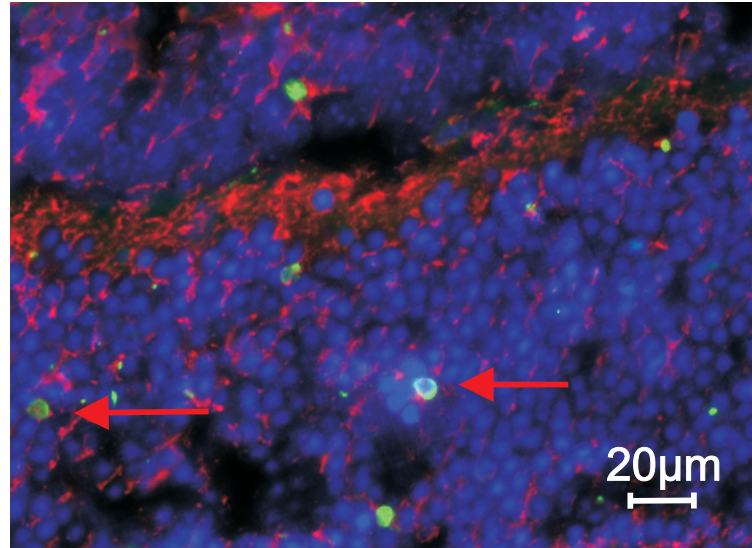


Figure 3.31: BRDU positive cells in the outer nuclear layer of NMDA lesioned TGF- β RII- deficient mice 24h after NMDA injection: The cells show up in animals with a strong lesion of the outer nuclear layer, independent of the genotype and disappear 2 days after injection. This appears to be a effect of DNA repair.

11 animals only one BRDU positive Müller glia cell was found. For the second experiment TGF- β RII deficient mice and wildtype littermates were killed two days after the NMDA injection as depicted in figure 3.30 like in the Smad7 model (n = 6 wt/11 het). In these retinae, no BRDU positive cells were found in the outer nuclear layer. Some scattered BRDU positive cells were found in the ganglion cell layer.

3.4.4 Nestin and GFAP expression after NMDA treatment

Nestin and GFAP expression after NMDA treatment in Smad7^{fl/-} mice

A possible influence of the Smad7 deficiency on the activation of Müller glia cells can be analyzed by performing a Nestin staining after the NMDA lesion. For the experiment, 6 week old mice were injected with NMDA and killed 3 days later.

The effect of an NMDA treatment on the Nestin level of the Müller glia cells can be seen for example in Figure 3.32 where the processes of the Müller glia cells appear in green (Nestin) after the NMDA lesion. This points to an increased Nestin expression after the NMDA injection, which is a well known reaction after any lesion in the eye. For a statistical analysis, the stainings were rated with the

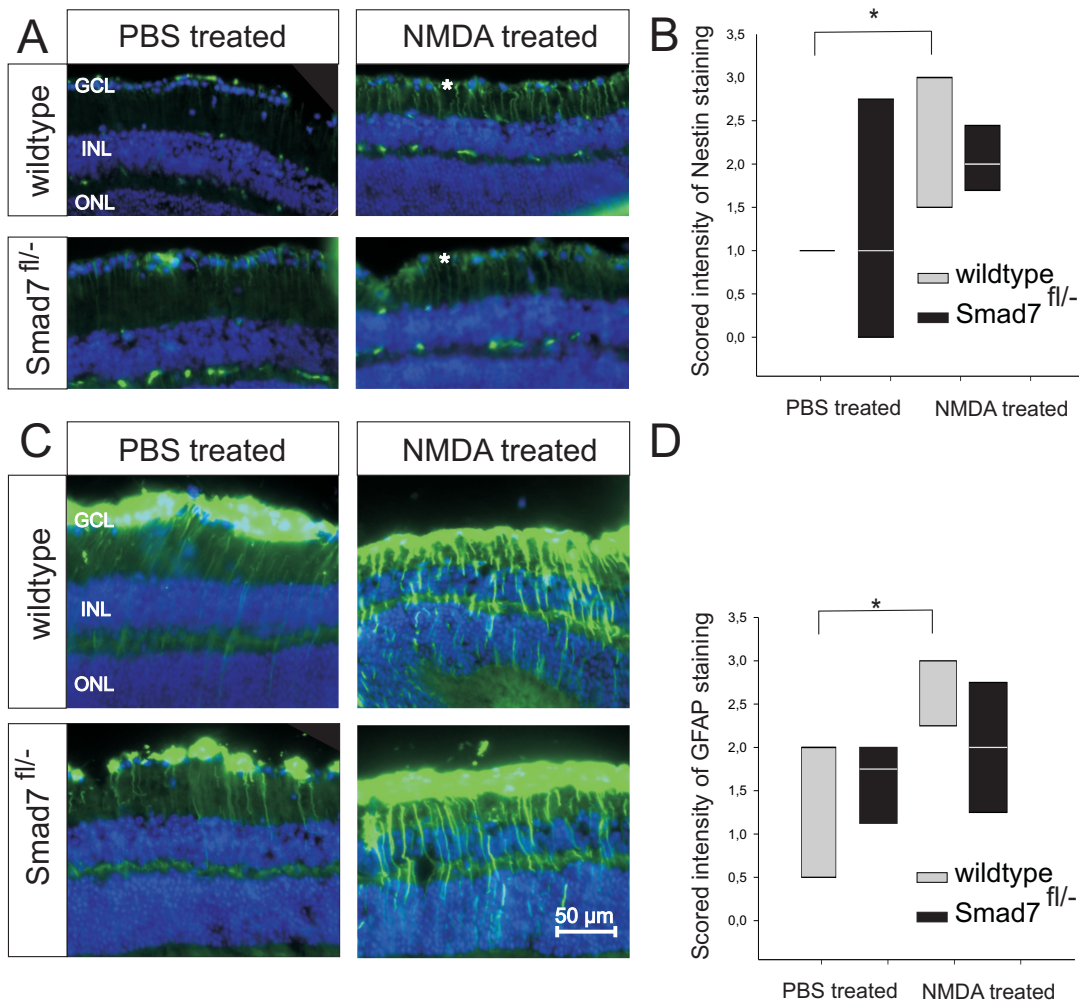


Figure 3.32: Nestin and GFAP expression after NMDA lesion in *Smad7^{fl/fl}* mice: (A) Nestin staining after NMDA/PBS injection: Comparing the staining after PBS and after NMDA injection, it can be seen that the Nestin level in the Müller glia foot processes (marked with an asterisk (*)) rises significantly after NMDA injection. (B) Using the scoring method, it could be shown that the Nestin level rises significantly in the wildtype mice, but not in the *Smad7^{fl/fl}* mice. This is owed to the higher base level of the Nestin staining in the PBS treated *Smad7^{fl/fl}* mice eye, that was already found in 3 week old mice, see section 3.3.7 ($n = 7/4/4/4$, $p = 0.042$). (C) The micrographs in this figure show an obvious elevation in GFAP expression in Müller glia cells after NMDA injection in *Smad7^{fl/fl}* mice and their wildtype littermates. This is a well known reaction of Müller glia cells to a lesion. The *Smad7* deficiency itself appears to have no influence on the GFAP expression and accordingly on the activation of the Müller glia cells. As the focus lay on the Müller glia cells the staining in the ganglion cell layer, caused by GFAP positive astrocytes was not taken into account in the scoring. (D) The GFAP level was evaluated using the scoring method because of the background staining ($n = 5/4/4/4$, $p = 0.037$). ONL = outer nuclear layer; INL = inner nuclear layer; GCL = ganglion cell layer.

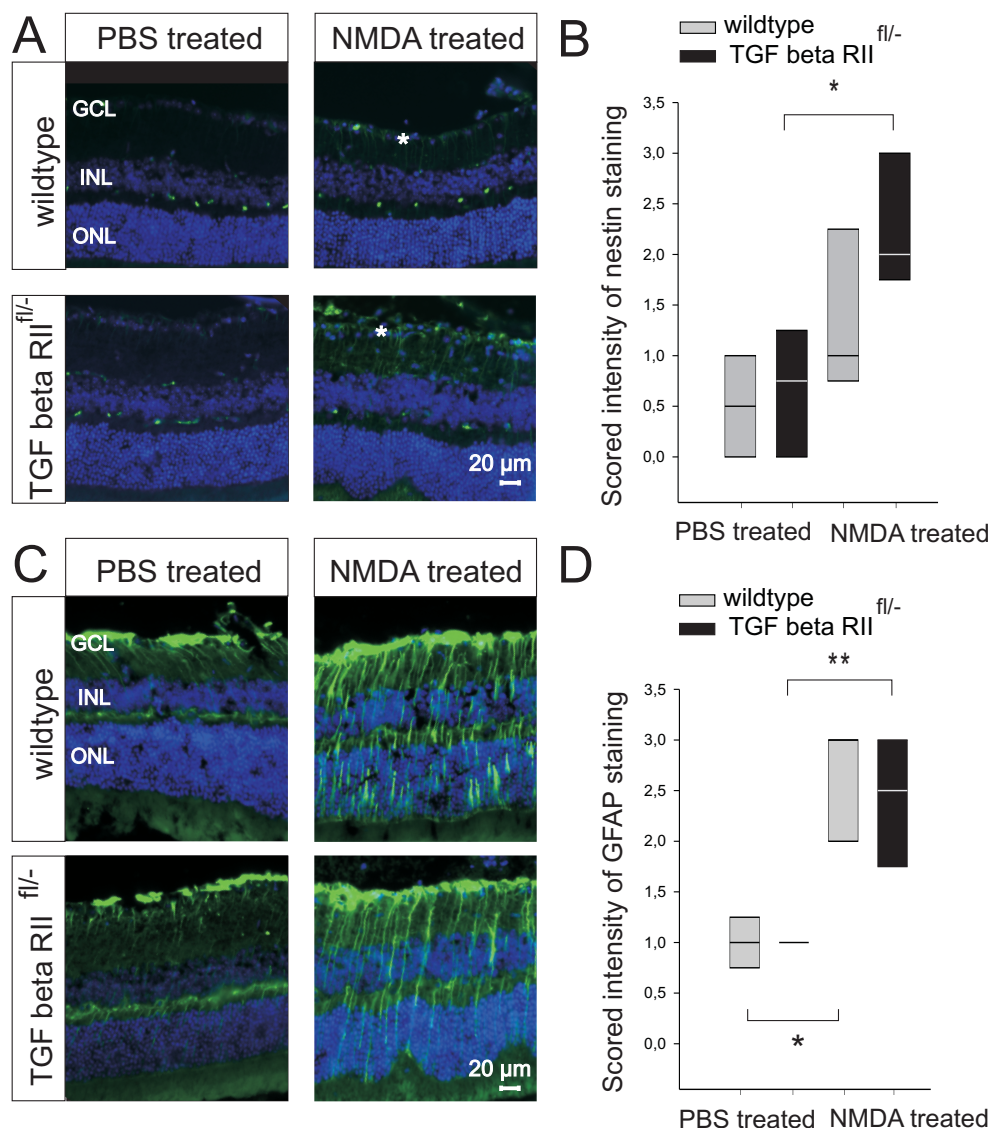


Figure 3.33: (A) The micrographs show Nestin stained retinæ from TGF- β RII^{fl/-} mice and their wildtype littermates. After NMDA injection, only a slight reaction in the form of Nestin expression is visible in the Müller glia foot processes (marked with an asterisk (*)) in TGF- β RII^{fl/-} mice and wildtypes. (B) With the scoring method, it can be seen that the heterozygous TGF- β RII^{fl/-} mice show a significant rise in Nestin expression. No significant difference can be found after the NMDA injection in wildtype mice. (C) Micrographs in this figure show a GFAP staining after an NMDA injection in TGF- β RII deficient mice and their wildtype littermates. The strong reaction of both, TGF- β RII^{fl/-} mice and wildtype littermates, to NMDA can easily be seen. (D) Using the scoring method, the GFAP staining intensity can be compared. In the wildtype littermates as well as in the TGF- β RII deficient mice a significantly higher GFAP expression can be found after NMDA injection, but the TGF- β RII deficiency does not appear to influence the GFAP expression. ONL = outer nuclear layer; INL = inner nuclear layer; GCL = ganglion cell layer.

scoring method, as described in sec. 2.4.12. This method is used when background stainings have a strong influence on the result of intensity measurements.

The graph in Figure 3.32 shows that the Nestin level rises significantly after an NMDA injection in wildtype mice. It also rises in Smad7^{fl/-} mice but not to a significant level. There appears to be no significant influence of the Smad7 deficiency on the reaction and activation of the Müller glia cells.

This experiment has also been done in an analogous way for GFAP (Figure 3.32). Here, the well documented rise in expression of GFAP after a lesion could also be found. But as in the experiment with Nestin, no significant difference between the Smad7^{fl/-} and the wildtype mice can be seen.

Nestin and GFAP expression after NMDA treatment in TGF- β RII^{fl/-} mice

The experiments were also carried out for the TGF- β RII deficient animals (Figure 3.33). Besides the anticipated increase of expression of Nestin and GFAP following the NMDA injection, no difference in reaction caused by the TGF- β RII deficiency could be found. We conclude that a deficiency of TGF- β RII has no influence on the activation of Müller glia cells after an NMDA lesion.

3.5 β -B1-CTGF overexpressing mice

As Connective tissue growth factor (CTGF) is a target protein of the TGF- β pathway, and is usually upregulated when the TGF- β pathway is activated, we wanted to see if an overexpression of CTGF in the eye had the same effect as a Smad7 deficiency. For this purpose mouse models were used that overexpress CTGF to different levels in the lens. Strain 1 has a low level of expression of CTGF, in Strain 5 the expression is higher and Strain 6 shows the highest levels. The strains were bred and provided by Benjamin Junglas and Rudolf Fuchshofer [153].

3.5.1 Increased retinal thickness

Interestingly the overexpression of CTGF leads to an impressive thickening of the retina. This effect is starting at the central retina in strain 1 where CTGF is expressed at low levels, and spreads over the whole retina as the CTGF levels rise in strains 5 and 6, see Figure 3.34. In strain 6 the retina of the CTGF overexpression mice is more than 20% thicker than in the wildtype animals. The effect of this dose dependent thickening can also be seen in the inner nuclear layer, which is also more than 20% thicker in strain 6 animals than in the wildtype mice.

3.5.2 Number of Müller glia cells

As the inner nuclear layer was thickened, we were interested in the number of Müller glia analogous to the experiments on Smad7^{fl/-} mice. Again 3 week old mice were used and the counting was done with the help of a glutamine synthetase staining. Also, counting and statistics were done analogous to the experiments with the Smad7 mice. But contrary to the Smad7 mice, no significant effect on the number of Müller glia was found in these mice, regardless of expression intensity.

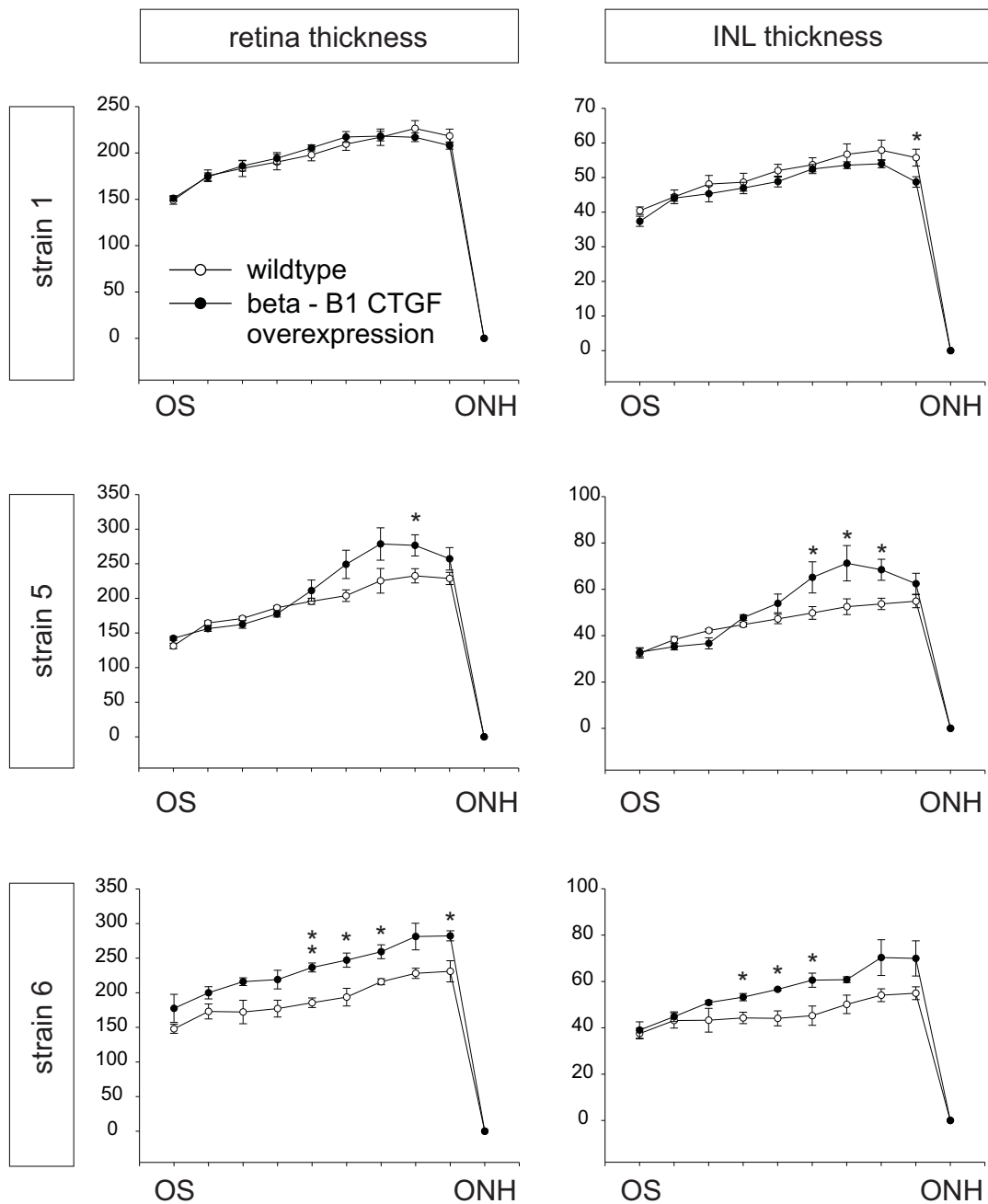


Figure 3.34: Measurement of retina thickness in different Connective tissue growth factor (CTGF) overexpressing strains. The thickening effect of the whole retina and the inner nuclear layer rises with the CTGF expression in the different mouse lines (strain 1: $n = 6/6$; strain 5: $n = 7/6$; strain 6: $n = 3/3$; $p < 0.05$).

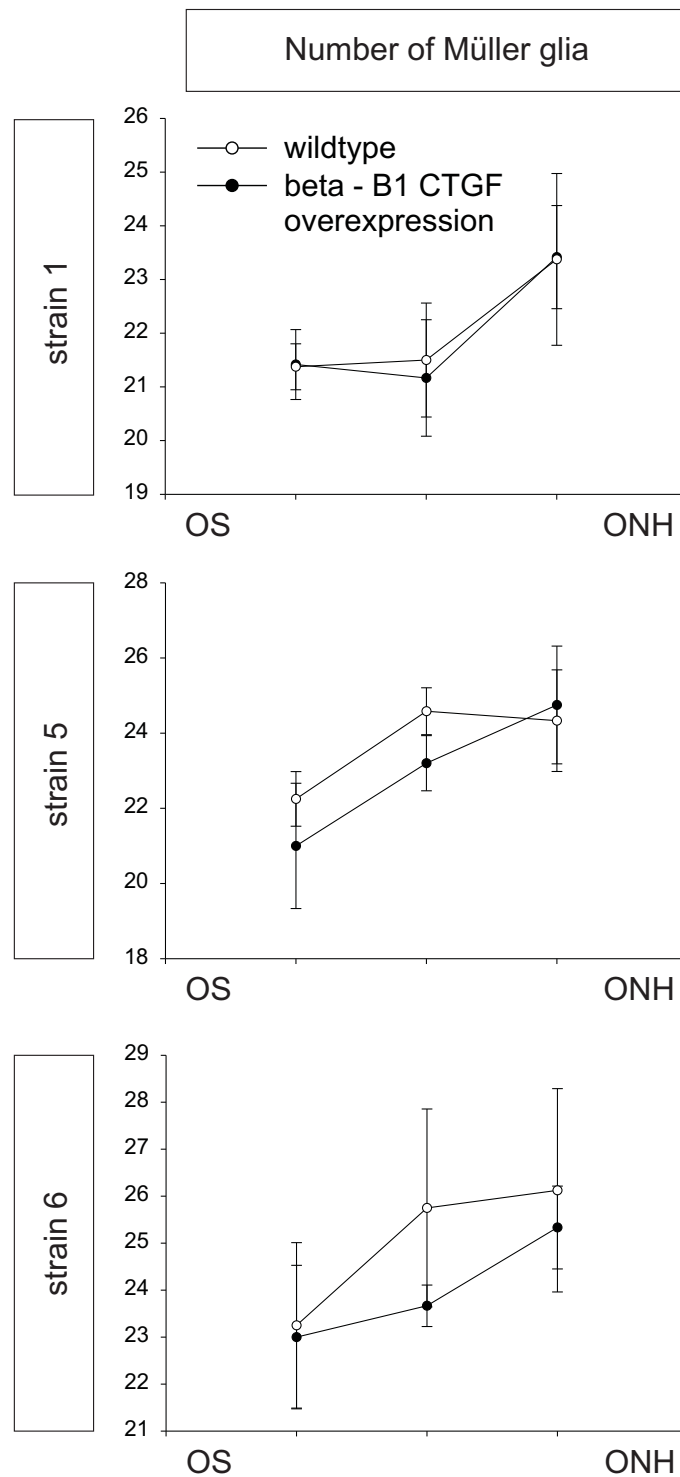


Figure 3.35: The number of Müller glia cells was evaluated in the central (close to the optic nerve head), medial and peripheral (close to the ora serrata) retina of the three CTGF overexpressing strains. In none of the strains a significant difference could be found. The number of Müller glia is not influenced by an overexpression of CTGF (strain 1: $n = 4/6$, strain 5: $n = 6/5$, strain 6: $n = 4/3$, $p < 0.05$). OS = Ora serrata; ONH = optic nerve head.

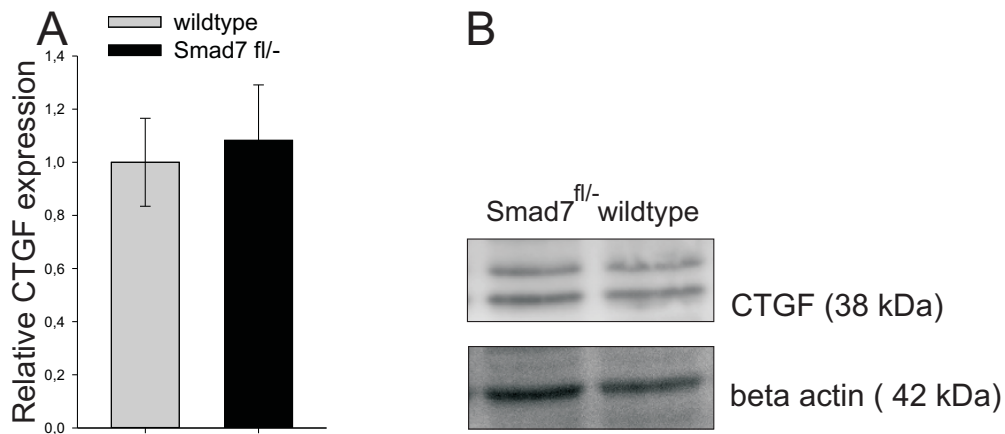


Figure 3.36: (A) Real-time PCR for CTGF in 3 week old $Smad7^{fl/-}$ mice: The mRNA level of CTGF is not significantly altered in $Smad7^{fl/-}$ mice ($n = 12/11$ (wt/het)). (B) Western blot for CTGF with retina protein from 3 week old $Smad7^{fl/-}$ mice and wildtype littermates: Similar to the result of the real-time PCR, the CTGF protein level is not altered in the $Smad7^{fl/-}$ mice. The housekeeper β -actin was used as a control ($n = 4/5$ (wt/het)).

No alteration in CTGF levels in $Smad7^{fl/-}$ mice

As CTGF is a target gene of the TGF- β pathway we speculated that the thickening in the retina of the CTGF overexpressing mice could be the same effect as seen in the $Smad7^{fl/-}$ mice. Since we did not observe changes in the number of Müller cells in the CTGF overexpressing mice, the CTGF level of 3 week old $Smad7^{fl/-}$ mice and their littermates was evaluated by quantitative real-time PCR using retinal RNA.

As Figure 3.36 A shows, no significant change could be found in the level of CTGF. Western blot analysis for CTGF showed no difference in the protein levels between the wildtype animals and the $Smad7$ deficient mice as well (figure 3.36 B), indicating that the proliferative effect, seen in the $Smad7$ deficient mice is not mediated through CTGF elevation. Nevertheless CTGF itself could possibly promote neuronal survival or increased proliferation, since the ONL and the INL are significantly thicker in those animals compared to the wildtype. But this could as well be an effect of increased extracellular matrix.

Chapter 4

Discussion

Based on the results presented in chapter 3, we conclude that TGF- β signaling has a significant effect on proliferation. It influences proliferation during development of the central retina, but its alteration does not provoke proliferation in the normal and injured adult retina. This conclusion rests upon:

- the generation of genetically modified mouse models, with a diminished or enhanced overall TGF- β signaling during development.
- the finding of an increase in the number of Müller glia along with enhanced thickness of the inner nuclear layer in mice with enhanced TGF- β signaling.
- the observation of increased proliferation during the development of the postnatal retina at P4, where the peak of Müller glia proliferation is observed, and the absence of influence on programmed cell death in retinal development in these mice.
- the increased expression of Nestin, a progenitor cell marker, in the central retina at P20 in mice with enhanced TGF- β signaling.
- the almost complete lack of Müller cell proliferation after exitotoxic damage in animals with diminished or enhanced TGF- β signaling.

In the following, we will discuss these results in detail.

4.1 Generation of mouse models with diminished or enhanced TGF- β signaling

With the help of the Cre LoxP system we were able to generate a mouse model deficient for Smad7, an inhibitor of TGF- β signaling, by deleting the floxed promoter region and exon I using the EIIa Cre recombinase. It was not possible to work with a homozygous deletion, because this turned out to be lethal at a late embryonic stage. The Smad7 deficiency could be demonstrated on mRNA level. Additionally, we could show by western-blot analysis for pSmad3, a receptor regulated Smad of the TGF- β pathway, that the TGF- β signaling in these animals was enhanced.

To generate a comparable model for a diminished TGF- β pathway, we used an analogous model to create TGF- β receptor II deficient mice by a heterozygous deletion of exon II of TGF- β receptor II. The TGF- β receptor II deficiency could be shown on protein level.

4.2 Influence of an altered TGF- β signaling on retinal thickness and cell number

4.2.1 Smad7 deficiency causes a thickened retina around the optic nerve head

In our study, the heterozygous deletion of Smad7 lead to a significantly thickened central retina at P20, including a thickened inner nuclear layer with an elevated number of Müller glia, as well as a thickened outer nuclear layer pointing to an increased number of photoreceptors. It is well possible that increased numbers of bipolar cells, amacrine cells or horizontal cells also contribute to the thickening of the inner nuclear layer.

The findings displayed show that an alteration of the TGF- β pathway affects different cell types in the retina. It is therefore tempting to speculate that this effect occurs very early in development, affecting the common progenitor cells of neurons and glia.

4.2.2 Induceable TGF- β RII homozygous deletion causes a thinned retina

As the heterozygous TGF- β RII deletion had no effect on retina thickness, we worked with an induceable mouse model with a homozygous deletion for TGF- β RII. For this mouse model, Tamoxifen induceable CAG Cre mice were crossed with TGF- β RII^{fl/fl} mice. The mice were bred and kindly provided by Barbara Braunger. The resulting induceable homozygous deletion of TGF- β RII in the retina caused an overall thinned retina. This appears to be an effect contrary to the retina thickening in the Smad7^{fl/-} mice.

4.3 Influence of the TGF- β pathway on proliferation and stem cell renewal

4.3.1 Increased proliferation in Smad7 deficient mice

Since the number of Müller cells was significantly elevated in the Smad7 deficient mice, we decided to investigate a possible pro-proliferative effect of the deficiency. For these experiments, P4 as the natural peak of Müller glia cell proliferation was chosen. Indeed, a significantly raised number of BRDU positive cells was found in the central retina of four day old mice. This indicates an increased proliferation as the cause of the thickened retina. An alteration in the apoptosis rate in the retinae could not be found at P8, the peak of Müller glia apoptosis. This, however, does not exclude a changed apoptosis rate in other stages of development.

	enhanced self renewal	prolonged proliferation	decelerated proliferation
more BRDU positive cells	+	=	+
increased final cell number	+	+	=

Table 4.1: An increased number of BRDU positive cells can be caused by enhanced self renewal or decelerated proliferation. An increased final number of cells can originate from enhanced self renewal and a prolonged proliferation period. Only an enhanced capacity for self renewal can cause both effects.

For the determination of the exact effect of Smad7 deficiency on cell proliferation, we gathered two main data points: In P20 we found an elevated number of Müller glia and a thickened retina, while in P4 an elevated number of BRDU positive cells was found.

Considering cell proliferation as cause for the elevated final number of retinal cells in P20, two effects could be responsible: The phase of proliferation could be prolonged in the retina of the newborn animal, or more stem cells could be proliferating in the same time frame. Both would lead to a higher final cell count in the retina of the adult animal. If we assume the same starting amount of cells, an increased number of proliferating cells at the same time can only be caused by an enhanced ability for self renewal.

Regarding the proliferation data in P4, the increased number of BRDU positive cells could also have two different reasons. On the one hand, single stem cells could require a prolonged time for one cell cycle, and in this way more cells could be seen proliferating at once. This would, however, not lead to an increased final cell count.

On the other hand, the cells could proliferate at normal speed but undergo additional rounds of proliferation, pointing to an enhanced self renewal capacity. This would also lead to an increased number of BRDU positive cells at any given time, if one assumes the same starting amount of stem cells.

Considering both, P4 and P20 data, we conclude that an enhanced self renewal capacity of the stem cells can explain our findings, see Table 4.1. This does not exclude that the timespan of proliferation could be additionally prolonged in the Smad7 deficient mice.

4.3.2 Direct effects of TGF- β on adult neural cells and embryonic stem cells

In our study, deficiency of Smad7 and enhanced TGF- β signaling lead to a thickened retina, increased proliferation and supposedly enhanced stem cell renewal.

Contrary to this, most publications working with effects of TGF- β on *adult* neural stem cells show TGF- β as an inhibitor of stem cell proliferation [70,88,100] or as a protector of stem cell quiescence [154]. TGF- β also had an anti-proliferative effect *in vitro* in retinal postnatal progenitors [102].

On the other hand, TGF- β was shown to have pro-proliferative effects and influences differentiation in *embryonic* stem cells: Watabe et al. showed that the treatment of ES cells with an inhibitor for type I receptor kinases (e.g. TGF- β RI), lead to a decrease of proliferation. This suggests that TGF- β , activin or nodal

is needed for the proliferation of embryonic stem cells [94]. In undifferentiated human embryonic stem cells TGF- β , activin or nodal signaling were observed, and their expression decreased upon early differentiation [95]. An inhibition of the TGF- β /activin/nodal signaling by SB431542 resulted in decreased expression of markers of undifferentiated cells [96–98]. This implies that TGF- β keeps the stem cells from differentiating and therefore supports self renewal.

The effects on proliferation and differentiation are similar to the ones occurring in our Smad7^{fl/-} mice. This suggests that the retina is thickened due to an effect on early stem cells. The described facts can be brought into line if one assumes that the retinal stem cells change their reaction to TGF- β in a certain phase of differentiation, as implied by the earlier findings described above.

Besides a direct effect of the altered TGF- β pathway, it is also possible that Smad7 or other components of the TGF- β pathway interact with other pathways or act through other mediators.

4.3.3 CTGF as a potential mediator

Connective tissue growth factor (CTGF) has been identified as a critical downstream mediator of TGF- β [155] signaling acting on the proliferation of connective tissue cells. It is additionally known to have a proliferative role in some cancer cell lines [156].

In a further part of our studies, mice with an overexpression of the connective tissue growth factor (CTGF) in the lens showed an extremely thickened retina similar to the less pronounced phenotype seen in the Smad7^{fl/-} mice. With rising concentrations of CTGF in CTGF overexpressing mouse strains, the thickening starts at the optic nerve head and gradually spreads until the whole retina is affected in the mouse strain with the highest CTGF expression.

These findings led to the hypothesis that the thickened retina in the Smad7^{fl/-} mice could be caused by a stronger TGF- β signaling and in turn a stronger CTGF signaling resulting in enhanced cell proliferation in the retina.

Contrary to this hypothesis, the CTGF overexpressing mice showed no difference in the number of Müller glia as the Smad7 deficient mice did, even as the retina was much more thickened than in the Smad7 deficient mice. This again could be evidence that the mechanisms leading to thickening in both cases are different from each other. It is for example well possible, that the thickening of the retina of the CTGF overexpressing mice can not be explained by a higher cell mass but by a expression of matrix proteins like proteoglycan. The proposition that both effects are of different origin is supported by the fact that in real-time PCR no elevated level of CTGF could be found in the retinae of Smad7^{fl/-} mice at P20.

4.3.4 Possible influence of an crosstalk between TGF- β and EGF-pathway on proliferation

Krampert et al. found that Smad7 modulates the neural stem/progenitor cell proliferation TGF- β - and BMP-independently in the brain [157]. They showed that enhanced proliferation after a Smad7 Exon1 deletion might be at least partially mediated by elevated signaling via the epidermal growth factor (EGF) receptor,

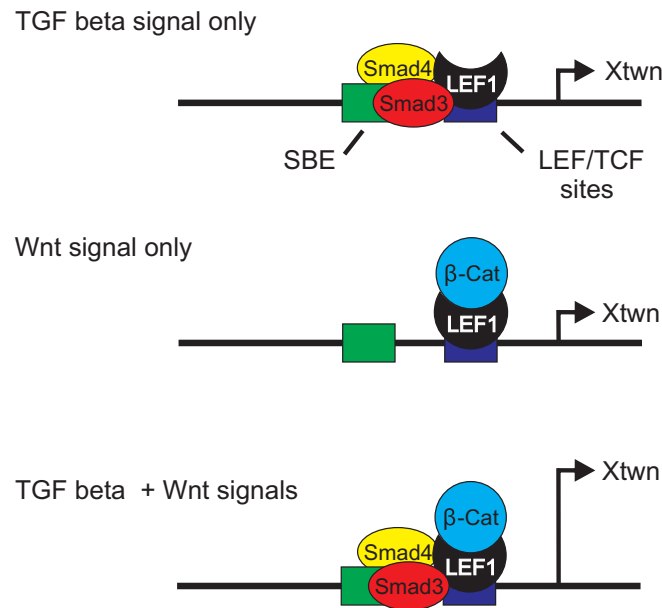


Figure 4.1: Crosstalk between the Wnt pathway and the TGF- β pathway during the activation of *Xtnw*, a target gene (Figure adapted from: [161]).

as the mutant cells showed higher expression and activation levels of the EGF receptor. Additionally this proliferation could be reduced by an EGF receptor inhibitor.

Also in cancer cells, which often act similar to stem cells, TGF- β was found to stimulate proliferation in some cases by crosstalk with the EGF pathway. Colon carcinoma cells for example are stimulated to proliferate by TGF- β via a Ras dependent mechanism [158, 159].

Having these findings in mind we tested the *Smad7^{fl/-}* mice for an activation of the EGF pathway by using western blot experiments. It could be shown that important proteins involved in the EGF signaling like ERK and Akt were neither altered in expression nor phosphorylation. The EGF pathway is therefore most likely not altered by *Smad7* deficiency.

4.3.5 Possible influence of an crosstalk between TGF- β and Wnt-pathway on proliferation

An interesting further potential cause for the increased proliferation in the *Smad7* deficient mice is the crosstalk between the wingless Type (Wnt)-pathway and the TGF- β pathway. The Wnt-signaling pathway is a known modulator of stem cell maintenance, cellular proliferation and differentiation [160].

Briefly, in the absence of Wnt signaling, glycogen synthase kinase 3 (GSK-3) phosphorylates β -catenin. This induces ubiquitination and degradation of β -catenin. When Wnt signaling is activated, GSK-3 activity is inhibited and β -catenin can accumulate and translocate to the nucleus. In the nucleus it associates with members of the lymphoid enhancer binding factor family (LEF/TCF). These are DNA binding proteins that activate targets of the Wnt pathway in association with β -catenin. Letamendia et al. showed that Smads physically interact with

LeF1/TCF and in this way cooperate to express *Xtwn*, a Wnt and TGF- β target gene (Figure 4.1) [161].

Taking the crosstalk between the two pathways into consideration, a hypothesis would be that a downregulation of the TGF- β pathway could cause a compensating upregulation of the Wnt pathway, resulting in an enhanced stem cell maintenance and a thickened retina due to enhanced stem cell renewal.

4.4 The possible role of Nestin in the progenitor cell population

4.4.1 Increased Nestin expression in *Smad7* deficient mice

In *Smad7^{fl/-}* mice an increased expression of Nestin, an important marker for neural stem/progenitor cells, was found at P20 in the central retina. This applies particularly to the foot processes of the Müller glia, facing the vitreous body, and was demonstrated in immunohistochemistry as well as on RNA level.

4.4.2 Nestin expression as a sign of activation, gliosis and structure stabilization

In general an increased Nestin expression is considered a sign of active Müller glia cells, e.g. going into gliosis or preparing for migration or proliferation. Together with an increased GFAP level it could point to a gliotic reaction, but the GFAP RNA level was not increased in the retinæ of these mice. In the case of gliosis, Nestin works as a stabilizing element that supports the retinal structure, e.g. following a lesion.

4.4.3 Polarized distribution of cell components

Besides stabilizing the cell structure, as cytoplasmatic protein, Nestin is also assumed to be involved in the asymmetric distribution of material between dividing stem cells and their differentiating daughter cells [120]. In this process Nestin itself, other cytoskeletal proteins and cellular factors are shared unequally between the daughter cells, making them follow different paths during development. This applies according to Bieberich et al. for Nestin in the neural tube, where ventricular cells continue to proliferate, while differentiated cells migrate to the surface.

In these cells the polarized distribution of material between dividing and differentiating cells appears to be caused by Nestin mediated disassembly and uneven partitioning of motile vimentin particles during mitosis [106, 162–164]. Following this observations we propose that Nestin could also influence the stemness of stem cells in the murine retina.

4.4.4 The possible role of Nestin in cell cycle control

Interestingly the significantly elevated Nestin expression is exactly in the same area as the elevated proliferation at P4. Therefore we suppose that Nestin could be involved in the control of the cell cycle in the progenitor cell population. A

fact supporting this hypothesis is that Nestin is known to play a major role in the stem cell renewal of neural stem cells: Park et al. found in their study that a Nestin knockout lead to the development of fewer neural stem cells in the neural tube [125].

Additionally it is known that Nestin constitutes a dynamic scaffold for the Cdk5 complex, which is responsible for the withdrawal from the cell cycle [107]. Nestin also has the ability to halt the differentiation of the myoblasts *in vitro* when it is overexpressed, by interacting with the Cdk5/p35 complex and controlling the cleavage of p35 to its degradation resistant form p25 [126].

To demonstrate these effects of Nestin in a Müller glia cell culture is difficult. As soon as a lesion occurs, Müller glia strongly express Nestin. For this reason Müller glia in cell culture show a much stronger Nestin expression than the unlesioned retina, where nearly no Nestin expression can be found in the retina of wildtype animals. This may also be the reason why a treatment with TGF- β in our studies could not further elevate the level of Nestin produced by the Müller glia in culture. Therefore the evidence for this hypothesis would have to be adduced by additional experiments in the *in vitro* models, for example by western blot analysis for the p35 and p25.

4.4.5 Nestin expression after NMDA lesion

After NMDA lesion in general, a tendency for increased levels of Nestin and GFAP can be seen in the experiments. This is a long known effect following lesions in the retina and appears to point to a beginning gliosis in the retinae. As this happens in wildtype animals as well as in animals with an altered TGF- β pathway, this reaction appears to be unrelated to the gene deletions and does not appear to influence the reactivity of the Müller glia cells in TGF- β RII/Smad7 deficient mice regarding proliferation and regeneration.

4.5 Influence of TGF- β signaling on proliferation in the lesioned adult retina

In our studies, sporadic BRDU positive cells were found in the outer nuclear layer of three of eleven tested TGF- β RII deficient mice, 24 h after NMDA lesion. Only one animal showed a single BRDU positive Müller glia cell. This reaction did not depend on the genotype of the mice (6 wt/5 het). When using these samples for a TUNEL assay, the same samples that showed BRDU positive cells revealed the highest number of TUNEL positive cells in the outer nuclear layer. While it is possible that Müller glia cells translocate in the direction of the outer nuclear layer, this movement takes several days according to Joly et al. [165]. In our study, the BRDU positive cells appeared one day after the NMDA injection and had disappeared in samples taken two days after the injection.

A possible explanation for these results can be found in the publication by Joly et al. [165]. They describe the occurrence of BRDU positive cells in the outer nuclear layer one day after light damage and the disappearance of these cells after two to three days. Joly et al. could explain this phenomenon as a DNA repair reaction by costaining the BRDU positive cells with ligase IV, a marker for DNA repair. As the results appear very similar to ours, even in their dependence on

a lesioned outer nuclear layer, we assume that the BRDU positive cells in our samples can be also explained by DNA repair. It appears that the TGF- β RII deficiency does not facilitate a proliferative reaction after NMDA lesion.

4.6 Constriction of the effects to the central retina

All effects of the Smad7 deficiency are found in the central retina. This could be due to the differentiation of the retina that starts at the center around the optic nerve head, and ends at the periphery [44]. As discussed above, we assume that TGF- β has a pro-proliferative effect on stem cells during certain, early stages of development. If the cells of the retina react to the alteration in signaling in this defined time frame, this could affect a certain part of the retinal cells, for example only the cells of the central retina, assuming that these cells are in the right stage of growth and differentiation to react to the signal at this point in time.

A second possibility could be that receptors like TGF- β RI or RII are more intensely expressed in the central retina than in the periphery. This could lead to a dose dependent effect of TGF- β . Working with the CTGF overexpressing mice we saw a dose dependent thickening that started around the optic nerve head and spread to the whole retina with increased expression of CTGF. In the mouse model with an inducible homozygous deletion of TGF- β RII we could see that the effect of the thinned retina was not constricted to the central retina like in the Smad7 deficient mice. Considering these facts, it is well possible that in a mouse model with an inducible homozygous deletion of Smad7, the effect on thickening and proliferation would not be restricted to the area around the optic nerve head. Up to now, however, there is no evidence for an uneven distribution of the receptors.

4.7 Outlook

We suppose that a reduced expression of Smad7 and an enhanced TGF- β signaling lead to a thickened retina and an increased number of Müller glia. Our results additionally indicate that a Smad7 deficiency causes an increased number of proliferating cells in the retinae of newborn mice. Together with an elevated cell number in the adult retina, this could point to an increased self renewal ability in the retinal progenitor cells leading to delayed differentiation.

Besides the effects on proliferation and cell number, a raised immunoreactivity for Nestin could be seen in adult Smad7 deficient mice. Whether or not the Nestin expression is a direct effect of the altered TGF beta pathway is still unclear. Injections of TGF beta/PBS in the eyes of wildtype animals could help to answer this question.

We assume that there is a direct connection between the increased Nestin expression in the central retina in adult animals, and the increased proliferation in newborn Smad7 deficient mice, that leads to a thickening in this part of the retina.

In myoblasts, Nestin is known to modulate the cleavage of p35, an activator protein of Cdk5 (Cyclin dependent kinase) to its degradation resistant form p25. Therefore it is able to halt myoblast differentiation by inhibition of the continuing activation of Cdk5 by p25 [126]. The same mechanism could also affect the differentiation of the progenitor cells in the mouse retina.

To verify this hypothesis regarding our mouse models, further experiments need to be conducted. Experiments with cultured Müller glia turned out to be difficult in this case, as the Nestin expression in Müller glia cells appears to rise heavily in culture after isolation. Instead it would be possible to work with freshly isolated progenitor cells from newborn Smad7 deficient mice with an inducible homozygous deletion of Smad7. Using this material it could be possible to check the cell cycle status by FACS analysis or do western blots on p35 and p25 to see if there is any difference in expression. For this experiments we already started breeding CAG Cre x Smad7^{fl/fl} mice to achieve a Tamoxifen-inducible homozygous deletion of Smad7 in the eye.

One other question remained unanswered. The Smad7 deficiency had an effect on the proliferation of the embryonic stem cell population, but could not cause proliferation of the Müller glia cells post-lesion. This is possibly again due to the TGF- β signaling having different effects on embryonic compared to adult stem/progenitor cells. It is possible that other signaling pathways have to be activated or repressed in addition, to achieve an effect. An experiment combining an EGF/FGF injection with a lesion in Smad7 deficient mice or animals with an inducible homozygous deletion would be a promising possibility. It also remains to be tested if a homozygous deletion of Smad7 in the retina causes a reaction after a lesion.

Chapter 5

Summary

There is evidence that Müller glia cells have some of the same characteristics as neuronal progenitor cells. Still, they do not proliferate under physiological conditions in the adult mammalian retina. As TGF- β is known to impair proliferation in the brain [100], we formulated the hypothesis that the progenitor cell populations in the retina could be also be influenced by TGF- β signaling.

Based on our results we were able to conclude that TGF- β signaling has a significant effect on the retina: It influences the proliferation during the development of the central retina, but does not provoke proliferation in the normal and injured adult retina when altered. To investigate the effects of the TGF- β pathway on Müller glia cells and their precursors, we studied three different mouse models: Smad7 deficient mice with enhanced TGF- β signaling, and mice with a heterozygous respectively inducible homozygous deletion of TGF- β RII as models for diminished TGF- β signaling. Smad7 deficient mice showed a significantly thickened inner and outer nuclear layer near the optic nerve head, and a significantly elevated number of Müller glia cells in the central retina. In mice carrying the inducible homozygous deletion of TGF- β RII, a slight, but significant thinning of the retina could be detected.

To evaluate the cause of the thickened retina in the Smad7 deficient mice, the rates of proliferation and apoptosis were measured by BrdU staining at P4 and TUNEL-labeling at P8. In these studies the Smad7 deficient mice showed an increased proliferation in the central retina at P4, which could apparently be the reason for the thickening of the retina, while the rate of apoptosis remained unchanged. Reduced expression of Smad7 also increased the expression of Nestin, a progenitor cell marker, in the central retina. This might well be closely connected to the increased proliferation in the central retina. To study the effect of altered TGF- β signaling on the proliferative reaction in the adult lesioned retina, we used NMDA injections on Smad7 and TGF- β RII deficient mice. Smad7 deficient mice showed no BRDU positive cells after NMDA injection, while in TGF- β deficient mice sporadic BRDU positive cells were found in the outer nuclear layer one day after injection. Most likely, this effect is due to DNA repair.

In a nutshell, the results show that TGF- β influences the proliferation in the central retina during development, while proliferation is absent in the normal or injured adult retina.

Abbreviations

°C	degree Celsius
AMD	age related macula degeneration
APS	ammonium peroxodisulfate
BSA	bovine serum albumin
CNTF	ciliary neurotrophic factor
cDNA	complementary DNA
CNS	central nervous system
CTGF	Connective tissue growth factor
DAPI	4',6-diamidino-2-phenylindol
dest.	distilled
DMEM	dulbecco's modified eagle medium
DMSO	dimethyl sulfoxide
DNA	deoxy- ribonucleic acid
dNTP	2'-deoxyribonucleotide-5'-triphosphate
EDTA	ethylene- diamine- tetraacetic- acid
EGF	epidermal growth factor
ELISA	enzyme linked immunosorbent assay
ES cells	embryonic stem cells
FCS	fetal calf serum
FGF	fibroblast growth factor
fl/fl	flox/flox
fw	forward
g	gram, standard gravity
G	gauge
GFAP	glial fibrillary acidic protein
GNB2L	guanine nucleotide binding protein 2L
GS	glutamine synthetase
GSK-3	glycogen synthase kinase 3
HRP	horseradish peroxidase
in vitro	studies outside of the living organism
in vivo	studies inside of the living organism
kg	kilogram
l	liter
LTBP	latent TGF- β binding protein
m	milli-, meter
M	molar (mol/l)
min	minute

mRNA	messenger ribonucleic acid
NMDA	N-methyl-D-aspartate
OD	optical density
PAGE	polyacrylamid-gelelectrophoresis
PBS	phosphate buffered saline
PCR	polymerase chain reaction
PFA	paraformaldehyde
Php	phosphate buffer
PNS	peripheral nervous system
rev	reverse retinal pigment epithelium
RPE	retinal pigment epithelium
rpm	rotations per minute
RT	reverse transcriptase, room temperature
s	second
Smad7	mothers against decapentaplegic homolog 7
TGF	transforming growth factor
Tris	tris-(hydroxymethyl-)aminoethan
V	volt
v/v	volume per volume
w/v	weight per volume
Wnt	wingless Type
wt	wildtype

List of Figures

1.1	Asymmetric division of stem cells	4
1.2	Architecture of the retina	5
1.3	Stem cell populations in the eye	5
1.4	Cell types regenerated from Müller glia	8
1.5	Architecture of the Müller glia cell	8
1.6	Time course of cell differentiation in the retina	9
1.7	Functions of Müller glia	10
1.8	TGF- β signaling	12
1.9	Nestin filaments in a cultured Müller cell	14
2.1	Schematic drawing of the function of the Cre/loxP System (adapted from [128]).	22
2.2	Schematic drawing of the Rosa LacZ mouse construct.	23
2.3	LacZ staining of Tamoxifen induced CAG Cre x Rosa Lac mice	24
2.4	Schematic drawing of the Smad7 ^{fl/fl} mouse construct.	24
2.5	Schematic drawing of the TGF- β RII ^{fl/fl} mouse construct.	25
2.6	Breeding procedure for a heterozygous deletion of Smad7 or TGF- β RII with EIIa Cre mice	25
2.7	The Principle of the deletion PCR	29
2.8	Example for a measurement on retinal thickness	36
2.9	Müller glia cell death and proliferation in newborn mice	40
2.10	Example for intensity measurement.	42
2.11	Scoring for Nestin staining intensity.	43
2.12	Scoring for GFAP staining intensity.	44
2.13	Staining of Müller glia with glutamine synthetase and counting scheme.	44
3.1	Mosaicism of EIIa Cre recombinase expression	58
3.2	Confirmation of the heterozygous Smad7 deletion on DNA and deficiency on RNA level	59
3.3	Confirmation of the TGF- β heterozygous deletion on DNA and deficiency on protein level	60
3.4	Light micrographs of sagittal eye sections of Smad7 deficient mice and their wildtype littermates	61
3.5	Light micrographs of sagittal eye sections of TGF- β RII deficient mice and their wildtype littermates	62
3.6	Measurement of retina thickness in Smad7 ^{fl/-} mice	63

3.7	Micrographs taken at the optic nerve in Smad7 ^{fl/-} mice	64
3.8	Measurement of the inner and outer nuclear layer thickness in Smad7 ^{fl/-} mice	64
3.9	Measurement of the retina thickness of TGF- β RII ^{fl/-} mice	65
3.10	Glutamine synthetase staining for Müller glia counting	66
3.11	Number of Müller glia in the retina in Smad7-deficient mice	66
3.12	Number of Müller glia in a 200 μ m segment in the retina of TGF- β RII ^{fl/-} and wildtype mice	67
3.13	Proliferation in 4 day old Smad7 ^{fl/-} mice	68
3.14	Apoptosis in 8 day old Smad7 ^{fl/-} mice	69
3.15	Proliferation of Müller glia cells <i>in vitro</i> after TGF- β 1 treatment . .	70
3.16	Nestin staining of the central and medial retina of 3 week old mice . .	72
3.17	GFAP expression on RNA level in Smad7 ^{fl/-} mice	73
3.18	Nestin expression in untreated TGF- β RII ^{fl/-} mice	74
3.19	Nestin and GFAP expression on RNA level in TGF- β RII ^{fl/-} mice .	74
3.20	Nestin expression in Müller glia cell culture after TGF- β 1 treatment	75
3.21	Western blot data of pSmad3 in Smad7 ^{fl/-} mice	75
3.22	Western blot data of proteins involved in EGF signaling in Smad7 ^{fl/-} mice	76
3.23	Morphology of a cross section of the optic nerve in Smad7 ^{fl/-} mice .	77
3.24	Axon count in NMDA treated Smad7 ^{fl/-} mice	77
3.25	Micrographs of the optic nerve of TGF- β RII	78
3.26	Axon count in NMDA/PBS treated TGF- β RII ^{fl/-} mice	78
3.27	TUNEL staining in NMDA treated retinæ of Smad7 ^{fl/-} mice	79
3.28	TUNEL positive cells after NMDA injection in Smad7 ^{fl/-} mice and their wildtype littermates	80
3.29	Apoptosis after NMDA lesion in TGF- β RII deficient mice	82
3.30	Scheme of NMDA and BRDU injections.	83
3.31	BRDU positive cells in the outer nuclear layer of NMDA lesioned TGF- β RII deficient mice 24h after NMDA injection	83
3.32	Nestin and GFAP expression after NMDA lesion in Smad7 ^{fl/-} mice .	84
3.33	Nestin and GFAP expression after NMDA lesion in TGF- β RII ^{fl/-} mice	85
3.34	Measurement of retinal thickness in different CTGF overexpressing strains	87
3.35	Number of Müller glia in CTGF overexpressing mice	88
3.36	Real-time PCR for CTGF in 3 week old Smad7 ^{fl/-} mice	89
4.1	Crosstalk between the Wnt pathway and the TGF- β pathway during the activation of Xtnn, a target gene (Figure adapted from: [161]). .	95

List of Tables

1.1	Types of intermediate filaments.	15
2.1	Laboratory chemicals	19
2.2	Laboratory consumables	19
2.3	Laboratory equipment	20
2.4	Protein and DNA - Ladders	21
2.5	Reaction kits	21
2.6	Mouse tail lysis buffer.	27
2.7	IRN DNA precipitation buffer.	27
2.8	PCR mix and program for EIIa Cre product: 700 bp.	28
2.9	PCR mixes for Smad7 fl/fl; TGF- β RII fl/fl; Smad7 deletion; TGF- β deletion.	28
2.10	PCR programs for Smad7 ^{fl/fl} and TGF- β RII ^{fl/fl}	28
2.11	5x glycerol mix.	28
2.12	PCR program for Smad7 deletion product and for TGF- β RII deletion	29
2.13	PCR mix and cycler program for Rosa LacZ.	30
2.14	PCR mix and Cycler program for SV 40	30
2.15	Genotyping primers.	31
2.16	Buffers for gel electrophoresis.	31
2.17	Chemicals and equipment for histology.	32
2.18	PBS heparin solution.	33
2.19	Buffers and solutions for cryo embedding and immunohistochemistry	33
2.20	Buffers and solutions for Epon embedding	35
2.21	Solutions for Richardson's staining	35
2.22	LacZ fixation buffer	41
2.23	LacZ washing buffer	41
2.24	LacZ staining solution	41
2.25	Primary antibodies for immunostaining	41
2.26	Secondary antibodies for immunostaining	42
2.27	Reaction mixture for cDNA synthesis	46
2.28	Cycler program for cDNA synthesis	46
2.29	Q-PCR primers.	47
2.30	Reaction mixture for real-time PCR	47
2.31	Cycler program for quantitative RT-PCR	48
2.32	Washing buffer for protein isolation.	49
2.33	Gel composition for SDS gel electrophoresis	50

2.34	Buffers for SDS gel electrophoresis.	50
2.35	Transfer buffer for western blotting.	51
2.36	Stacking scheme for western blotting.	51
2.37	TBS and TBST buffer for immunostaining.	51
2.38	Primary antibodies for immunostaining	52
2.39	Secondary antibodies.	52
2.40	Solutions for Coomassie staining and destaining.	52
2.41	Reagents, media and equipment for cell culture.	53
2.42	Müller cell medium.	53
2.43	Müller cell digestion solution.	54
4.1	Possible reasons for the thickened retina in Smad7 deficient mice . . .	93

List of publications

In chronological order:

- V. V. Zverlov, **M. Klupp**, J. Krauss, and W. H. Schwarz, Mutations in the scaffoldin gene, *cipA*, of *Clostridium thermocellum* with impaired cellulosome formation and cellulose hydrolysis: insertions of a new transposable element, IS1447, and implications for cellulase synergism on crystalline cellulose, *J. Bacteriol.*, vol. 190, p. 4321-4327, Jun 2008
- Z. Wang, C. Wilhelmsson, P. Hyrsli, T. G. Loof, P. Dobes, **M. Klupp**, O. Loseva, M. Morgelin, J. Ikle, R. M. Cripps, H. Herwald, and U. Theopold, Pathogen entrapment by transglutaminase - a conserved early innate immune mechanism, *PLoS Pathog.*, vol. 6, p. e1000763, Feb 2010.
- **M. Klupp**, R. Fuchshofer, B. Braunger, E. R. Tamm, and L. Aigner, Poster: Conditional Smad7 knockdown causes elevated number of müller glia and increased nestin expression in the central retina ; *ARVO - The Association for Research in Vision and Ophthalmology*; Fort Lauderdale, Florida, 2011.

Bibliography

- [1] N. Congdon, B. O'Colmain, C. C. Klaver, R. Klein, B. Munoz, D. S. Friedman, J. Kempen, H. R. Taylor, and P. Mitchell, "Causes and prevalence of visual impairment among adults in the United States," *Arch. Ophthalmol.*, vol. 122, pp. 477–485, Apr 2004. *Cited on page 1.*
- [2] S. J. Odelberg, "Unraveling the molecular basis for regenerative cellular plasticity," *PLoS Biol.*, vol. 2, p. E232, Aug 2004. *Cited on page 2.*
- [3] K. Gurley and A. Sánchez Alvarado, "Stem cells in animal models of regeneration," *StemBook*, ed. *The Stem Cell Research Community*, pp. StemBook, doi/10.3824/stembook.1.32.1, Dec 2008. *Cited on page 2.*
- [4] S. R. Y. Cajal, "Degeneration and regeneration of the nervous system," *Oxford University*, vol. Vol. 2, pp. 558–582, 1928. *Cited on page 2.*
- [5] J. ALTMAN, "Are new neurons formed in the brains of adult mammals?," *Science*, vol. 135, pp. 1127–1128, Mar 1962. *Cited on page 2.*
- [6] The National Institutes of Health resource for stem cell research, "<http://stemcells.nih.gov/info/basics/basics1.asp>," 2012. *Cited on pages 2 and 3.*
- [7] B. Alberts *et al.*, *Molecular biology of the cell*. Garland Science, 4th ed., 2004. *Cited on pages 2, 3 and 4.*
- [8] F. Arai, A. Hirao, M. Ohmura, H. Sato, S. Matsuoka, K. Takubo, K. Ito, G. Y. Koh, and T. Suda, "Tie2/angiopoietin-1 signaling regulates hematopoietic stem cell quiescence in the bone marrow niche," *Cell*, vol. 118, pp. 149–161, Jul 2004. *Cited on page 3.*
- [9] A. G. Smith, "Embryo-derived stem cells: of mice and men," *Annu. Rev. Cell Dev. Biol.*, vol. 17, pp. 435–462, 2001. *Cited on page 3.*
- [10] D. J. Anderson, F. H. Gage, and I. L. Weissman, "Can stem cells cross lineage boundaries?," *Nat. Med.*, vol. 7, pp. 393–395, Apr 2001. *Cited on page 3.*
- [11] S. J. Morrison, "Stem cell potential: can anything make anything?," *Curr. Biol.*, vol. 11, pp. 7–9, Jan 2001. *Cited on page 3.*
- [12] A. J. Wagers, R. I. Sherwood, J. L. Christensen, and I. L. Weissman, "Little evidence for developmental plasticity of adult hematopoietic stem cells," *Science*, vol. 297, pp. 2256–2259, Sep 2002. *Cited on page 3.*

- [13] F. Arai and T. Suda, "Quiescent stem cells in the niche," *StemBook*, ed. *The Stem Cell Research Community*, pp. StemBook, doi/10.3824/stembook.1.32.1, Dec 2008. doi/10.3824/stembook.1.6.1, <http://www.stembook.org>. *Cited on page 3.*
- [14] A. Kubota, K. Nishida, K. Nakashima, and Y. Tano, "Conversion of mammalian Müller glial cells into a neuronal lineage by in vitro aggregate-culture," *Biochem. Biophys. Res. Commun.*, vol. 351, pp. 514–520, Dec 2006. *Cited on page 3.*
- [15] M. O. Karl and T. A. Reh, "Regenerative medicine for retinal diseases: activating endogenous repair mechanisms," *Trends Mol Med*, vol. 16, pp. 193–202, Apr 2010. *Cited on pages 3, 5, 6, 7, 8, 9 and 10.*
- [16] M. A. Dyer and C. L. Cepko, "Regulating proliferation during retinal development," *Nat. Rev. Neurosci.*, vol. 2, pp. 333–342, May 2001. *Cited on page 5.*
- [17] V. Tropepe, B. L. Coles, B. J. Chiasson, D. J. Horsford, A. J. Elia, R. R. McInnes, and D. van der Kooy, "Retinal stem cells in the adult mammalian eye," *Science*, vol. 287, pp. 2032–2036, Mar 2000. *Cited on page 4.*
- [18] S. A. Cicero, D. Johnson, S. Reyntjens, S. Frase, S. Connell, L. M. Chow, S. J. Baker, B. P. Sorrentino, and M. A. Dyer, "Cells previously identified as retinal stem cells are pigmented ciliary epithelial cells," *Proc. Natl. Acad. Sci. U.S.A.*, vol. 106, pp. 6685–6690, Apr 2009. *Cited on page 4.*
- [19] A. Moshiri, J. Close, and T. A. Reh, "Retinal stem cells and regeneration," *Int. J. Dev. Biol.*, vol. 48, no. 8-9, pp. 1003–1014, 2004. *Cited on page 4.*
- [20] M. Araki, "Regeneration of the amphibian retina: role of tissue interaction and related signaling molecules on RPE transdifferentiation," *Dev. Growth Differ.*, vol. 49, pp. 109–120, Feb 2007. *Cited on page 6.*
- [21] T. A. Reh, M. Jones, and C. Pittack, "Common mechanisms of retinal regeneration in the larval frog and embryonic chick," *Ciba Found. Symp.*, vol. 160, pp. 192–204, 1991. *Cited on page 6.*
- [22] S. Sakami, P. Etter, and T. A. Reh, "Activin signaling limits the competence for retinal regeneration from the pigmented epithelium," *Mech. Dev.*, vol. 125, no. 1-2, pp. 106–116, 2008. *Cited on page 6.*
- [23] P. A. Raymond and P. F. Hitchcock, "How the neural retina regenerates," *Results Probl Cell Differ*, vol. 31, pp. 197–218, 2000. *Cited on page 6.*
- [24] R. L. Bernardos, L. K. Barthel, J. R. Meyers, and P. A. Raymond, "Late-stage neuronal progenitors in the retina are radial Müller glia that function as retinal stem cells," *J. Neurosci.*, vol. 27, pp. 7028–7040, Jun 2007. *Cited on page 6.*
- [25] J. E. Braisted, T. F. Essman, and P. A. Raymond, "Selective regeneration of photoreceptors in goldfish retina," *Development*, vol. 120, pp. 2409–2419, Sep 1994. *Cited on page 6.*
- [26] A. J. Fischer and T. A. Reh, "Exogenous growth factors stimulate the regeneration of ganglion cells in the chicken retina," *Dev. Biol.*, vol. 251, pp. 367–379, Nov 2002. *Cited on page 6.*

- [27] P. A. Raymond, L. K. Barthel, R. L. Bernardos, and J. J. Perkowski, "Molecular characterization of retinal stem cells and their niches in adult zebrafish," *BMC Dev. Biol.*, vol. 6, p. 36, 2006. *Cited on page 6.*
- [28] P. Yurco and D. A. Cameron, "Cellular correlates of proneural and Notch-delta gene expression in the regenerating zebrafish retina," *Vis. Neurosci.*, vol. 24, no. 3, pp. 437–443, 2007. *Cited on page 6.*
- [29] S. C. Kassen, R. Thummel, L. A. Campochiaro, M. J. Harding, N. A. Bennett, and D. R. Hyde, "CNTF induces photoreceptor neuroprotection and Müller glial cell proliferation through two different signaling pathways in the adult zebrafish retina," *Exp. Eye Res.*, vol. 88, pp. 1051–1064, Jun 2009. *Cited on page 6.*
- [30] A. A. Calinescu, P. A. Raymond, and P. F. Hitchcock, "Midkine expression is regulated by the circadian clock in the retina of the zebrafish," *Vis. Neurosci.*, vol. 26, pp. 495–501, Nov 2009. *Cited on page 6.*
- [31] R. Thummel, S. C. Kassen, J. E. Montgomery, J. M. Enright, and D. R. Hyde, "Inhibition of Müller glial cell division blocks regeneration of the light-damaged zebrafish retina," *Dev Neurobiol*, vol. 68, pp. 392–408, Feb 2008. *Cited on page 6.*
- [32] B. V. Fausett, J. D. Gumerson, and D. Goldman, "The proneural basic helix-loop-helix gene *ascl1a* is required for retina regeneration," *J. Neurosci.*, vol. 28, pp. 1109–1117, Jan 2008. *Cited on page 6.*
- [33] A. Bringmann, I. Iandiev, T. Pannicke, A. Wurm, M. Hollborn, P. Wiedemann, N. N. Osborne, and A. Reichenbach, "Cellular signaling and factors involved in Müller cell gliosis: neuroprotective and detrimental effects," *Prog Retin Eye Res*, vol. 28, pp. 423–451, Nov 2009. *Cited on page 6.*
- [34] J. A. Sahel, D. M. Albert, S. Lessell, H. Adler, T. L. McGee, and J. Konrad-Rastegar, "Mitogenic effects of excitatory amino acids in the adult rat retina," *Exp. Eye Res.*, vol. 53, pp. 657–664, Nov 1991. *Cited on page 6.*
- [35] S. Ooto, T. Akagi, R. Kageyama, J. Akita, M. Mandai, Y. Honda, and M. Takahashi, "Potential for neural regeneration after neurotoxic injury in the adult mammalian retina," *Proc. Natl. Acad. Sci. U.S.A.*, vol. 101, pp. 13654–13659, Sep 2004. *Cited on pages 6 and 7.*
- [36] J. Wan, H. Zheng, Z. L. Chen, H. L. Xiao, Z. J. Shen, and G. M. Zhou, "Preferential regeneration of photoreceptor from Müller glia after retinal degeneration in adult rat," *Vision Res.*, vol. 48, pp. 223–234, Jan 2008. *Cited on page 7.*
- [37] J. Wan, H. Zheng, H. L. Xiao, Z. J. She, and G. M. Zhou, "Sonic hedgehog promotes stem-cell potential of Müller glia in the mammalian retina," *Biochem. Biophys. Res. Commun.*, vol. 363, pp. 347–354, Nov 2007. *Cited on page 7.*
- [38] J. L. Close, J. Liu, B. Gumuscu, and T. A. Reh, "Epidermal growth factor receptor expression regulates proliferation in the postnatal rat retina," *Glia*, vol. 54, pp. 94–104, Aug 2006. *Cited on page 7.*
- [39] M. A. Dyer and C. L. Cepko, "Control of Müller glial cell proliferation and activation following retinal injury," *Nat. Neurosci.*, vol. 3, pp. 873–880, Sep 2000. *Cited on page 7.*

- [40] M. O. Karl, S. Hayes, B. R. Nelson, K. Tan, B. Buckingham, and T. A. Reh, "Stimulation of neural regeneration in the mouse retina," *Proc. Natl. Acad. Sci. U.S.A.*, vol. 105, pp. 19508–19513, Dec 2008. *Cited on pages 7 and 81.*
- [41] A. Bringmann, T. Pannicke, J. Grosche, M. Francke, P. Wiedemann, S. N. Skatchkov, N. N. Osborne, and A. Reichenbach, "Müller cells in the healthy and diseased retina," *Prog Retin Eye Res*, vol. 25, pp. 397–424, Jul 2006. *Cited on pages 7, 9 and 10.*
- [42] S. R. Robinson and Z. Dreher, "Müller cells in adult rabbit retinae: morphology, distribution and implications for function and development," *J. Comp. Neurol.*, vol. 292, pp. 178–192, Feb 1990. *Cited on page 8.*
- [43] D. L. Turner and C. L. Cepko, "A common progenitor for neurons and glia persists in rat retina late in development," *Nature*, vol. 328, no. 6126, pp. 131–136, 1987. *Cited on page 7.*
- [44] R. W. Young, "Cell differentiation in the retina of the mouse," *Anat. Rec.*, vol. 212, pp. 199–205, Jun 1985. *Cited on pages 7, 9, 39, 40 and 98.*
- [45] A. Reichenbach and S. Robinson, "The involvement of Müller cells in the outer retina," in *Neurobiology and clinical aspects of the outer retina* (M. Djamgoz, S. Archer, and S. Vallergera, eds.), vol. p.395–416, Chapman and Hall, Nov. 1995. *Cited on page 9.*
- [46] C. L. Poitry-Yamate, S. Poitry, and M. Tsacopoulos, "Lactate released by Müller glial cells is metabolized by photoreceptors from mammalian retina," *J. Neurosci.*, vol. 15, pp. 5179–5191, Jul 1995. *Cited on page 9.*
- [47] T. Kuwabara and D. G. Cogan, "Retinal glycogen," *Arch. Ophthalmol.*, vol. 66, pp. 680–688, Nov 1961. *Cited on page 9.*
- [48] B. Pfeiffer-Guglielmi, M. Francke, A. Reichenbach, B. Fleckenstein, G. Jung, and B. Hamprecht, "Glycogen phosphorylase isozyme pattern in mammalian retinal Müller (glial) cells and in astrocytes of retina and optic nerve," *Glia*, vol. 49, pp. 84–95, Jan 2005. *Cited on page 9.*
- [49] E. A. Newman, D. A. Frambach, and L. L. Odette, "Control of extracellular potassium levels by retinal glial cell K⁺ siphoning," *Science*, vol. 225, pp. 1174–1175, Sep 1984. *Cited on page 9.*
- [50] E. A. Nagelhus, M. L. Veruki, R. Torp, F. M. Haug, J. H. Laake, S. Nielsen, P. Agre, and O. P. Ottersen, "Aquaporin-4 water channel protein in the rat retina and optic nerve: polarized expression in Müller cells and fibrous astrocytes," *J. Neurosci.*, vol. 18, pp. 2506–2519, Apr 1998. *Cited on page 9.*
- [51] E. A. Newman, "A physiological measure of carbonic anhydrase in Müller cells," *Glia*, vol. 11, pp. 291–299, Aug 1994. *Cited on page 9.*
- [52] H. Brew and D. Attwell, "Electrogenic glutamate uptake is a major current carrier in the membrane of axolotl retinal glial cells," *Nature*, vol. 327, no. 6124, pp. 707–709, 1987. *Cited on page 9.*
- [53] T. Rauen, W. R. Taylor, K. Kuhlbrodt, and M. Wiessner, "High-affinity glutamate transporters in the rat retina: a major role of the glial glutamate transporter GLAST-1 in transmitter clearance," *Cell Tissue Res.*, vol. 291, pp. 19–31, Jan 1998. *Cited on page 9.*

- [54] B. Biedermann, A. Bringmann, and A. Reichenbach, "High-affinity GABA uptake in retinal glial (Müller) cells of the guinea pig: electrophysiological characterization, immunohistochemical localization, and modeling of efficiency," *Glia*, vol. 39, pp. 217–228, Sep 2002. *Cited on page 9.*
- [55] P. J. Linser and A. A. Moscona, "Induction of glutamine synthetase in embryonic neural retina: its suppression by the gliatoxic agent alpha-amino adipic acid," *Brain Res.*, vol. 227, pp. 103–119, Jan 1981. *Cited on page 9.*
- [56] D. V. Pow and S. R. Robinson, "Glutamate in some retinal neurons is derived solely from glia," *Neuroscience*, vol. 60, pp. 355–366, May 1994. *Cited on page 9.*
- [57] M. Schutte and P. Werner, "Redistribution of glutathione in the ischemic rat retina," *Neurosci. Lett.*, vol. 246, pp. 53–56, Apr 1998. *Cited on page 9.*
- [58] D. V. Pow and D. K. Crook, "Immunocytochemical evidence for the presence of high levels of reduced glutathione in radial glial cells and horizontal cells in the rabbit retina," *Neurosci. Lett.*, vol. 193, pp. 25–28, Jun 1995. *Cited on page 9.*
- [59] S. R. Das, N. Bhardwaj, H. Kjeldbye, and P. Gouras, "Muller cells of chicken retina synthesize 11-cis-retinol," *Biochem. J.*, vol. 285 (Pt 3), pp. 907–913, Aug 1992. *Cited on page 9.*
- [60] C. Giaume, F. Kirchhoff, C. Matute, A. Reichenbach, and A. Verkhratsky, "Glial: the fulcrum of brain diseases," *Cell Death Differ.*, vol. 14, pp. 1324–1335, Jul 2007. *Cited on pages 9 and 10.*
- [61] K. Franze, J. Grosche, S. N. Skatchkov, S. Schinkinger, C. Foja, D. Schild, O. Uckermann, K. Travis, A. Reichenbach, and J. Guck, "Muller cells are living optical fibers in the vertebrate retina," *Proc. Natl. Acad. Sci. U.S.A.*, vol. 104, pp. 8287–8292, May 2007. *Cited on pages 9 and 10.*
- [62] R. F. Miller and J. E. Dowling, "Intracellular responses of the Müller (glial) cells of mudpuppy retina: their relation to b-wave of the electroretinogram," *J. Neurophysiol.*, vol. 33, pp. 323–341, May 1970. *Cited on page 9.*
- [63] R. Wen and B. Oakley, "K(+)-evoked Müller cell depolarization generates b-wave of electroretinogram in toad retina," *Proc. Natl. Acad. Sci. U.S.A.*, vol. 87, pp. 2117–2121, Mar 1990. *Cited on page 9.*
- [64] E. A. Newman and L. L. Odette, "Model of electroretinogram b-wave generation: a test of the K⁺ hypothesis," *J. Neurophysiol.*, vol. 51, pp. 164–182, Jan 1984. *Cited on page 9.*
- [65] E. Seuntjens, L. Umans, A. Zwijsen, M. Sampaolesi, C. M. Verfaillie, and D. Huylebroeck, "Transforming Growth Factor type beta and Smad family signaling in stem cell function," *Cytokine Growth Factor Rev.*, vol. 20, no. 5-6, pp. 449–458, 2009. *Cited on page 10.*
- [66] J. Massague, S. W. Blain, and R. S. Lo, "TGFbeta signaling in growth control, cancer, and heritable disorders," *Cell*, vol. 103, pp. 295–309, Oct 2000. *Cited on page 10.*
- [67] M. P. de Caestecker, E. Piek, and A. B. Roberts, "Role of transforming growth factor-beta signaling in cancer," *J. Natl. Cancer Inst.*, vol. 92, pp. 1388–1402, Sep 2000. *Cited on page 10.*

- [68] R. Derynck, R. J. Akhurst, and A. Balmain, "TGF-beta signaling in tumor suppression and cancer progression," *Nat. Genet.*, vol. 29, pp. 117–129, Oct 2001. *Cited on page 10.*
- [69] K. Miyazono, P. ten Dijke, and C. H. Heldin, "TGF-beta signaling by Smad proteins," *Adv. Immunol.*, vol. 75, pp. 115–157, 2000. *Cited on page 10.*
- [70] L. Aigner and U. Bogdahn, "TGF-beta in neural stem cells and in tumors of the central nervous system," *Cell Tissue Res.*, vol. 331, pp. 225–241, Jan 2008. *Cited on pages 10, 11, 13 and 93.*
- [71] O. Dreesen and A. H. Brivanlou, "Signaling pathways in cancer and embryonic stem cells," *Stem Cell Rev.*, vol. 3, pp. 7–17, Jan 2007. *Cited on page 10.*
- [72] P. ten Dijke and H. M. Arthur, "Extracellular control of TGFbeta signalling in vascular development and disease," *Nat. Rev. Mol. Cell Biol.*, vol. 8, pp. 857–869, Nov 2007. *Cited on pages 10 and 11.*
- [73] Y. Y. Wan and R. A. Flavell, "'Yin-Yang' functions of transforming growth factor-beta and T regulatory cells in immune regulation," *Immunol. Rev.*, vol. 220, pp. 199–213, Dec 2007. *Cited on page 10.*
- [74] R. B. Luwor, A. H. Kaye, and H. J. Zhu, "Transforming growth factor-beta (TGF-beta) and brain tumours," *J Clin Neurosci*, vol. 15, pp. 845–855, Aug 2008. *Cited on page 10.*
- [75] M. J. Goumans, Z. Liu, and P. ten Dijke, "TGF-beta signaling in vascular biology and dysfunction," *Cell Res.*, vol. 19, pp. 116–127, Jan 2009. *Cited on page 10.*
- [76] J. Massague, "TGF-beta signal transduction," *Annu. Rev. Biochem.*, vol. 67, pp. 753–791, 1998. *Cited on page 11.*
- [77] R. Derynck and R. J. Akhurst, "Differentiation plasticity regulated by TGF-beta family proteins in development and disease," *Nat. Cell Biol.*, vol. 9, pp. 1000–1004, Sep 2007. *Cited on page 11.*
- [78] X. Yan, Z. Liu, and Y. Chen, "Regulation of TGF-beta signaling by Smad7," *Acta Biochim. Biophys. Sin. (Shanghai)*, vol. 41, pp. 263–272, Apr 2009. *Cited on pages 11 and 12.*
- [79] M. Bottner, K. Krieglstein, and K. Unsicker, "The transforming growth factor-betas: structure, signaling, and roles in nervous system development and functions," *J. Neurochem.*, vol. 75, pp. 2227–2240, Dec 2000. *Cited on page 11.*
- [80] S. Dennler, M. J. Goumans, and P. ten Dijke, "Transforming growth factor beta signal transduction," *J. Leukoc. Biol.*, vol. 71, pp. 731–740, May 2002. *Cited on page 11.*
- [81] J. P. Annes, J. S. Munger, and D. B. Rifkin, "Making sense of latent TGFbeta activation," *J. Cell. Sci.*, vol. 116, pp. 217–224, Jan 2003. *Cited on page 11.*
- [82] I. Nunes, P. E. Gleizes, C. N. Metz, and D. B. Rifkin, "Latent transforming growth factor-beta binding protein domains involved in activation and transglutaminase-dependent cross-linking of latent transforming growth factor-beta," *J. Cell Biol.*, vol. 136, pp. 1151–1163, Mar 1997. *Cited on page 11.*

- [83] J. Massague and R. R. Gomis, "The logic of TGFbeta signaling," *FEBS Lett.*, vol. 580, pp. 2811–2820, May 2006. *Cited on page 11.*
- [84] J. Massague, "How cells read TGF-beta signals," *Nat. Rev. Mol. Cell Biol.*, vol. 1, pp. 169–178, Dec 2000. *Cited on pages 11 and 12.*
- [85] R. Derynck and X. H. Feng, "TGF-beta receptor signaling," *Biochim. Biophys. Acta*, vol. 1333, pp. F105–150, Oct 1997. *Cited on page 11.*
- [86] A. B. Roberts and R. Derynck, "Meeting report: signaling schemes for TGF-beta," *Sci. STKE*, vol. 2001, p. pe43, Dec 2001. *Cited on pages 11 and 12.*
- [87] R. Derynck, Y. Zhang, and X. H. Feng, "Smads: transcriptional activators of TGF-beta responses," *Cell*, vol. 95, pp. 737–740, Dec 1998. *Cited on page 12.*
- [88] M. Kandasamy, R. Reilmann, J. Winkler, U. Bogdahn, and L. Aigner, "Transforming Growth Factor-Beta Signaling in the Neural Stem Cell Niche: A Therapeutic Target for Huntington's Disease," *Neurol Res Int*, vol. 2011, p. 124256, 2011. *Cited on pages 12 and 93.*
- [89] L. Izzi and L. Attisano, "Ubiquitin-dependent regulation of TGFbeta signaling in cancer," *Neoplasia*, vol. 8, pp. 677–688, Aug 2006. *Cited on page 12.*
- [90] Y. Inoue and T. Imamura, "Regulation of TGF-beta family signaling by E3 ubiquitin ligases," *Cancer Sci.*, vol. 99, pp. 2107–2112, Nov 2008. *Cited on page 12.*
- [91] C. S. Hill, "Nucleocytoplasmic shuttling of Smad proteins," *Cell Res.*, vol. 19, pp. 36–46, Jan 2009. *Cited on page 12.*
- [92] L. C. Fuentealba, E. Eivers, A. Ikeda, C. Hurtado, H. Kuroda, E. M. Pera, and E. M. De Robertis, "Integrating patterning signals: Wnt/GSK3 regulates the duration of the BMP/Smad1 signal," *Cell*, vol. 131, pp. 980–993, Nov 2007. *Cited on page 12.*
- [93] K. H. Wrighton and X. H. Feng, "To (TGF)beta or not to (TGF)beta: fine-tuning of Smad signaling via post-translational modifications," *Cell. Signal.*, vol. 20, pp. 1579–1591, Sep 2008. *Cited on page 12.*
- [94] T. Watabe and K. Miyazono, "Roles of TGF-beta family signaling in stem cell renewal and differentiation," *Cell Res.*, vol. 19, pp. 103–115, Jan 2009. *Cited on pages 12, 13 and 94.*
- [95] L. Vallier, M. Alexander, and R. A. Pedersen, "Activin/Nodal and FGF pathways cooperate to maintain pluripotency of human embryonic stem cells," *J. Cell. Sci.*, vol. 118, pp. 4495–4509, Oct 2005. *Cited on pages 13 and 94.*
- [96] G. J. Inman, F. J. Nicolas, J. F. Callahan, J. D. Harling, L. M. Gaster, A. D. Reith, N. J. Laping, and C. S. Hill, "SB-431542 is a potent and specific inhibitor of transforming growth factor-beta superfamily type I activin receptor-like kinase (ALK) receptors ALK4, ALK5, and ALK7," *Mol. Pharmacol.*, vol. 62, pp. 65–74, Jul 2002. *Cited on pages 13 and 94.*
- [97] J. F. Callahan, J. L. Burgess, J. A. Fornwald, L. M. Gaster, J. D. Harling, F. P. Harrington, J. Heer, C. Kwon, R. Lehr, A. Mathur, B. A. Olson, J. Weinstock, and N. J. Laping, "Identification of novel inhibitors of the transforming growth factor beta1 (TGF-beta1) type 1 receptor (ALK5)," *J. Med. Chem.*, vol. 45, pp. 999–1001, Feb 2002. *Cited on pages 13 and 94.*

- [98] D. James, A. J. Levine, D. Besser, and A. Hemmati-Brivanlou, "TGF-beta/activin/nodal signaling is necessary for the maintenance of pluripotency in human embryonic stem cells," *Development*, vol. 132, pp. 1273–1282, Mar 2005. *Cited on pages 13 and 94.*
- [99] S. Falk, H. Wurdak, L. M. Ittner, F. Ille, G. Sumara, M. T. Schmid, K. Draganova, K. S. Lang, C. Paratore, P. Leveen, U. Suter, S. Karlsson, W. Born, R. Ricci, M. Gotz, and L. Sommer, "Brain area-specific effect of TGF-beta signaling on Wnt-dependent neural stem cell expansion," *Cell Stem Cell*, vol. 2, pp. 472–483, May 2008. *Cited on page 13.*
- [100] F. P. Wachs, B. Winner, S. Couillard-Despres, T. Schiller, R. Aigner, J. Winkler, U. Bogdahn, and L. Aigner, "Transforming growth factor-beta1 is a negative modulator of adult neurogenesis," *J. Neuropathol. Exp. Neurol.*, vol. 65, pp. 358–370, Apr 2006. *Cited on pages 13, 93 and 101.*
- [101] S. Temple, "The development of neural stem cells," *Nature*, vol. 414, pp. 112–117, Nov 2001. *Cited on page 13.*
- [102] J. L. Close, B. Gumuscu, and T. A. Reh, "Retinal neurons regulate proliferation of postnatal progenitors and müller glia in the rat retina via TGF β signaling," *Development*, vol. 132, no. 13, pp. 3015–3026, 2005. *Cited on pages 13 and 93.*
- [103] T. Ikeda, Y. Homma, K. Nisida, K. Hirase, C. Sotozono, S. Kinoshita, and D. G. Puro, "Expression of transforming growth factor-beta s and their receptors by human retinal glial cells," *Curr. Eye Res.*, vol. 17, pp. 546–550, May 1998. *Cited on page 13.*
- [104] C. Wiese, A. Rolletschek, G. Kania, P. Blyszczuk, K. V. Tarasov, Y. Tarasova, R. P. Wersto, K. R. Boheler, and A. M. Wobus, "Nestin expression—a property of multi-lineage progenitor cells?," *Cell. Mol. Life Sci.*, vol. 61, pp. 2510–2522, Oct 2004. *Cited on pages 14 and 15.*
- [105] P. M. Steinert, Y. H. Chou, V. Prahlad, D. A. Parry, L. N. Marekov, K. C. Wu, S. I. Jang, and R. D. Goldman, "A high molecular weight intermediate filament-associated protein in BHK-21 cells is nestin, a type VI intermediate filament protein. Limited co-assembly in vitro to form heteropolymers with type III vimentin and type IV alpha-internexin," *J. Biol. Chem.*, vol. 274, pp. 9881–9890, Apr 1999. *Cited on page 14.*
- [106] Y. H. Chou, S. Khuon, H. Herrmann, and R. D. Goldman, "Nestin promotes the phosphorylation-dependent disassembly of vimentin intermediate filaments during mitosis," *Mol. Biol. Cell*, vol. 14, pp. 1468–1478, Apr 2003. *Cited on pages 14 and 96.*
- [107] C. M. Sahlgren, H. M. Pallari, T. He, Y. H. Chou, R. D. Goldman, and J. E. Eriksson, "A nestin scaffold links Cdk5/p35 signaling to oxidant-induced cell death," *EMBO J.*, vol. 25, pp. 4808–4819, Oct 2006. *Cited on pages 14, 15 and 97.*
- [108] J. Dahlstrand, L. B. Zimmerman, R. D. McKay, and U. Lendahl, "Characterization of the human nestin gene reveals a close evolutionary relationship to neurofilaments," *J. Cell. Sci.*, vol. 103 (Pt 2), pp. 589–597, Oct 1992. *Cited on page 14.*

- [109] J. Dahlstrand, M. Lardelli, and U. Lendahl, "Nestin mRNA expression correlates with the central nervous system progenitor cell state in many, but not all, regions of developing central nervous system," *Brain Res. Dev. Brain Res.*, vol. 84, pp. 109–129, Jan 1995. *Cited on page 15.*
- [110] S. Fukuda, F. Kato, Y. Tozuka, M. Yamaguchi, Y. Miyamoto, and T. Hisatsune, "Two distinct subpopulations of nestin-positive cells in adult mouse dentate gyrus," *J. Neurosci.*, vol. 23, pp. 9357–9366, Oct 2003. *Cited on page 15.*
- [111] T. Nakamura, G. Xi, Y. Hua, J. T. Hoff, and R. F. Keep, "Nestin expression after experimental intracerebral hemorrhage," *Brain Res.*, vol. 981, pp. 108–117, Aug 2003. *Cited on page 15.*
- [112] S. Hockfield and R. D. McKay, "Identification of major cell classes in the developing mammalian nervous system," *J. Neurosci.*, vol. 5, pp. 3310–3328, Dec 1985. *Cited on page 15.*
- [113] C. Andressen, E. Stocker, F. J. Klinz, N. Lenka, J. Hescheler, B. Fleischmann, S. Arnhold, and K. Addicks, "Nestin-specific green fluorescent protein expression in embryonic stem cell-derived neural precursor cells used for transplantation," *Stem Cells*, vol. 19, no. 5, pp. 419–424, 2001. *Cited on page 15.*
- [114] E. Cattaneo and R. McKay, "Proliferation and differentiation of neuronal stem cells regulated by nerve growth factor," *Nature*, vol. 347, pp. 762–765, Oct 1990. *Cited on page 15.*
- [115] S. Holmin, C. von Gertten, A. C. Sandberg-Nordqvist, U. Lendahl, and T. Mathiesen, "Induction of astrocytic nestin expression by depolarization in rats," *Neurosci. Lett.*, vol. 314, pp. 151–155, Nov 2001. *Cited on page 15.*
- [116] Y. Li and M. Chopp, "Temporal profile of nestin expression after focal cerebral ischemia in adult rat," *Brain Res.*, vol. 838, pp. 1–10, Aug 1999. *Cited on page 15.*
- [117] T. Nakagawa, O. Miyamoto, N. A. Janjua, R. N. Auer, S. Nagao, and T. Itano, "Localization of nestin in amygdaloid kindled rat: an immunoelectron microscopic study," *Can J Neurol Sci*, vol. 31, pp. 514–519, Nov 2004. *Cited on page 15.*
- [118] C. M. Sahlgren, A. Mikhailov, J. Hellman, Y. H. Chou, U. Lendahl, R. D. Goldman, and J. E. Eriksson, "Mitotic reorganization of the intermediate filament protein nestin involves phosphorylation by cdc2 kinase," *J. Biol. Chem.*, vol. 276, pp. 16456–16463, May 2001. *Cited on page 15.*
- [119] D. C. Hess, W. D. Hill, A. Martin-Studdard, J. Carroll, J. Brailer, and J. Carothers, "Bone marrow as a source of endothelial cells and NeuN-expressing cells After stroke," *Stroke*, vol. 33, pp. 1362–1368, May 2002. *Cited on page 15.*
- [120] E. Bieberich, S. MacKinnon, J. Silva, S. Noggle, and B. G. Condie, "Regulation of cell death in mitotic neural progenitor cells by asymmetric distribution of prostate apoptosis response 4 (PAR-4) and simultaneous elevation of endogenous ceramide," *J. Cell Biol.*, vol. 162, pp. 469–479, Aug 2003. *Cited on pages 15 and 96.*
- [121] T. Biagiotti, M. D'Amico, I. Marzi, P. Di Gennaro, A. Arcangeli, E. Wanke, and M. Olivetto, "Cell renewing in neuroblastoma: electrophysiological and immunocytochemical characterization of stem cells and derivatives," *Stem Cells*, vol. 24, pp. 443–453, Feb 2006. *Cited on page 15.*

- [122] H. Kambara, H. Okano, E. A. Chiocca, and Y. Saeki, “An oncolytic HSV-1 mutant expressing ICP34.5 under control of a nestin promoter increases survival of animals even when symptomatic from a brain tumor,” *Cancer Res.*, vol. 65, pp. 2832–2839, Apr 2005. *Cited on page 15.*
- [123] S. K. Thomas, C. A. Messam, B. A. Spengler, J. L. Biedler, and R. A. Ross, “Nestin is a potential mediator of malignancy in human neuroblastoma cells,” *J. Biol. Chem.*, vol. 279, pp. 27994–27999, Jul 2004. *Cited on page 15.*
- [124] L. C. Wei, M. Shi, R. Cao, L. W. Chen, and Y. S. Chan, “Nestin small interfering RNA (siRNA) reduces cell growth in cultured astrocytoma cells,” *Brain Res.*, vol. 1196, pp. 103–112, Feb 2008. *Cited on page 15.*
- [125] D. Park, A. P. Xiang, F. F. Mao, L. Zhang, C. G. Di, X. M. Liu, Y. Shao, B. F. Ma, J. H. Lee, K. S. Ha, N. Walton, and B. T. Lahn, “Nestin is required for the proper self-renewal of neural stem cells,” *Stem Cells*, vol. 28, pp. 2162–2171, Dec 2010. *Cited on pages 15 and 97.*
- [126] H. M. Pallari, J. Lindqvist, E. Torvaldson, S. E. Ferraris, T. He, C. Sahlgren, and J. E. Eriksson, “Nestin as a regulator of Cdk5 in differentiating myoblasts,” *Mol. Biol. Cell*, vol. 22, pp. 1539–1549, May 2011. *Cited on pages 16, 97 and 99.*
- [127] P. C. Orban, D. Chui, and J. D. Marth, “Tissue- and site-specific DNA recombination in transgenic mice,” *Proc. Natl. Acad. Sci. U.S.A.*, vol. 89, pp. 6861–6865, Aug 1992. *Cited on page 22.*
- [128] P. K. Stricklett, R. D. Nelson, and D. E. Kohan, “The Cre/loxP system and gene targeting in the kidney,” *Am. J. Physiol.*, vol. 276, pp. F651–657, May 1999. *Cited on pages 22 and 105.*
- [129] M. Lakso, J. G. Pichel, J. R. Gorman, B. Sauer, Y. Okamoto, E. Lee, F. W. Alt, and H. Westphal, “Efficient in vivo manipulation of mouse genomic sequences at the zygote stage,” *Proc. Natl. Acad. Sci. U.S.A.*, vol. 93, pp. 5860–5865, Jun 1996. *Cited on page 23.*
- [130] K. Sakai and J. Miyazaki, “A transgenic mouse line that retains Cre recombinase activity in mature oocytes irrespective of the cre transgene transmission,” *Biochem. Biophys. Res. Commun.*, vol. 237, pp. 318–324, Aug 1997. *Cited on page 23.*
- [131] I. Kleiter, J. Song, D. Lukas, M. Hasan, B. Neumann, A. L. Croxford, X. Pedré, N. Hövelmeyer, N. Yogev, A. Mildner, M. Prinz, E. Wiese, K. Reifenberg, S. Bitner, H. Wiendl, L. Steinman, C. Becker, U. Bogdahn, M. F. Neurath, A. Steinbrecher, and A. Waisman, “Smad7 in T cells drives T helper 1 responses in multiple sclerosis and experimental autoimmune encephalomyelitis,” *Brain*, vol. 133, no. 4, pp. 1067–1081, 2010. *Cited on pages 24, 26, 29, 58 and 59.*
- [132] A. Chytil, M. A. Magnuson, C. V. Wright, and H. L. Moses, “Conditional inactivation of the TGF- β type II receptor using cre:lox,” *genesis*, vol. 32, no. 2, pp. 73–75, 2002. *Cited on pages 24, 26 and 29.*
- [133] B. Junglas, S. Kuespert, A. A. Seleem, T. Struller, S. Ullmann, M. Bosl, A. Bossert, J. Kostler, R. Wagner, E. R. Tamm, and R. Fuchshofer, “Connective tissue growth factor causes glaucoma by modifying the actin cytoskeleton of the trabecular meshwork,” *Am. J. Pathol.*, vol. 180, pp. 2386–2403, Jun 2012. *Cited on page 25.*

- [134] K. Mullis, F. Faloona, S. Scharf, R. Saiki, G. Horn, and H. Erlich, "Specific enzymatic amplification of DNA in vitro: the polymerase chain reaction," *Cold Spring Harb. Symp. Quant. Biol.*, vol. 51 Pt 1, pp. 263–273, 1986. *Cited on page 27.*
- [135] K. C. Richardson, L. Jarett, and E. H. Finke, "Embedding in epoxy resins for ultrathin sectioning in electron microscopy," *Stain Technol.*, vol. 35, pp. 313–323, Nov 1960. *Cited on page 34.*
- [136] M. Almasieh, A. M. Wilson, B. Morquette, J. L. Cueva Vargas, and A. Di Polo, "The molecular basis of retinal ganglion cell death in glaucoma," *Prog Retin Eye Res.*, vol. 31, pp. 152–181, Mar 2012. *Cited on page 36.*
- [137] Y. Gavrieli, Y. Sherman, and S. A. Ben-Sasson, "Identification of programmed cell death in situ via specific labeling of nuclear DNA fragmentation," *J. Cell Biol.*, vol. 119, pp. 493–501, Nov 1992. *Cited on page 37.*
- [138] R. W. Young, "Cell death during differentiation of the retina in the mouse," *J. Comp. Neurol.*, vol. 229, pp. 362–373, Nov 1984. *Cited on pages 39 and 40.*
- [139] P. Chomczynski and N. Sacchi, "Single-step method of RNA isolation by acid guanidinium thiocyanate-phenol-chloroform extraction," *Analytical Biochemistry*, vol. 162, no. 1, pp. 156 – 159, 1987. *Cited on page 45.*
- [140] R. Higuchi, C. Fockler, G. Dollinger, and R. Watson, "Kinetic PCR analysis: real-time monitoring of DNA amplification reactions," *Biotechnology (N.Y.)*, vol. 11, pp. 1026–1030, Sep 1993. *Cited on page 46.*
- [141] U. K. Laemmli, "Cleavage of structural proteins during the assembly of the head of bacteriophage T4," *Nature*, vol. 227, pp. 680–685, Aug 1970. *Cited on page 49.*
- [142] D. Hicks and Y. Courtois, "The growth and behaviour of rat retinal Müller cells in vitro. 1. An improved method for isolation and culture," *Exp. Eye Res.*, vol. 51, pp. 119–129, Aug 1990. *Cited on page 54.*
- [143] D. Seitz, "Einfluss des Wachstumsfaktors Norrin auf Endothel- und Vorläuferzellen," *Diplomarbeit am Lehrstuhl für Embryologie und Humananatomie, Regensburg*, Feb. 2008. *Cited on page 54.*
- [144] D. L. Turner and C. L. Cepko, "A common progenitor for neurons and glia persists in rat retina late in development," *Nature*, vol. 328, no. 6126, pp. 131–136, 1987. *Cited on page 58.*
- [145] C. E. Holt, T. W. Bertsch, H. M. Ellis, and W. A. Harris, "Cellular determination in the *Xenopus* retina is independent of lineage and birth date," *Neuron*, vol. 1, pp. 15–26, Mar 1988. *Cited on page 58.*
- [146] R. Wetts and S. E. Fraser, "Multipotent precursors can give rise to all major cell types of the frog retina," *Science*, vol. 239, pp. 1142–1145, Mar 1988. *Cited on page 58.*
- [147] D. L. Turner, E. Y. Snyder, and C. L. Cepko, "Lineage-independent determination of cell type in the embryonic mouse retina," *Neuron*, vol. 4, pp. 833–845, Jun 1990. *Cited on page 58.*

- [148] P. G. Layer, R. Alber, P. Mansky, G. Vollmer, and E. Willbold, "Regeneration of a chimeric retina from single cells in vitro: cell-lineage-dependent formation of radial cell columns by segregated chick and quail cells," *Cell Tissue Res.*, vol. 259, pp. 187–198, Feb 1990. *Cited on page 58.*
- [149] R. W. Williams and D. Goldowitz, "Structure of clonal and polyclonal cell arrays in chimeric mouse retina," *Proc. Natl. Acad. Sci. U.S.A.*, vol. 89, pp. 1184–1188, Feb 1992. *Cited on page 58.*
- [150] S. C. Fields-Berry, A. L. Halliday, and C. L. Cepko, "A recombinant retrovirus encoding alkaline phosphatase confirms clonal boundary assignment in lineage analysis of murine retina," *Proc. Natl. Acad. Sci. U.S.A.*, vol. 89, pp. 693–697, Jan 1992. *Cited on page 58.*
- [151] A. Reichenbach, M. Ziegert, J. Schnitzer, S. Pritz-Hohmeier, P. Schaaf, W. Schober, and H. Schneider, "Development of the rabbit retina. V. The question of 'columnar units'," *Brain Res. Dev. Brain Res.*, vol. 79, pp. 72–84, May 1994. *Cited on page 58.*
- [152] M. Krampert, S. R. Chirasani, F. P. Wachs, R. Aigner, U. Bogdahn, J. M. Yingling, C. H. Heldin, L. Aigner, and R. Heuchel, "Smad7 regulates the adult neural stem/progenitor cell pool in a transforming growth factor beta- and bone morphogenetic protein-independent manner," *Mol. Cell. Biol.*, vol. 30, pp. 3685–3694, Jul 2010. *Cited on page 75.*
- [153] B. Junglas, A. H. Yu, U. Welge-Lussen, E. R. Tamm, and R. Fuchshofer, "Connective tissue growth factor induces extracellular matrix deposition in human trabecular meshwork cells," *Exp. Eye Res.*, vol. 88, pp. 1065–1075, Jun 2009. *Cited on page 86.*
- [154] L. Li and R. Bhatia, "Stem cell quiescence," *Clin. Cancer Res.*, vol. 17, pp. 4936–4941, Aug 2011. *Cited on page 93.*
- [155] G. R. Grotendorst, "Connective tissue growth factor: a mediator of TGF-beta action on fibroblasts," *Cytokine Growth Factor Rev.*, vol. 8, pp. 171–179, Sep 1997. *Cited on page 94.*
- [156] M. Kidd, S. Schimmack, B. Lawrence, D. Alaimo, and I. M. Modlin, "EGFR/TGF beta and TGF beta/CTGF Signaling in Neuroendocrine Neoplasia: Theoretical Therapeutic Targets," *Neuroendocrinology*, Jun 2012. *Cited on page 94.*
- [157] M. Krampert, S. R. Chirasani, F. P. Wachs, R. Aigner, U. Bogdahn, J. M. Yingling, C. H. Heldin, L. Aigner, and R. Heuchel, "Smad7 regulates the adult neural stem/progenitor cell pool in a transforming growth factor beta- and bone morphogenetic protein-independent manner," *Mol. Cell. Biol.*, vol. 30, pp. 3685–3694, Jul 2010. *Cited on page 94.*
- [158] R. L. Elliott and G. C. Blobe, "Role of transforming growth factor Beta in human cancer," *J. Clin. Oncol.*, vol. 23, pp. 2078–2093, Mar 2005. *Cited on page 95.*
- [159] Z. Yan, X. Deng, and E. Friedman, "Oncogenic Ki-ras confers a more aggressive colon cancer phenotype through modification of transforming growth factor-beta receptor III," *J. Biol. Chem.*, vol. 276, pp. 1555–1563, Jan 2001. *Cited on page 95.*

- [160] E. M. Lad, S. H. Cheshier, and M. Y. Kalani, “Wnt-signaling in retinal development and disease,” *Stem Cells Dev.*, vol. 18, no. 1, pp. 7–16, 2009. *Cited on page 95.*
- [161] A. Letamendia, E. Labbe, and L. Attisano, “Transcriptional regulation by Smads: crosstalk between the TGF-beta and Wnt pathways,” *J Bone Joint Surg Am*, vol. 83-A Suppl 1, no. Pt 1, pp. S31–39, 2001. *Cited on pages 95, 96 and 106.*
- [162] P. Rakic, “Specification of cerebral cortical areas,” *Science*, vol. 241, pp. 170–176, Jul 1988. *Cited on page 96.*
- [163] K. Frederiksen and R. D. McKay, “Proliferation and differentiation of rat neuroepithelial precursor cells in vivo,” *J. Neurosci.*, vol. 8, pp. 1144–1151, Apr 1988. *Cited on page 96.*
- [164] K. Michalczyk and M. Ziman, “Nestin structure and predicted function in cellular cytoskeletal organisation,” *Histol. Histopathol.*, vol. 20, pp. 665–671, Apr 2005. *Cited on page 96.*
- [165] S. Joly, V. Pernet, M. Samardzija, and C. Grimm, “Pax6-positive Müller glia cells express cell cycle markers but do not proliferate after photoreceptor injury in the mouse retina,” *Glia*, vol. 59, pp. 1033–1046, Jul 2011. *Cited on page 97.*

Danksagung

Mein herzlicher Dank gilt Allen, die zum Gelingen dieser Arbeit beigetragen haben. Besonders danken möchte ich:

- Prof. Tamm, der mir die Möglichkeit gegeben hat, meine Doktorarbeit an seinem Lehrstuhl anzufertigen und all meine Ideen immer voll unterstützt hat.
- Prof. Aigner, für das interessante Projekt und das Mentoring meiner Arbeit.
- Prof. Langmann für das Mentoring meiner Arbeit.
- Barbara, ohne deren persönlichen Einsatz und fachliche Anleitung diese Doktorarbeit nicht zustande gekommen wäre. Ganz dickes Dankeschön!
- Rudi, für die Adoption meines Projekts und für seine geduldige Hilfe in der schwierigen Anfangsphase.
- Meinem zukünftigen Mann Michael, der mich durch alle Hochs und Tiefs dieser Doktorarbeit begleitet hat. Du bist der Beste!
- Meinen Eltern Rosi und Herbert, die mich während meiner ganzen Ausbildung immer unterstützt haben.
- Stephi, Leonie, Christiane, Barbara und Michael fürs Korrekturlesen.
- Allen meinen Doktorandenkollegen, die immer ein offenes Ohr für Fachliches und Persönliches hatten.
- Unseren technischen Assistentinnen Margit, Silvia, Angelika und besonders Elke für die Unterstützung und die vielen netten Gespräche.